UNIVERSITA' DEGLI STUDI DELL'INSUBRIA

DOTTORATO DI RICERCA IN BIOTECNOLOGIE - XXVIII CICLO

Evaluation of microarray technology and cell line models in modern toxicology

Docente guida: Prof. **Emanuela Maserati**

Tesi di Dottorato di: **Marco Fabbri**
Matricola: **720419**

Dipartimento di Medicina Clinica e Sperimentale - Università degli Studi dell'Insubria

Anno Accademico 2014-2015

Contents

Summary

Modern toxicology puts together existing knowledge of classical biology with new technologies to study effects of perturbations and to predict adverse outcomes resulting from those perturbations. Modern toxicology employs high throughput technology as microarray and cell lines as *in vitro* models to investigate the effect of potential toxic compounds.

In my thesis I evaluate the usefulness and reproducibility of microarray technology and cell line models. I have been mainly interested in the study of the effects on the regulation of gene transcription in cell lines. I used HepG2 cell line as a model for liver to study cadmium-induced cytotoxicity, Caco-2 as model for intestinal epithelial to study nanoparticles and HeLa cells from cervical cancer to evaluate genomic instability.

Cadmium is currently classified as carcinogen for human. In my first study, gene expression is used to explain the possible toxic mechanism of cadmium carcinogenity, using HepG2 cell line. A suggested mechanism of cadmium-induced carcinogenicity involves defects in the cell response to DNA damage and in the resistance to apoptosis. In this regard, I focused on the tumour suppressor protein P53, since its inactivation is a common feature found in human cancers and it is a crucial component of the cellular response to DNA damage. The results presented in this thesis demonstrate that in HepG2 cells exposed to cadmium, P53 was

correctly moved and accumulated into the nucleus to accomplish its function as a transcription factor. However, in spite of this correct nuclear localization, the signals for the cell cycle arrest were not activated. In this context, the important mediator of cell cycle arrest P21, a P53 downstream protein, was upregulated at the gene level but not at the protein level. These results could be explained by the involvement of a post-transcriptional activity mediated by miRNA, as demonstrated by the upregulation of mir-372 in cadmium-treated HepG2 cells, which was able to affect p21 expression and to promote cell proliferation.

Recent advances in materials science have resulted in the creation of particles in the nano-scale range and their use is spreading. This creates the need to evaluate their possible toxic effect on human health. In the second study, gene expression is applied to evaluate nanoparticle effect on Caco-2 cells as *in vitro* model of intestinal epithelial cells. The main focus was to compare the effect of gold nanoparticles (AuNP) of two sizes (30 nm and 5 nm), using microarray technology. Smaller AuNPs (5 nm) inhibit Caco-2 cell growth. Gene expression analysis shows a broad range of responses induced by small size AuNPs. A bioinformatics reconstruction of the possible pathways regulated by smaller AuNPs indicates that Caco-2 cells activate defence responses even if it was not enough to prevent the observed toxic effect. The response at the transcriptome level upon exposure to larger AuNPs (30 nm) is very weak. This effect can be due to the low uptake of these larger AuNPs.

The third study focuses on the issue concerning cell line variability using different batches of HeLa cells obtained from different laboratories. The microarray expression analysis was performed on different batches of HeLa cells exposed to hypoxic conditions. In response to a hypoxic stimulus, each cell line batch activated different pathways, although the regulation of genes related to hypoxia is conserved. A genetic analysis show the high level of extensive chromosome instability in HeLa clones obtained from different laboratories. Each clone accumulates genomic variability in a time-dependent manner. The large differences in gene expression profiles suggest that the use of uncharacterized clones may lead to faulty conclusions and to irreproducible results in studies of gene function and pathway analysis.

In the three papers presented in this thesis I have not only shown the reproducibility of microarray by comparison to real time PCR, the gold standard technique for mRNA quantification, but also the potential to create possible model for the mechanistic effects on biological pathways.

In my thesis I have used different cell lines as *in vitro* models. They have shown that they have many advantages and that can give strong support for modern toxicology and be used to study biological mechanism. However, a possible drawback, which should be taken into account, is highlighted in the third study showing a high variability in the responses of different batches of the same cell line.

Aim of the thesis

The focus of my PhD study was the application of high throughput technology to investigate cellular models which may be highly informative for the study of human pathological conditions and of the effects of toxic compounds. I have been mainly interested in the study of the effects of different compounds on the regulation of gene transcription and in the evaluation of cell lines as *in vitro* models. To this end I used Caco-2 as model of intestinal epithelial cell to study cadmium, HepG2 as a model of hepatic cell, to study nanoparticles and HeLa cells from cervical cancer to evaluate genomic instability after having been cultured in different laboratories for several years.

I mainly studied the transcriptional responses that I evaluated by a high throughput technology such as microarray. This technology allows evaluating the expression of the entire genome in a single experiment. Furthermore, I investigated microRNAs, small RNAs that regulate the expression of thousands of genes at post-transcriptional, both in normal physiologic and pathological conditions.

Introduction

Modern toxicology

Recent improvements in biological understanding and technologies (high throughput), have allowed the contemplation of a new approach to understand disease and toxicology. This modern approach puts together existing knowledge of classical biology with new chemical and biological information about the effect of perturbations, leading to a hypothesis-based approach to predict adverse outcomes resulting from those perturbations. This general approach has been termed Adverse Outcome Pathway (AOP), as described by Ankely and colleagues [1]. An AOP describes the events that occur after a chemical exposure, starting from the interaction of the chemical with a biomolecule (e.g., protein, receptor) that it is called the Molecular Initiating Event (MIE), followed by a description of the cellular and tissue perturbations that can produce a toxicological effect also called adverse outcome. The cells respond to the change in their environment to maintain physiological condition but when they are not still able to maintain physiological condition, different processes are induced. In assessing cellular stress, Warringer and colleagues [2] suggested three phases of response: the most immediate response occurs via protein stabilization and modification, followed by translational reprogramming and finally by a slower, and more energy costing transcriptional response.

Toxicogenomics

The history of molecular biology starts with the discovery of DNA structure by Watson and Crick (1953), 20 years later, Southern blot and Northern blot allowed to "visualize" the presence of genetic material. Nowadays, Southern and Northern blots are not frequently used. These methods are now replaced with more rapid and higher throughput methods that need very small amounts of sample material and enable analyses of molecular events at a whole-genomic level.

The most enabling technology for such approaches is the microarray chip, first published in the mid-1990's [3]. The result was a miniature array that could allow the probing of the whole-genomic transcript profile.

The application of array technology in toxicology experiments provided the basis for the emergence of a new field, the toxicogenomics. Today, the term toxicogenomics represents the interface of multiple functional genomics approaches applied to understand mechanisms of toxicity.

The possibility to characterize the population of transcribed genes led to the creation of a new term, the transcriptome [4]. This concept defines the complete set of transcribed genes expressed as messenger RNAs for a particular species. The transcriptome, therefore, represents the universe of RNA messengers that may code for proteins. Only approximately 5% of genes are active in a particular cell at any given point in time. Most of the genes are

repressed, and this control may occur at either the transcriptional or the translational level. Since the regulation of protein expression at the level of transcription is more efficient, control mainly takes place at this level. The gene expression profile of a cell determines its function, phenotype and response to external stimuli. Therefore, gene expression profiles can help to elucidate cellular functions, biochemical pathways and regulatory mechanisms. In addition, gene expression profiles of disease cells or tissues, compared with normal controls, may promote the understanding of disease pathology and identify new therapeutic options, improving diagnosis and clarifying prognosis.

MicroRNA

MicroRNA (miRNA), a biologically relevant group of RNA molecules is gaining interest. Involvement of miRNAs for gene regulation and their biogenesis have been described in few review articles [5]–[7]. *In silico* prediction estimates that ∼60% of human mRNAs could be targets of miRNAs [8]. Similar to mRNA, miRNAs are expressed in a tissue- or cell-specific manner. MiRNAs can potentially regulate every aspect of cellular processes such as differentiation, proliferation, apoptosis, and necrosis as well as a large range of physiological processes [9].

The miRNA regulatory networks are complex because a single miRNA can target numerous mRNAs, often in combination with

other miRNAs; thus, an understanding of miRNA roles in toxicological processes requires an overall toxicogenomics approach. Studies that employ toxicogenomics have been performed, e.g., to evaluate the miRNA responses in rodent livers in order to identify potential biomarkers for toxicological risk assessment [10].

High throughput technologies

Microarray

Microarray is a high throughput technology for detection and characterization of DNA and RNA. This whole genome technology can be applied for different analysis, transcription analysis, detection and characterization of genetic variants [11] and toxicology [12]. The microarray is a collection of microscopic DNA spots attached to a solid surface [11]. Each spot contains a few picomole amount of a specific probe. Probes can be a short sequence of a gene or a DNA element used for hybridization of RNA or DNA in the sample (target) under stringent conditions. The probes are produced and attached to a solid surface by a covalent binding to a chemical matrix in commercial microarrays. According to different manufacturers the solid surface can be a glass or a silicon chip, alternatively, microarrays can be constructed by the direct synthesis of oligonucleotide probes on solid surfaces.

Microarrays allow measure global changes in gene expression (Fig.1). The signal is detected, quantified, integrated and normalized with software and reflect the gene expression profile or molecular portrait of a given biological sample. However, this molecular analysis depends on the number and type of probes spotted on a slide, thus in microarrays, only molecules that are searched, can be found.

Numerous commercial microarray platforms covering human or model animal genomes are commercially available.
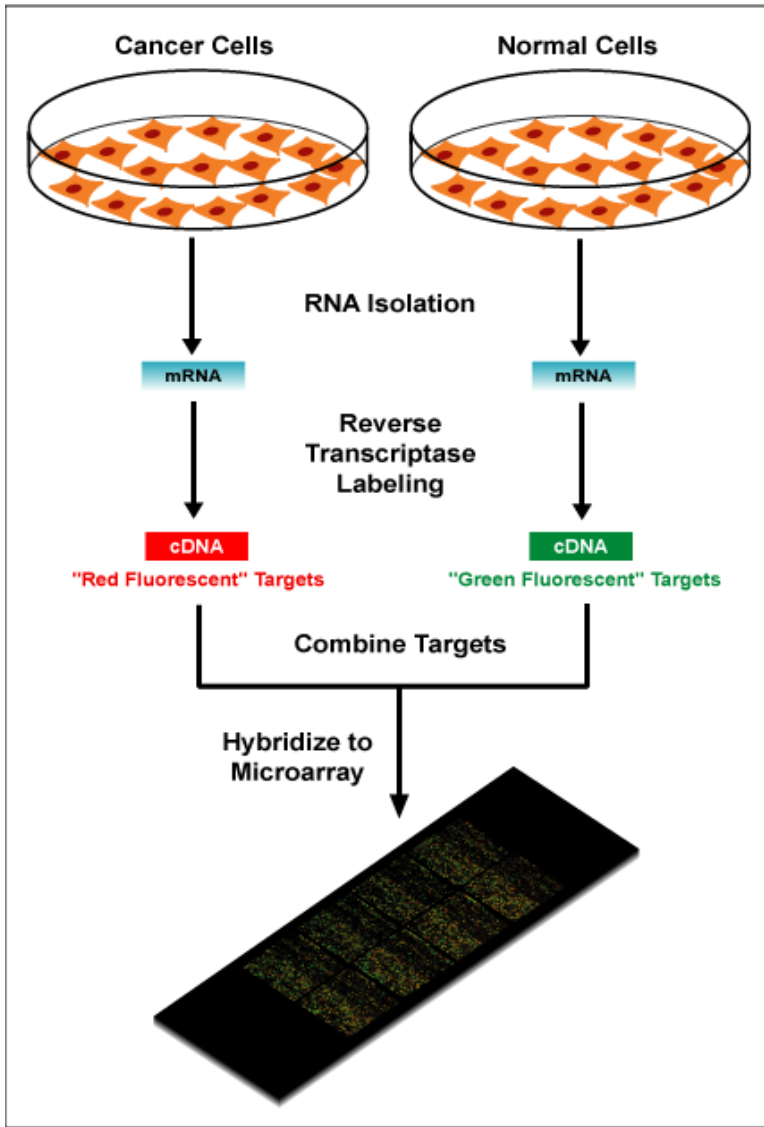
Fig 1. Schematic representation of a typical gene expression study.
The mRNA of two samples is isolated and labelled. The labelled RNA is
hybridized on the slide. In the last step the signal is detected, quantified,
integrated and normalized.

Microfluidic cards

Microfluidic Cards are high throughput tools for quantitative analysis of mRNA or miRNA transcripts using a real-time PCR protocol. This technology utilizes a microfluidic card with 384 reaction chambers and eight sample loading ports. In the studies of coding transcripts, the reaction chambers are preloaded with user selected or predefined panels of TaqMan Gene Expression Assays [13]. These assays enable real-time monitoring of a PCR reaction via hydrolysis of an oligonucleotide probe which has been dual labelled with fluorescent dye and quencher. Applications of TaqMan Array Cards include verification of microarray results, as well as hypothesis driven testing of panels of genes selected for their biological functions and relationships.

Bioinformatics analysis

The spread of toxicogenomics to the forefront as an area of research investigation [14], followed the initial success of large-scale genome projects to areas such as cancer, immunology and development. The first toxicogenomics experiments follow transcript changes after exposure of cells or tissues to a compound. The validation of the hypothesis that these changes lead to a possibility to group compounds with similar effects and to propose mechanistic insights previously unknown with the chemical action. This approach requires technical precision of processing

components of the experiments, and complex computational and bioinformatics approaches. With the abundance of the genomic data collected from series of microarray experiments, scientists realized that databases and analytical tools were essential in order to effectively manage and present the data into a new approach [15]. Scientists with different backgrounds began to develop analytical tools and to share resources for microarray gene expression data.

Gene expression analysis

Analysis of gene expression data can follow different approaches including class discovery, comparison, prediction, and pathway analysis.

One the most successful and used analytical tools developed for microarray are the clustering algorithm. The Eisen laboratory [16] implemented the use of the hierarchical clustering methodology (creating groups of genes and samples based on similarity of expression measurements) to analyse cell cycle time course [17] and displayed the relationship of the genes according to their distance relative to one another on a dendrogram expression illustrated by a colour gradient heat map. The result of the clustering of gene expression data is an assessment of the co-expression of genes within or between samples and the presumed coregulation of genes based on regulatory processes. Waring and colleagues [18] were one of the first groups to use clustering to analyse toxicogenomics data. Strong correlation between the

histopathology, clinical chemistry, and gene expression profiles from rats treated with different known hepatotoxicants was revealed, and genes were identified with expression level that correlated strongly with effects on clinical chemistry parameters.

At the very least, investigators in the field of toxicogenomics are often interested in a basic question of whether or not there are a set of gene expression profiles that can separate two or more classes of samples according to a particular exposure condition or phenotype.

There are some regulatory pathways catalogued in biological resources [19], most of these regulatory networks are constructed from gene interactions evaluated under normal conditions and that can be regulated in responses to environmental factors, toxicants, and other forms of stressors.

The study of biological pathways is a key to understand the different processes inside a cell: proteins exert their function not in isolation but in a tightly controlled network of interactions and reactions. Activation of a pathway typically leads to a change of state in the cell: as examples, a set of genes is transcribed, new molecules are assembled, molecules are secreted, or new signals are recognized. Pathways come in different flavours, depending on their functions in the cell, the three main types being metabolic pathways, gene regulatory pathways and signalling pathways.

Biological pathways are generally derived from experimental work in cell culture or model organisms. Many different studies are collected and integrated over time by initiatives like KEGG [19],

Reactome [20], BioCyc [21], or the user-curated WikiPathways [22].

Prediction of microRNA targets

MicroRNAs (miRNAs) play an important role in posttranscriptional regulation of target genes both in plant and animal cells. It is estimated that more than half of mammalian coding-genes are regulated by miRNAs and most human mRNAs are potential target of miRNAs [8], [23]. MiRNAs downregulate gene expression mostly by imperfect binding to complementary sites within transcript sequences. This imperfect binding suppresses their translation, stimulate their deadenylation and degradation or induce their cleavage [5], [24]. MiRNAs have been shown to be crucial for the majority of physiological processes. Therefore, their deregulation has been associated with many diseases such as cancer, cardiovascular and neurodegenerative diseases or metabolic disorders [25]. Hence, miRNA expression analysis has a diagnostic value, and the comparison with healthy miRNA levels is one of the promising therapeutic approaches [26]. Effective prediction of miRNA-mRNA interactions in animal systems remains challenging due to the interaction complexity, and a limited knowledge of rules governing these processes. Therefore, it is necessary to take advantage of the newest findings in miRNA biology and their targets prediction algorithms to find possible miRNA-mRNA interactions.

Cell lines as *in vitro* models

The use of toxicogenomics was applied to the study of *in vitro* experiments, and several studies have shown the validity of toxicogenomics-based *in vitro* systems for toxicity evaluation. One of the first studies [18] was promising, followed by a report on the use of primary cultured rat hepatocytes to identify two toxicological classes [27]. However, it is known that *in vitro* systems are different from *in vivo* studies, mainly in metabolic functions that are important for drug toxicity. By comparing various animal-free liver models against liver tissue in terms of their gene expression profiles, Boess and colleagues [28] demonstrated that the gene expression of primary hepatocyte cultures has moderate similarity to the liver, whereas two selected cell lines are quite different from whole liver. The authors suggested that although *in vitro* experiments are an indispensable research tool, the limitations of the experimental design of cell culture studies should be kept in mind [29].

Cell culture technologies form the basis of most alternative methods in toxicology. They are a mature technology, but still some limitations remain. It is important to be aware of limitations that impact on the predictive value of test systems based on cell cultures [30]. The main question is, how well the cell in culture reproduces the cell in the organism, in particular about its state of differentiation and its response patterns in an artificial environment. Differentiation can be seen as the cellular equivalent

of the phenotype at the level of an organism: which genes are expressed at a given time point and which functionality do they allow? This critical appraisal of the problems of current cell culture techniques does not mean that *in vitro* systems are not useful, but stresses the need to critically evaluate the predictive value of these models in each and every case. This emphasizes the need for validation, either in a formal sense for standardised tests or as a quality assurance process for the *in vitro* models in research and cell based screening approaches. Furthermore, cell lines can change with time.

HepG2

HepG2 cell line was isolated from a human hepatocellular carcinoma and it is one of the most used human hepatic cell model [31]. Although some studies attribute sufficient metabolic activities to these cells [32], they are in general considered to lack substantial liver-specific functions and hepatic enzyme activity [33]. The human origin of this hepatic cell line and its high rate of cellular proliferation, which represents a sensitive end-point for cytotoxicity potential, still make the HepG2 cells a relevant cell line in basal toxicity testing.

The main advantage of HepG2 cells is that they have retained the activities of several phase I and phase II xenobiotic metabolising enzymes [34]. The HepG2 cells are able to form structures typical of normal hepatocytes, express liver-specific functions, are metal responsive, and, more in general, are well characterized, thus

making them a useful model for mechanistic studies on cadmium carcinogenicity [35], [36].

Caco-2

Caco-2 cell line was initially used as an *in vitro* model system for studying human intestinal permeability for its characteristics shared with the small intestinal epithelium as to cell morphology, polarity, and enterocytic differentiation [37]. Its suitability for intestinal permeability screening was initially confirmed when strong correlations between *in vitro* Caco-2 and *in vivo* human intestinal permeability measurements were observed for some passively absorbed drugs [38], [39]. Since then, Caco-2 has been used to screen the intestinal permeability of an increasingly diverse population of compounds. Yee [40] had reported that Caco-2 may accurately predict the human intestinal permeability or absorption of compounds regardless of transcellular, paracellular, and carrier-mediated transport mechanisms. However, there are Caco-2 permeability results that disagree with measured human intestinal permeability rates or measured extents of human intestinal absorption [41], [42].

HeLa

HeLa was the first human cell line established [43] and has then become the most widely used human cell line in biological research. Its application as a model of living organism has

contributed to the characterization of important biological processes described in more than 70000 publications. This cell line originates from a cervical cancer tumour of a patient named Henrietta Lacks, who died of cancer in 1951 [44]. One of the earliest uses of HeLa cells was to develop the vaccine against the polio virus [45].

The HeLa cells has contributed to many fundamental scientific breakthroughs, these cells have been employed to investigate cancer, AIDS mechanisms [46], and the effects of drugs, toxins and radiation [47]. These cells have also been used in the Nobel-winning experiments that led to the discovery of telomeric activity [48].

Furthermore, to verify the gene-editing effects involved in specific cellular processes, gene expression profiles and proteome analyses have been applied to HeLa cells [49]. The widespread use of this cell line is mainly due to the easy handling and manipulation in different conditions.

Several published studies reported that HeLa cells are characterized by extensive chromosome instability. Cytogenetic analysis of HeLa led to observe numerous chromosome aberrations, and extensive chromosome instability.

HeLa cells have a hypertriploid (3n+) karyotype and produce heterogeneous cell populations [50], [51]. These cells differ in both their total number of chromosomes and in the number of specific chromosomes [52]. When Chu and colleagues examined parental HeLa cell lines and a series of clones derived from the primary

cells, they found wide variation in modal chromosome numbers [53]. Ghosh and colleagues [54] observed variation of stemline karyotype and rise of stable independent karyotype subpopulations from the "HeLa cell line (modal number 69)". Similarly, Macville and colleagues reported that 60% of the parental HeLa cells have a modal chromosome number of 78, and noted the emergence of a phenotypically distinct subpopulation of cells with their own stable karyotype (N=73) [55], [56].

Treatments

Cadmium

Cadmium is a highly persistent pollutant harmful to humans and animals, listed as one of the top ten hazardous substances by the Agency for Toxic Substances and Disease [57].

The long biological half-life of cadmium makes it a cumulative toxin, so long past exposures could still result in direct toxic effects of the residual metal [58]. Unfortunately, there are no proven effective treatments for chronic cadmium intoxication [58]. The long residence time of cadmium is due to metallothionein (MT), a metal-binding protein that is induced at the transcriptional level by cadmium and strongly binds the metal [59]. Cadmium accumulates mainly in the liver where it is bound to metallothionein [60]. The body has limited capacity to respond to cadmium exposure, as the liver cannot transform the metal to a less toxic species and it is only

poorly excreted, making long-term storage a viable option to reduce toxic effect with this toxic element.

Cadmium and its inorganic compounds were currently classified as a Group 1 carcinogen for human by IARC (International Agency for Research on Cancer) [61]. There was strong evidence specially based on experimental studies regarding cadmium carcinogenicity [62]. Cadmium is able to produce malignant tumours in multiple organs following long term and chronic exposure [59]. Besides experimental studies, epidemiological studies have also confirmed the potential cadmium carcinogenicity [63].

Although cadmium can produce genotoxic and mutagenic events, these generally require high doses [59]. Cadmium will not form stable DNA adducts and, since it is not a redox active metal, indirect oxidative DNA damage is unlikely as a primary carcinogenic mechanism. Thus, epigenetic non-genotoxic or indirect genotoxic mechanisms may apply. Such mechanisms could include aberrant gene expression resulting in stimulation of cell proliferation or blockage of apoptosis. Both these potential mechanisms could result in carcinogenic transformation in the absence of cadmium-induced genetic damage. Alternatively, cadmium can inhibit repair of DNA [64] which could be an indirect source of mutational events. Together with upregulation of mitogenic signalling, perturbed DNA repair and the resulting indirect genotoxicity could be key events in carcinogenesis [65].

Gold nanoparticles

Recent advances in material science have resulted in the creation of particles in the nano-scale range. However, years of research in this field, coupled with technological advances, have brought transformation in nanomaterial (NM) synthesis capabilities [66]. The consequent needs to assess the safety of NMs and identify their cellular responses have given rise to the field of nanotoxicology, which has now been in existence for over a decade [67].

The observed cellular reactions associated with NM exposure have identified a differential response that can be directly linked to their distinct physicochemical parameters [68], [69], demonstrating that small changes in NM properties can alter subsequent behaviour and cellular interactions. In addition to identify the NM properties that induce cytotoxicity, current investigations are in progress to evaluate the mechanisms behind these responses. Results of these inquiries have found that excess production of stress response and modifications to protein and gene expression precedes cellular death [70], [71].

Gold belongs to the group of noble metals and has been used in medical applications for centuries [71]. In recent years, nano-gold based applications were designed and gold nanoparticles (AuNPs) were synthesized with the idea that noble metal characteristics of gold would be preserved even when synthesized and used at nano-scale, thus being bio-compatible [72]. AuNPs and their derivatives undergo continuous development for their use in clinical diagnostics, as drug delivery systems or therapeutic agents [73]. In

general, AuNPs are well tolerated *in vivo* [74], although some toxicity of AuNPs was also reported *in vitro* [75], [76].

Hypoxia

Hypoxia and activation of hypoxia signalling pathways are associated with aggressive malignancy. Hypoxia inducible factor (HIF) is the key transcription factor mediating responses to hypoxia. Many common genes are among HIF target genes and genes implicated in dysregulated tumour metabolism.

Hypoxia inducible factor-1 (HIF-1) was initially identified as a transcriptional regulator that is bound to the hypoxia-response element of the erythropoietin [77]. It was initially believed that the entire underlying oxygen sensing apparatus was only involved in the regulation of erythropoietin. Later studies of the hypoxia-response element showed that the response pathway operated much more widely [78]. Consequently it became clear that HIF-1 has a wide range of transcriptional targets [79].

The Hypoxia inducible factor (HIF) senses and modulate cellular responses to hypoxia. HIF is a heterodimer: one of three alpha (α) subunits and a beta (β) subunit. HIF-β is constantly expressed, instead HIF-α is induced by hypoxia. HIF-1α is the most well-established member of the HIF family; the other two members of the basic–helix–loop–helix-PAS (bHLH-PAS) superfamily are HIF-2α (endothelial PAS domain protein 1 or HIF1α-like-factor), which also stabilizes hypoxia and binds to the aryl hydrocarbon

26

receptor nuclear translocator (ARNT) and HIF-3α [80]. HIF-1α is a transcriptional activator and a master regulator for the expression of genes involved in the response to hypoxia in most mammalian cells [81].

Results

Research Article

Cadmium Impairs p53 Activity in HepG2 Cells

C. Urani,[1] P. Melchioretto,[1] M. Fabbri,[2,3] G. Bowe,[2] E. Maserati,[3] and L. Gribaldo[2]

[1] *Department of Earth and Environmental Sciences, University of Milano Bicocca, piazza della Scienza 1, 20126 Milan, Italy*
[2] *Institute for Health and Consumer Protection, Joint Research Centre, Via Enrico Fermi 2749, 21027 Ispra, Italy*
[3] *Dipartimento di Medicina Clinica e Sperimentale, Università dell'Insubria, 21100 Varese, Italy*

Correspondence should be addressed to C. Urani; chiara.urani@unimib.it

Cadmium and cadmium compounds are contaminants of the environment, food, and drinking water and are important constituents of cigarette smoke. Cd exposure has also been associated with airborne particulate CdO and with Cd-containing quantum dots in medical therapy. Adverse cadmium effects reported in the literature have stimulated during recent years an ongoing discussion to better elucidate cadmium outcomes at cell and molecular level. The present work is designed to gain an insight into the mechanism of p53 impairment at gene and protein level to understand Cd-induced resistance to apoptosis. We used a hepatoma cell line (HepG2) derived from liver, known to be metal responsive. At genotoxic cadmium concentrations no cell cycle arrest was observed. The p53 at gene and protein level was not regulated. Fluorescence images showed that p53 was correctly translocated into the nucleus but that the p21$^{Cip1/WAF-1}$, a downstream protein of p53 network involved in cell cycle regulation, was not activated at the highest cadmium concentrations used. The miRNAs analysis revealed an upregulation of mir-372, an miRNA able to affect p21$^{Cip1/WAF-1}$ expression and promote cell cycle progression and proliferation. The role of metallothioneins and possible conformational changes of p53 are discussed.

1. Introduction

Cadmium (Cd) is a toxic element present in air, soil, sediment, and water. It is released into the environment through the waste from heavy metal mining, manufactures of nickel-cadmium batteries, and from other industrial and agricultural activities. It is ubiquitously present in the environment and in food, thus leading to a potential risk of human exposure. Nonoccupational exposure is mainly from diet and smoking, due to an accumulation of Cd in tobacco plants [1]. More recently, Cd exposure has been associated with airborne particulate CdO and with Cd-containing quantum dots in medical therapy [2, 3]. Targets of Cd toxicity include liver, lung, kidney cortex, bone, the cardiovascular system, and the immune system ([4], see the reviews [5–7]).

Cd and Cd compounds have been classified as human carcinogens (Group 1) by the World Health Organization's International Agency for Research on Cancer [8] and by the National Toxicology Program [9]. Although Cd carcinogenicity has been recognized by epidemiological studies and animal experiments, the underlying mechanisms are still

matter of research activities. Proposed mechanisms have been recently reviewed [10, 11] and range from thiol-containing protein affection and consequent production of reactive oxygen species, and interference with essential metals. Moreover, the deregulation of the cellular response to DNA damage and the resistance to apoptosis are among other proposed mechanisms involved in Cd-induced carcinogenicity [5].

The tumor suppressor protein p53 is a crucial component of the cellular response to DNA damage, and it is primarily involved in defense mechanisms by transcriptional activation of genes responsible of growth arrest and apoptosis for the elimination of heavily damaged cells. The inactivation of p53 is one common feature found in human cancers [12]. Cd has been demonstrated to interfere with the structure and function of p53 [5], although opposite effects have been reported. Namely, some authors refer to the induction of the p53-mediated stress response [13], while others demonstrated an inactivation of p53 via structural changes [14].

In this study we focused on the p53 pathway at gene and protein level to better investigate the involvement of this tumor suppressor protein in Cd-induced carcinogenesis.

A microRNA analysis was further performed to evidence a possible role of these small and noncoding regulatory molecules.

We used the HepG2 cells as a model of human origin from a target organ. The HepG2 cells are able to form structures typical of normal hepatocytes, express liver-specific functions, are metal responsive, and, more in general, are well characterized, thus making them a useful model for mechanistic studies on Cd carcinogenicity [15–19].

2. Materials and Methods

2.1. Cell Line and Culture Conditions. HepG2 cells were routinely grown in a monolayer culture in the presence of Opti-MEM medium (Invitrogen, San Giuliano Milanese, MI, Italy) supplemented with 10% heat inactivated fetal bovine serum (Invitrogen) and 1% antibiotics. The cells were maintained in an incubator at 37°C and humidified atmosphere of 5% CO_2. The medium was replaced twice a week and the cells were trypsinized and diluted every 7 days at 1 : 3 ratio. The cells were transferred either into 165 cm^2 flasks (Costar, Euroclone, Pero, MI, Italy) for protein preparations and cell cycle analysis, or into 8 cm^2 plastic dishes (Costar) for immunofluorescence analysis. Cells grown in complete culture medium represented the controls. A 1 mM stock solution of $CdCl_2$ monohydrate 97% purity (Cd, BDH Italia, Rome, Italy) was prepared in sterile MilliQ water (Millipore, Vimodrone, MI, Italy), and further dilutions were prepared in complete culture medium just before use.

2.2. Cell Cycle Analysis. The cells were seeded (7 × 10^5 cells/Petri dishes) and treated (10 μM Cd, 24, 48, and 72 hours) 24 h after seeding. Treated and control cells were harvested by trypsinization, collected by centrifugation (200 g, 5 min), and washed in PBS. The samples were further centrifuged (200 g, 5 min) to remove the PBS, fixed in cold ethanol, and stored at −20°C until use. Defrosted samples were centrifuged (200 g, 10 min) to remove ethanol and were incubated (15 min) for RNA hydrolysis and DNA staining using the DNA Prestain kit (Coulter Reagents, Beckman Coulter). Cell cycle distribution was analyzed by flow cytometry (Becton Dickinson Italia, Buccinasco, MI, Italy). The percentage of cells in each phase was estimated by FlowJo software using the Dean-Jett-Fox best fit and compared to untreated control cells.

2.3. p53 Extraction and Immunochemical Analysis. HepG2 cells (5 × 10^6 cells/flask) were exposed to increasing Cd concentrations (0.1–10 μM) for 24 h. At the end of the exposure time, the cells were harvested by trypsinization, collected by centrifugation (200 g, 10 min), and washed with PBS to remove Cd excess. The cells were collected again by centrifugation (200 g, 10 min), and homogenates of total proteins were obtained by resuspension in sample buffer (0.05 M Tris-HCl, pH 6.8, containing 2% SDS, 10% glycerol, 10% β-mercaptoethanol) containing 1 mM PMSF freshly added prior use. Homogenates were boiled for 5 min, passed 3-4 times through a syringe needle (22 ga Ø), and stored at −80°C until use. Total protein content was estimated by the Lowry method [20] using BSA as a standard.

Fifty μg of total proteins was separated on 10% NuPAGE gels (Invitrogen) in MOPS running buffer (Invitrogen, cat. number NP0001) and transferred onto a nitrocellulose membrane and processed for immunochemical analysis. A p53 monoclonal antibody (StressGen, Vinci-Biochem, Vinci, FI, Italy) was used, and the membrane incubation was run overnight at 4°C. After incubation with the secondary antibody (mouse IgG alkaline phosphatase conjugate, Sigma), the specific bands were visualized by the colorimetric substrates BCIP/NBT (Fast, Sigma).

2.4. p53 Immunofluorescence Localization. HepG2 cells were plated (100.000 cells/cm^2) on glass coverslips and left to recover at 37°C in incubator. The next day, the cells were treated with Cd (2, and 10 μM) for 24 h. After treatment, the cells were rinsed with PBS, fixed with methanol (5 min, −20°C), and processed for immunofluorescence labeling of the p53 protein. Primary antibody mouse anti-p53 (SterssGen) at 1 : 50 dilution in PBS + 1% BSA was used, and the cells were incubated for 1 h at 37°C. After saturation with PBS and PBS + 1% BSA, the cells were labeled with 1 : 100 Alexa Fluor 594 (Molecular Probes, Invitrogen) and incubated for 45 min at 37°C in humidified atmosphere. Then, samples were washed in PBS and distilled water, stained with DAPI (4′,6-diamidino-2-phenylindole) for nuclei visualization, and air-dried prior mounting. The coverslips were viewed on a Zeiss Axioplan microscope equipped with epifluorescence optics and a digital camera (CoolSnap-ProColors Media Cybernetics, Bethesda, MA, USA), and images were taken and stored using the Image Proplus software (Media Cybernetics).

2.5. $p21^{Cip1/WAF-1}$ Immunochemical Analysis. HepG2 homogenates obtained as described in *par.2.4* were used to evaluate the $p21^{Cip1/WAF-1}$ expression in Cd-treated cells (0.1–10 μM). Fifty μg of homogenated proteins was separated by electrophoresis in 12% NuPage gels (Invitrogen) and processed as previously described [16] to enhance membrane transfer and retention of low molecular weight proteins. Mouse anti-$p21^{Cip1/WAF-1}$ was used as a primary antibody (Invitrogen). Anti-mouse alkaline phosphatase conjugate (Sigma, St. Louis, MO, USA) was used as a secondary antibody, and protein binding was visualized by the colorimetric substrate BCIP/NBT (Sigma-Aldrich, Milano Italy).

2.6. MicroRNA Expression Profiling. RNA was extracted using the MIRVANA kit (AMBION) according to the manufacturer's instructions. Concentration and quality were determined by Nanodrop. Total RNA was reverse transcribed with Taqman MicroRNA Reverse Transcription Kit using Megaplex RT Primers (Applied Biosystems). Real-time PCR reactions were carried out on preconfigured microfluidic cards (Taqman Array MicroRNA Cards, set A, V2.2 and set B, V3, Applied Biosystems) allowing the detection of about 754 unique assays specific and four candidate endogenous control assays.

Two biological replicates for control and two for $10\,\mu$M Cd were tested. Experimental data were then analyzed by SDS 2.3 software (Applied Biosystems) and the relative expression values were calculated using as endogenous control U6 for miRNA. MiRNAs with a threshold cycle <33 that showed a log fold change greater than one in samples treated with cadmium as compared to control samples were considered as induced.

2.7. Statistical Analysis. Student's *t*-test or ANOVA (multiple range test) was used for comparisons. The software package Statgraphics Plus version 5.0 (Statistical Graphics Corp., Manugistic Inc. Rockville, MD, USA) was used for the statistical analysis.

3. Results

3.1. Cell Cycle Progression Is Not Affected by Cd Exposure in HepG2 Cells. We previously demonstrated by MTT assay that Cd concentrations used in the present work induce a maximum of 20% loss of viability at $10\,\mu$M Cd. The IC_{50} value (50% of the reduction of cell viability) was computed to be $25.5\,\mu$M [16].

Cadmium induces DNA damage in HepG2 cells, as previously reported [22, 23], and as confirmed by our experiments on single-strand breaks formation (data not shown).

In the presence of DNA damage (e.g., single strand breaks), the cell systems have evolved multiple mechanisms to avoid damage propagation. Among these, responses working in mammalian cells include the cell cycle check points control mechanisms, as well as apoptosis for the elimination of heavily damaged cells.

Our results showed that in HepG2 cells exposed to the highest Cd concentration ($10\,\mu$M) for different time points (24, 48, and 72 h), there was no effect on cell cycle progression. The distribution of cell population among the cell cycle phases (G1, S, G2/M) did not change when statistically compared to controls (Figure 1(a)), even after 72 h of Cd exposure (Figures 1(a) and 1(b)).

3.2. p53 Expression and Localization in Cd-Stressed HepG2 Cells. The p53 tumor suppressor protein is a key regulator of cell cycle arrest and of apoptosis. In response to DNA damage, the p53 is normally activated and accumulated to exert its DNA-binding activity for the regulation of genes involved either in G1 cell cycle arrest or apoptosis. To understand the mechanism behind the cell cycle progression in the presence of a genotoxic effect of Cd, we analyzed the p53 expression. At molecular level, we focused on the genes related to the p53 signalling pathway. Interestingly, the map of KEGG shows that the p53 gene was not regulated at the transcriptional level (Figure 2). At protein level, immunochemical results confirmed that there is no clear evidence of an upregulation of this transcription factor in Cd-exposed (0.1–$10\,\mu$M) samples (Figure 3).

We next analyzed the subcellular localization of p53 by indirect immunofluorescence in the presence of genotoxic Cd concentrations (2 and $10\,\mu$M) to verify whether the p53 was correctly localized to exert its function. Fluorescence images showed that in control cells the p53 signal is spread and localizes throughout the cytoplasm (Figures 4(a)–4(c)). In cells treated with DNA-damaging concentrations of Cd (2 and $10\,\mu$M), the p53 fluorescence signal is increasingly concentrated and accumulated in areas that co-localize with the nuclei (Figures 4(d)–4(f) and 4(g)–4(i)), as expected by a transcription factor. To quantitatively express the nuclear localization of the p53, a wide population (400–1000 cells/controls or Cd) of stained cells coming from independent experiments and different coverslips was counted. In controls only $10 \pm 3,2\%$ of the cells showed a p53 nuclear localization, confirming the predominant cytoplasmic distribution in unstressed cells, while in Cd-treated samples an increasing percentage of the cells showed that the transcription factor moves into the nucleus (Cd $2\,\mu$M $30 \pm 9,2\%$, and Cd $10\,\mu$M $67 \pm 18\%$) to activate downstream genes. The extent of p53 nuclear localization in controls and in Cd-treated cells is summarized quantitatively in Figure 5.

3.3. $p21^{Cip1/WAF\text{-}1}$ Levels in Cd-Stressed HepG2 Cells. To better understand the p53 pathway and regulatory activity, we have analyzed the expression of the $p21^{Cip1/WAF\text{-}1}$ protein. The $p21^{Cip1/WAF\text{-}1}$ is a downstream protein known to be regulated also by p53 to trigger cell cycle arrest in DNA damaged cells. At gene level, *$p21^{Cip1/WAF\text{-}1}$* was upregulated, as shown by the p53 signalling pathway (Figure 2, in red). Nevertheless, levels of $p21^{Cip1/WAF\text{-}1}$ protein were comparable to controls at the lower Cd concentrations and decreased at 5 and $10\,\mu$M Cd (Figure 3).

3.4. miRNA Modulation. We have analyzed the modulation of these small and noncoding molecules, acting at posttranscriptional level, to unravel the apparent contrast between the *p21* gene upregulation and the p21 protein downregulation at high Cd concentrations (5 and $10\,\mu$M).

The effects of $10\,\mu$M Cd on miRNAs were evaluated with microfluidic cards and the focus was on the upregulated miRNAs. In Cd-treated samples we identified two miRNAs that were upregulated: hsa-mir-138 and hsa-mir-372.

4. Discussion

The aim of this study was to investigate the role of the p53 tumor suppressor at gene and protein level in order to contribute to the comprehension of the reported resistance to apoptosis in Cd-treated cells [5]. Cadmium carcinogenicity has been recognized by epidemiological studies and animal experiments, as recently reviewed [6, 8]; however, the overall mechanism is still unclear. In addition, conflicting results concerning the effects of Cd on biological systems are present in the literature [13, 14], possibly justified by a recently demonstrated hormetic effect of this metal [24, 25]. Current evidence suggests that Cd carcinogenicity is not due to a direct genotoxic effect of this metal. Multiple indirect mechanisms, the interference with the cell response to DNA damage, the deregulation of cell growth, and the resistance to

(a)

(b)
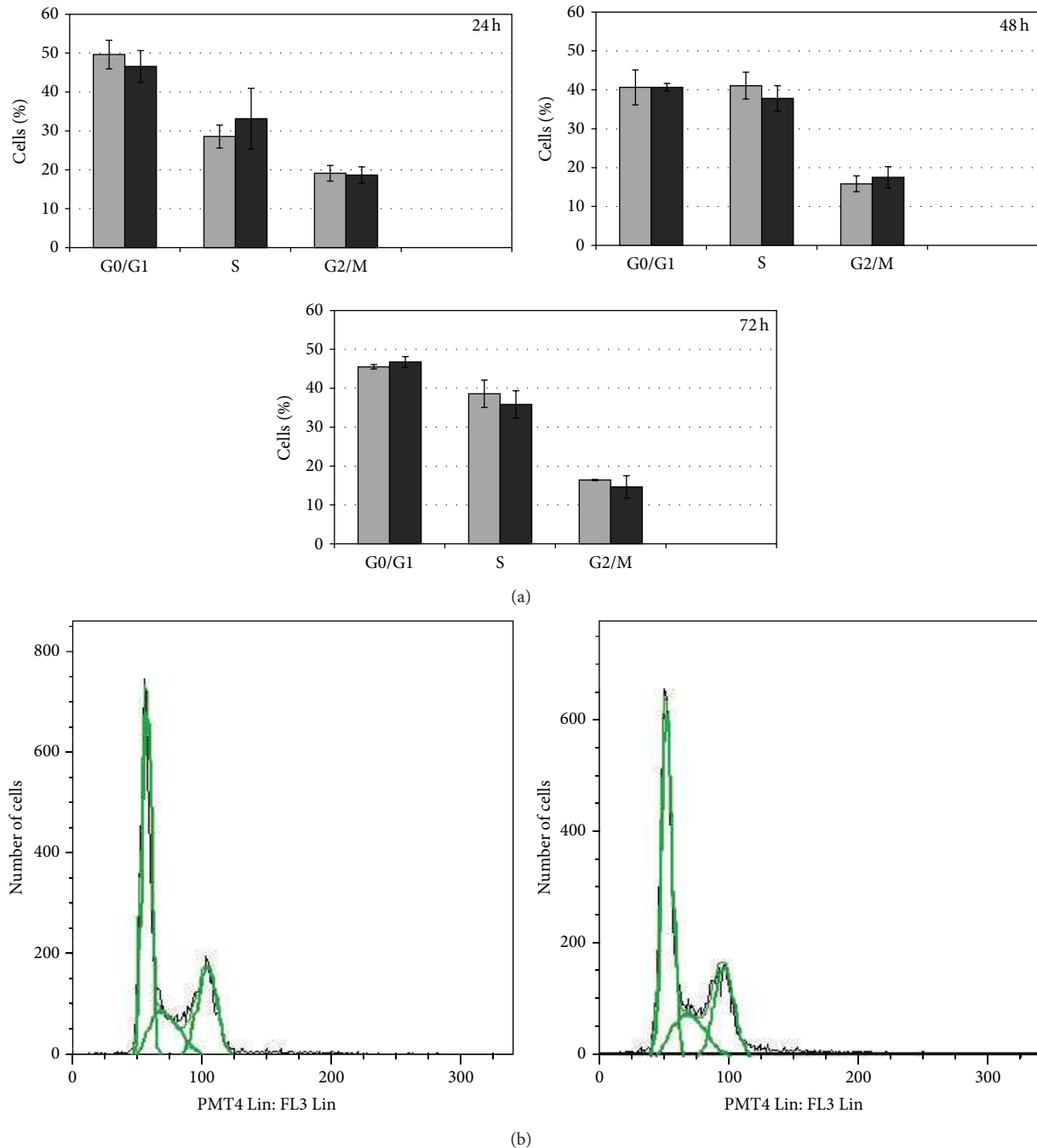
FIGURE 1: Effects of CdCl$_2$ on cell cycle distribution of HepG2 cells. HepG2 cells were cultured in the presence of $10\,\mu$M Cd concentration for different time points (24, 48, and 72 h). (a) The distribution of the cell population in the different cell cycle phases of treated cells (black bar) is always comparable to controls (grey bar) at all tested time points. In (b) an example of histogram obtained by flow cytometer analysis is displayed; the DNA content (x axis) is plotted against the cell number (y axis). Cells from three independent experiments were analyzed.

apoptosis are more accredited mechanisms which account for Cd carcinogenicity [5, 7, 11].

In HepG2 cells and, more in general, in mammalian cells cadmium exerts the genotoxic effect through reactive oxygen species generation, causing DNA strand breaks and chromosomal aberrations ([22], for a review see [5]). The DNA damage response is rigorously coordinated by multiple

mechanisms, among which the p53 has a key role. The p53 is essential in the regulation of the cell cycle arrest and apoptosis for the processing of DNA damage and for restoring genomic stability or eliminating heavily damaged cells [26]. Our experiments demonstrated that in Cd-treated HepG2 cells, these regulatory mechanisms were not activated. Namely, no cell cycle arrest was induced at the highest Cd concentration
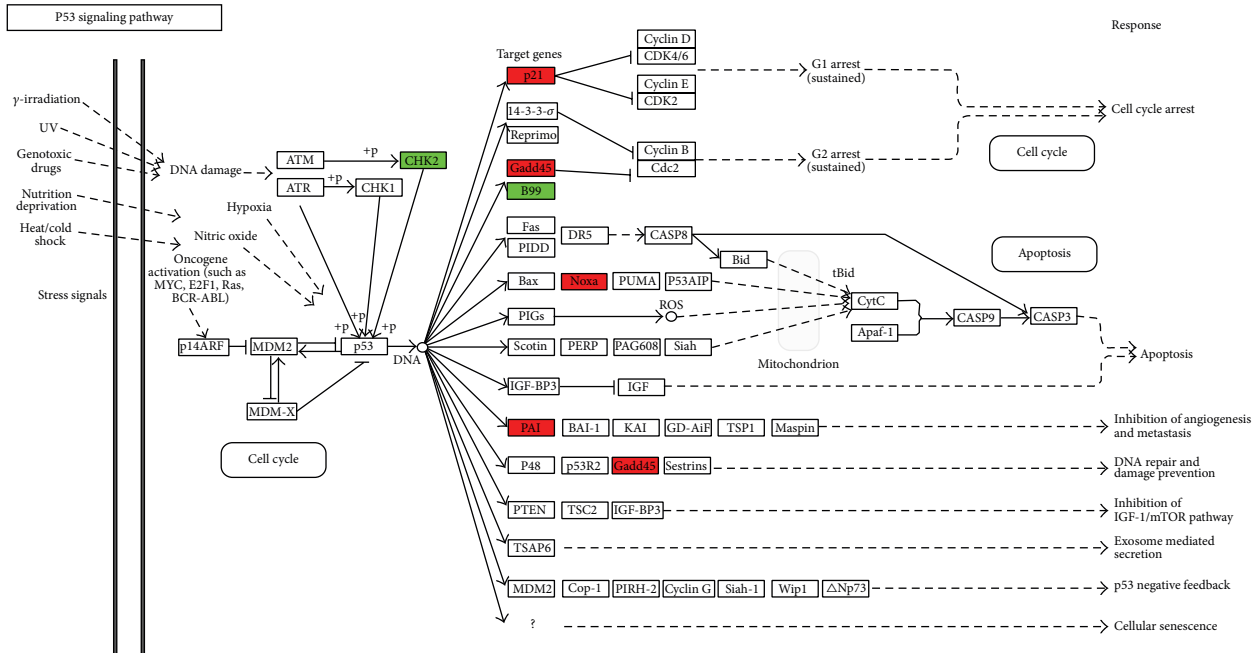
Figure 2: Representation of the p53 signaling pathway map from KEGG. The genes identified as regulated in 10 μm Cd-treated HepG2 cells are colored in the p53 signaling pathway map. The genes in red are upregulated and those in green are downregulated. Genes identified as regulated have a false discovery rate corrected P value smaller than 0.05 and fold change greater than 2.
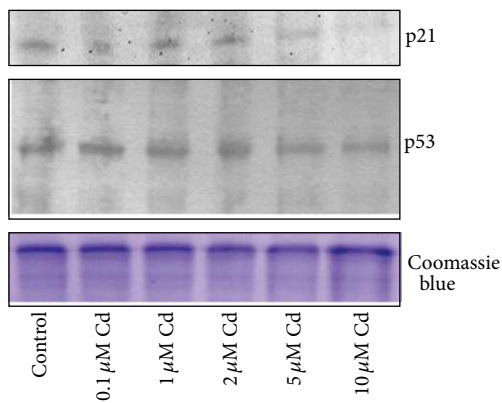
Figure 3: Effect of CdCl$_2$ on p53 and p21$^{Cip1/WAF-1}$ protein expression. HepG2 homogenated proteins (50 μg/lane) were separated on 12% gels or 10% gels, transferred onto nitrocellulose membrane, and probed for p21$^{Cip1/WAF-1}$ or p53 protein expression, respectively. Representative Western blots are shown. Parallel gels stained with Coomassie Blue G250 for equal protein loading evaluation were performed.

tested (10 μM), and no p53 upregulation was observed, as visualized at gene as well as at protein level. In response to stress, the p53 is normally accumulated in the nucleus and converted into an active DNA-binding form to control several sets of genes to prevent the proliferation of cells carrying a DNA damage [27]. To the best of our knowledge, our results of fluorescence microscopy show for the first time that the p53 was increasingly accumulated into the nucleus in Cd-treated

HepG2 cells, according to the activity of a transcription factor. However, despite this correct localization in stressed cells, the p53 was not able to activate the downstream signals of cell cycle regulation and arrest to allow the DNA repair. This data is supported by the result on the p21$^{Cip1/WAF-1}$, a p53 downstream protein responsible for the cell cycle arrest [26]. Indeed, in our samples the p21$^{Cip1/WAF-1}$ showed levels comparable to controls or downregulated in Cd-treated HepG2. Therefore, this lack of regulation could account for the normal progression of the HepG2 cells into the cell cycle phases that we observed.

The uncontrolled proliferation of DNA-damaged cells and the acquisition of apoptotic resistance are important steps in the malignant transformation process. In this context, our results on the impairment of p53 pathway activity go through this direction. HepG2 cells, albeit derived from a human hepatoma, express a wild type and an inducible p53 activity, well documented previously [28]. However, previous works [3, 14] suggest that this activity could be impaired by conformational changes in the wild type p53 protein, as demonstrated in MCF7 and A549 cells exposed to soluble and particulate Cd compounds. The impairment of p53 activity could also be explained by our recent findings on microRNA (miRNA) levels in Cd-exposed HepG2 [29]. The miRNAs are small and noncoding RNAs which play a key role in gene expression at the posttranscriptional level, targeting mRNAs for cleavage or translational repression. We previously found that a large percentage of downregulated miRNAs belong to the let-7 family. The let-7 family is reported to have oncosuppressor functions as it regulates processes including cell division and DNA repair. In this regard, very interestingly
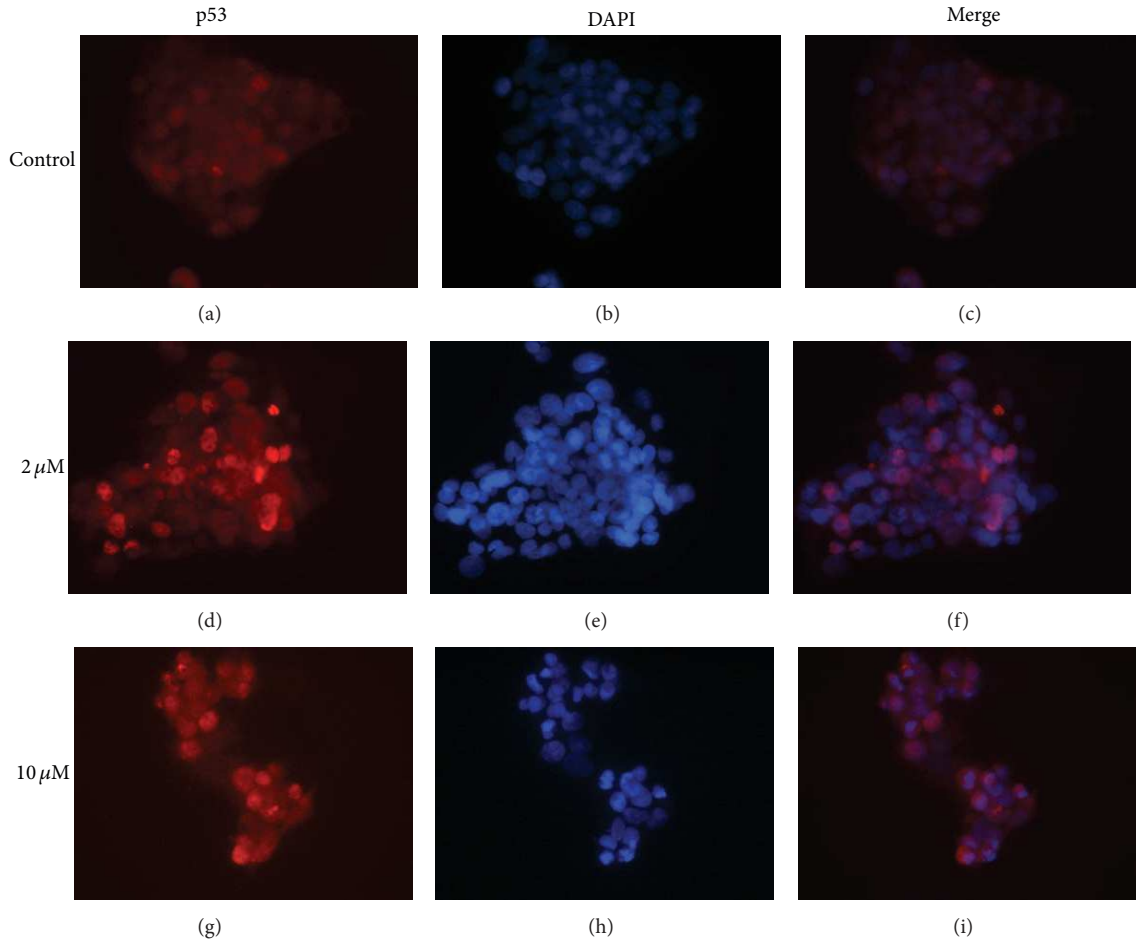
FIGURE 4: Visualization of p53 localization in CdCl$_2$-treated HepG2 cells. Fixed and p53 stained cells were visualized by indirect probing with Alexa Fluor antibody. In control HepG2 (a), a spread distribution of the p53 is shown throughout the cells, while the treatment with Cd increases the nuclear localization of the protein (d, g). (a, d, g) cells probed for p53 in controls (a), 2 μM (d), and 10 μM (g) Cd concentrations. (b, e, h) cells stained with DAPI for the nuclei visualization in controls (b), 2 μM (e), and 10 μM (h) Cd concentrations. Merge is represented in (c, f, i) images. Microscopy magnification: 400x.

it was recently described [30] that let-7a and let-7b expression are dependent on the p53 activity. Moreover, miRNAs are reported to have control activities on p21 at posttranscriptional level [31, 32] further sustaining our data on p21 expression at gene and protein level. Indeed, we suggest that the apparent contrast between $p21^{Cip1/WAF-1}$ upregulation at gene level and no modulation or downregulation at protein level could be possibly explained by the posttranscriptional activity of miRNAs. These findings support our data on the impaired function of this transcription factor. In order to further explain the lack of regulation of the p53 we analyzed the miRNA expression in Cd-treated HepG2. We analysed a panel of miRNA regulated upon stimulation of Cd, and we identified that two were upregulated after Cd exposure: mir-372 and mir-138, both connected to carcinogenesis [33, 34]. Wu and colleagues [32] showed that mir-372 can bind to the 3'UTR of p21$^{Cip1/WAF-1}$ affecting its expression. Furthermore, the expression of mir-372 can promote cell proliferation and cell-cycle progression [34]. This mechanism warrants further investigation, but the work by Wu and colleagues together

with our data on mir-372 upregulation provides hints on the involvement of miRNAs in the toxic mechanism induced by cadmium promoting proliferation activities. The second miRNA that we found upregulated, mir-138, was recently described to have oncosuppressor functions and its downregulation was associated with head and neck squamous cell carcinoma (HNSCC). However, while the deregulation of miR-138 is frequently observed in HNSCC and other cancer types, the exact role of miR-138 in tumorigenesis remains elusive [33]. Thus further functions and regulatory activities of this miRNA need to be deeply depicted.

Another possible mechanism that could contribute to the impairment of p53 activity and subsequent inhibition of the cell cycle arrest in HepG2 cells is the interference of metallothioneins (MTs). The expression and induction of this low molecular weight family of proteins are associated with protection against oxidative stress, cytotoxicity, and DNA damage. Cd is a transcriptional modulator, among others, of MT gene expression, and this family of metal-binding proteins appears also to play a key role in the prevention of
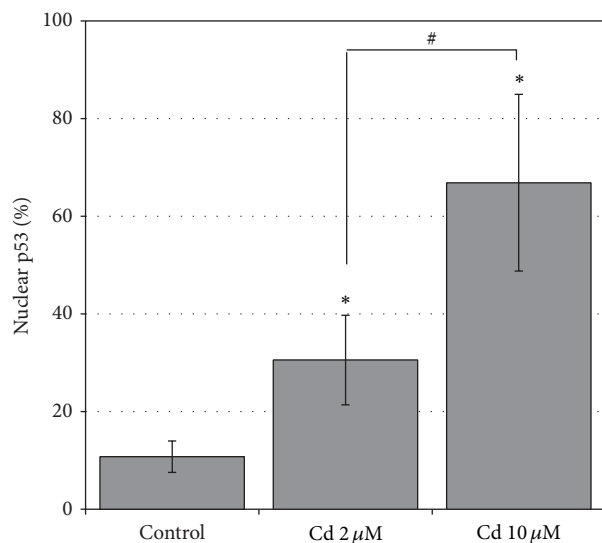
FIGURE 5: Quantification of the p53 nuclear localization. Percentage (mean ± SD) of HepG2 cells showing the p53 nuclear localization in the controls and in Cd-treated cells (2 and 10 μM). The mean ± SD values of at least 3 independent samples are shown; a number of $400 < n < 1000$ cells were counted. Significantly different from control: $^*P < 0.5$; significantly different between Cd treatments: $^\#P < 0.05$.

apoptosis, acting as regulators of p53 folding and activity [35]. In addition, MT null cells are more susceptible to apoptotic death after exposure to apoptosis-inducing agents, and the involvement of MT in controlling apoptotic mechanisms was suggested in the past [36]. MTs were also proposed as proteins involved in the regulation of p53 stability and DNA-binding activity, along with a protective function in Cd-induced toxicity [37]. In HepG2 cells, MTs are strongly upregulated in the presence of Cd, as previously demonstrated by our group. [16, 21, 38]. These data sustain the speculation of a role for MT as negative regulators of apoptosis and of p53 activity [35].

5. Conclusions

In conclusion, as depicted and summarized in Figure 6, we demonstrated for the first time that in HepG2 cells exposed to Cd, the p53 was correctly moved and accumulated into the nucleus to exert its function of transcription factor. However, besides this correct nuclear localization, the signals for the cell cycle arrest were not activated. In this context, the p21$^{\text{Cip1/WAF-1}}$, a p53 downstream protein and an important mediator of cell cycle arrest, was upregulated at gene level but not at protein level. These results could be explained by a posttranscriptional activity by the miRNA, as demonstrated by the upregulation of mir-372 in Cd-treated HepG2 cells, able to affect p21$^{\text{Cip1/WAF-1}}$ expression and to promote cell proliferation. In this complex network, it seems of crucial importance to further investigate the relation between miRNA activity and p53 impairment.

The influence of Cd on p53 inactivation by conformational changes is under investigation by our group to more
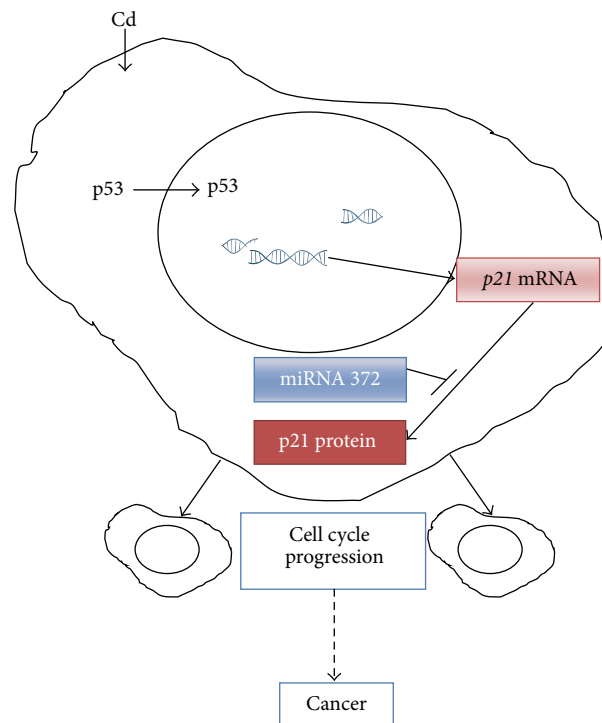
FIGURE 6: Overview of cadmium effects. (1) Cadmium is accumulated into HepG2 cells [21] and indirectly causes a genotoxic damage [22, 23] (data not shown); (2) the p53 is visualized into the nucleus, as expected, to exert its function of transcription factor; (3) the $p21^{Cip1/WAF-1}$ gene ($p21$ mRNA) is upregulated, although no protein upregulation is observed possibly due to a posttranscriptional regulation by miRNA-372; (4) no cell cycle arrest is observed, thus leading to the transmission of DNA damage and ultimately to cancer.

deeply elucidate the apoptotic resistance and the mechanism of Cd-carcinogenicity. Our results support the hypothesis of Cd as a double-edge sward factor [11], as it induces DNA damage and inhibits its repair.

Abbreviations

CdCl$_2$·H$_2$O: Cd
FBS: Fetal bovine serum
MT: Metallothioneins
PMSF: Phenylmethylsulfonyl fluoride
SDS: Sodium dodecyl sulphate.

Conflict of Interests

The authors declare that there is no conflict of interests regarding the publication of this paper.

Acknowledgments

References

[1] S. Satarug and M. R. Moore, "Adverse health effects of chronic exposure to low-level cadmium in foodstuffs and cigarette smoke," *Environmental Health Perspectives*, vol. 112, no. 10, pp. 1099–1103, 2004.

[2] M. P. Waalkes, "Cadmium carcinogenesis," *Mutation Research*, vol. 533, no. 1-2, pp. 107–120, 2003.

[3] T. Schwerdtle, F. Ebert, C. Thuy, C. Richter, L. H. F. Mullenders, and A. Hartwig, "Genotoxicity of soluble and particulate cadmium compounds: impact on oxidative dna damage and nucleotide excision repair," *Chemical Research in Toxicology*, vol. 23, no. 2, pp. 432–442, 2010.

[4] L. Friberg and M. Vahter, "Assessment of exposure to lead and cadmium through biological monitoring: results of a UNEP/WHO global study," *Environmental Research*, vol. 30, no. 1, pp. 95–128, 1983.

[5] A. Hartwig, "Cadmium and cancer," *Metal Ions in Life Sciences*, vol. 11, pp. 491–507, 2013.

[6] IARC, *A Review of Human Carcinogens, Part C: Arsenic, Metals, Fibers, and Dusts*, IARC, Lyon, France, 2012.

[7] M. Filipič, "Mechanisms of cadmium induced genomic instability," *Mutation Research*, vol. 733, no. 1-2, pp. 69–77, 2012.

[8] IARC, *Supplement: Cadmium and Cadmium Compounds. IARC Monographs on the Evaluation of Carcinogenic Risks To Humans*, IARC, Lyon, France, 1997.

[9] NTP, (National Toxicology Program), "Tenth report on carcinogens," Department of Health and Human Services III-42-III-44, Research Triangle Park, NC, USA, 2000.

[10] A. Martelli, E. Rousselet, C. Dycke, A. Bouron, and J.-M. Moulis, "Cadmium toxicity in animal cells by interference with essential metals," *Biochimie*, vol. 88, no. 11, pp. 1807–1814, 2006.

[11] G. Bertin and D. Averbeck, "Cadmium: cellular effects, modifications of biomolecules, modulation of DNA repair and genotoxic consequences (a review)," *Biochimie*, vol. 88, no. 11, pp. 1549–1559, 2006.

[12] M. Hollstein, D. Sidransky, B. Vogelstein, and C. C. Harris, "p53 Mutations in human cancers," *Science*, vol. 253, no. 5015, pp. 49–53, 1991.

[13] S. Chatterjee, S. Kundu, S. Sengupta, and A. Bhattacharyya, "Divergence to apoptosis from ROS induced cell cycle arrest: effect of cadmium," *Mutation Research*, vol. 663, no. 1-2, pp. 22–31, 2009.

[14] C. Méplan, K. Mann, and P. Hainaut, "Cadmium induces conformational modifications of wild-type p53 and suppresses p53 response to DNA damage in cultured cells," *Journal of Biological Chemistry*, vol. 274, no. 44, pp. 31663–31670, 1999.

[15] M. M. P. Zegers and D. Hoekstra, "Mechanisms and functional features of polarized membrane traffic in epithelial and hepatic cells," *Biochemical Journal*, vol. 336, no. 2, pp. 257–269, 1998.

[16] C. Urani, P. Melchioretto, C. Canevali, and G. F. Crosta, "Cytotoxicity and induction of protective mechanisms in HepG2 cells exposed to cadmium," *Toxicology in Vitro*, vol. 19, no. 7, pp. 887–892, 2005.

[17] V. Mersch-Sundermann, S. Knasmüller, X.-J. Wu, F. Darroudi, and F. Kassie, "Use of a human-derived liver cell line for the detection of cytoprotective, antigenotoxic and cogenotoxic agents," *Toxicology*, vol. 198, no. 1–3, pp. 329–340, 2004.

[18] P. F. Dehn, C. M. White, D. E. Conners, G. Shipkey, and T. A. Cumbo, "Characterization of the human hepatocellular carcinoma (HepG2) cell line as an in vitro model for cadmium toxicity studies," *In Vitro Cellular and Developmental Biology—Animal*, vol. 40, pp. 172–181, 2004.

[19] J. Shea, T. Moran, and P. F. Dehn, "A bioassay for metals utilizing a human cell line," *Toxicology in Vitro*, vol. 22, no. 4, pp. 1025–1031, 2008.

[20] H. Lowry, N. J. Rosenbrought, A. L. Farr, and R. L. Randall, "Protein measurement with the Folin phenol reagent," *The Journal of Biological Chemistry*, vol. 193, no. 1, pp. 265–275, 1951.

[21] C. Urani, P. Melchioretto, C. Canevali, F. Morazzoni, and L. Gribaldo, "Metallothionein and hsp70 expression in HepG2 cells after prolonged cadmium exposure," *Toxicology in Vitro*, vol. 21, no. 2, pp. 314–319, 2007.

[22] T. Fatur, M. Tušek, I. Falnoga, J. Ščančar, T. T. Lah, and M. Filipič, "DNA damage and metallothionein synthesis in human hepatoma cells (HepG2) exposed to cadmium," *Food and Chemical Toxicology*, vol. 40, no. 8, pp. 1069–1076, 2002.

[23] A. O. Lawal and E. Ellis, "Differential sensitivity and responsiveness of three human cell lines HepG2, 1321N1 and HEK 293 to cadmium," *Journal of Toxicological Sciences*, vol. 35, no. 4, pp. 465–478, 2010.

[24] G. Jiang, W. Duan, L. Xu, S. Song, C. Zhu, and L. Wu, "Biphasic effect of cadmium on cell proliferation in human embryo lung fibroblast cells and its molecular mechanism," *Toxicology in Vitro*, vol. 23, no. 6, pp. 973–978, 2009.

[25] M. Mantha and C. Jumarie, "Cadmium-induced hormetic effect in differentiated caco-2 cells: ERK and p38 activation without cell proliferation stimulation," *Journal of Cellular Physiology*, vol. 224, no. 1, pp. 250–261, 2010.

[26] S. L. Harris and A. J. Levine, "The p53 pathway: positive and negative feedback loops," *Oncogene*, vol. 24, no. 17, pp. 2899–2908, 2005.

[27] T. Inoue, L. Wu, J. Stuart, and C. G. Maki, "Control of p53 nuclear accumulation in stressed cells," *FEBS Letters*, vol. 579, no. 22, pp. 4978–4984, 2005.

[28] K. Boehme, Y. Dietz, P. Hewitt, and S. O. Mueller, "Activation of P53 in HepG2 cells as surrogate to detect mutagens and promutagens in vitro," *Toxicology Letters*, vol. 198, no. 2, pp. 272–281, 2010.

[29] M. Fabbri, C. Urani, M. G. Sacco, C. Procaccianti, and L. Gribaldo, "Whole genome analysis and microRNAs regulation in HepG2 cells exposed to cadmium," *ALTEX*, vol. 29, no. 2, pp. 173–182, 2012.

[30] A. D. Saleh, J. E. Savage, L. Cao et al., "Cellular stress induced alterations in microrna let-7a and let-7b expression are dependent on p53," *PLoS ONE*, vol. 6, no. 10, Article ID e24429, 2011.

[31] N. Tsuchiya, M. Izumiya, H. Ogata-Kawata et al., "Tumor suppressor miR-22 determines p53-dependent cellular fate through post-transcriptional regulation of p21," *Cancer Research*, vol. 71, no. 13, pp. 4628–4639, 2011.

[32] S. Wu, S. Huang, J. Ding et al., "Multiple microRNAs modulate p21$^{Cip1/WAF1}$ expression by directly targeting its 3′ untranslated region," *Oncogene*, vol. 29, no. 15, pp. 2302–2308, 2010.

[33] Y. Jin, D. Chen, R. J. Cabay, A. Wang, D. L. Crowe, and X. Zhou, "Role of microRNA-138 as a potential tumor suppressor in head

and neck squamous cell carcinoma," *International Review of Cell and Molecular Biology*, vol. 303, pp. 357–385, 2013.

[34] H. Gu, X. Guo, L. Zou, H. Zhu, and J. Zhang, "Upregulation of microRNA-372 associates with tumor progression and prognosis in hepatocellular carcinoma," *Molecular and Cellular Biochemistry*, vol. 375, pp. 23–30, 2013.

[35] R. Shimoda, W. E. Achanzar, W. Qu et al., "Metallothionein is a potential negative regulator of apoptosis," *Toxicological Sciences*, vol. 73, no. 2, pp. 294–300, 2003.

[36] Y. Kondo, J. M. Rusnak, D. G. Hoyt, C. E. Settineri, B. R. Pitt, and J. S. Lazo, "Enhanced apoptosis in metallothionein null cells," *Molecular Pharmacology*, vol. 52, no. 2, pp. 195–201, 1997.

[37] L. Z. Fan and M. G. Cherian, "Potential role of p53 on metallothionein induction in human epithelial breast cancer cells," *British Journal of Cancer*, vol. 87, no. 9, pp. 1019–1026, 2002.

[38] C. Urani, P. Melchioretto, and L. Gribaldo, "Regulation of metallothioneins and ZnT-1 transporter expression in human hepatoma cells HepG2 exposed to zinc and cadmium," *Toxicology in Vitro*, vol. 24, no. 2, pp. 370–374, 2010.
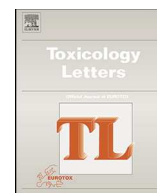
Changes in Caco-2 cells transcriptome profiles upon exposure to gold nanoparticles

CrossMark

Edyta Bajak [a,1], Marco Fabbri [a,b,1], Jessica Ponti [a], Sabrina Gioria [a], Isaac Ojea-Jiménez [a], Angelo Collotta [c], Valentina Mariani [a], Douglas Gilliland [a], François Rossi [a,*], Laura Gribaldo [d,**]

[a] European Commission, Joint Research Centre (JRC), Institute for Health and Consumer Protection (IHCP), Nanobiosciences (NBS) Unit, via E. Fermi 2749, 21027 Ispra (VA), Italy
[b] Department of Clinical and Experimental Medicine, University of Insubria, via J. Dunant, 5, 21100 Varese, Italy
[c] European Commission, JRC, IHCP, Molecular Biology and Genomics (MBG) Unit, via E. Fermi 2749, 21027 Ispra (VA), Italy
[d] European Commission, JRC, IHCP, Chemical Assessment and Testing (CAT) Unit, via E. Fermi 2749, 21027 Ispra (VA), Italy

HIGHLIGHTS

- Biological effects (toxicity, uptake and changes in gene expression patterns) on Caco-2 cells of citrate-stabilized 5 nm and 30 nm AuNPs were compared.
- Exposure to 5 nm AuNPs had much stronger effect on gene expression as compared to treatment with 30 nm AuNPs.
- Nrf2 signaling stress response was among the highly activated pathways.

ABSTRACT

Higher efficacy and safety of nano gold therapeutics require examination of cellular responses to gold nanoparticles (AuNPs). In this work we compared cellular uptake, cytotoxicity and RNA expression patterns induced in Caco-2 cells exposed to AuNP (5 and 30 nm). Cellular internalization was dose and time-dependent for both AuNPs. The toxicity was observed by colony forming efficiency (CFE) and not by Trypan blue assay, and exclusively for 5 nm AuNPs, starting at the concentration of $200\,\mu M$ (24 and 72 h of exposure). The most pronounced changes in gene expression (Agilent microarrays) were detected at 72 h ($300\,\mu M$) of exposure to AuNPs (5 nm). The biological processes affected by smaller AuNPs were: RNA/zinc ion/transition metal ion binding (decreased), cadmium/copper ion binding and glutathione metabolism (increased). Some Nrf2 responsive genes (several metallothioneins, HMOX, G6PD, OSGIN1 and GPX2) were highly up regulated. Members of the selenoproteins were also differentially expressed. Our findings indicate that exposure to high concentration of AuNPs (5 nm) induces metal exposure, oxidative stress signaling pathways, and might influence selenium homeostasis. Some of detected cellular responses might be explored as potential enhancers of anti-cancer properties of AuNPs based nanomedicines.

© 2015 The Authors. Published by Elsevier Ireland Ltd. This is an open access article under the CC BY license (http://creativecommons.org/licenses/by/4.0/).

1. Introduction

Nanotechnology and nanomedicine bring novel approaches into clinics, revolutionizing diagnosis and treatment options for diverse groups of patients. Engineered nanomaterials (ENMs) are also widely used in other consumer products and applications increasing the likelihood of human exposure to nanomaterials (Staggers et al., 2008). The exposure to ENMs can take place not only during their synthesis, production and usage, but also at other stages of the life cycle (e.g., waste deposition/combustion, material

* Corresponding author. Fax: +39 0332 78 5787.
** Corresponding author. Fax: +39 0332 78 5707.
E-mail addresses: edyta.bajak@ec.europa.eu (E. Bajak),
marco.fabbri@uninsubria.it (M. Fabbri), jessica.ponti@ec.europa.eu (J. Ponti),
sabrina.gioria@ec.europa.eu (S. Gioria), isaac.ojea-jimenez@ec.europa.eu
(I. Ojea-Jiménez), angelo.collotta@ec.europa.eu (A. Collotta),
valentina.mariani@gmail.com (V. Mariani), douglas.gillland@ec.europa.eu
(D. Gilliland), francois.rossi@jrc.ec.europa.eu (F. Rossi),
laura.gribaldo@ec.europa.eu (L. Gribaldo).
[1] Contributed equally to this work.

recycling) of a given nanomaterial. Therefore, in order to assure the safety of human population and environment, toxicological profiling of cellular responses to ENMs and proper risk assessment of nanomaterials should be performed (Maynard, 2012). The (nano) toxicological hazard identification and characterization are also required for improvement of the safety and efficacy of nanomedicines, including nano gold based formulations used in biomedical applications. Moreover, studies focused on the consequences of the long-term exposures to ENMs, including gold nanoparticles (AuNPs), are needed (Kunzmann et al., 2011).

Gold belongs to the group of noble metals and has been used in medical applications for centuries (Bhattacharya and Mukherjee, 2008). In recent years, nano gold based applications were designed and AuNPs synthesized with the idea that noble metal characteristics (in bulk) of gold would be preserved even when synthesized and used at nano scale, thus being bio-compatible (Connor et al., 2005). AuNPs and their derivatives undergo continuous development for their use in clinical diagnostics, as drug delivery systems or therapeutic agents (Dykman and Khlebtsov, 2012). In general, AuNPs are well tolerated in vivo (Hainfeld et al., 2006), although some toxicity of AuNPs was also reported in vitro (Pernodet et al., 2006; Chuang et al., 2013; Coradeghini et al., 2013; Mironova et al., 2014).

As methodologies develop, "omics" based research platforms can complement the classical tools for cytotoxicity testing in (nano) toxicology field. Therefore, identification and characterization of biological responses can be achieved at molecular levels compromising biomarkers/endpoints that can include whole or parts of transcriptome, proteome, metabolome, epigenome and/or genome of the in vitro/in vivo system under investigation (Hamadeh et al., 2002). Although toxicogenomics and other "omics" methods are currently easily accessible and cost effective, to date only a few studies applied transcriptomics or proteomics tools in the study of AuNPs induced/mediated cellular responses (Esther et al., 2005; Yang et al., 2010; Li et al., 2011; Qu et al., 2013; Gioria et al., 2014).

All living organisms respond to diverse stress stimuli. Depending on the biological context of given exposure/stressor, its severity and duration, cells within tissue/organ react to stimuli by evoking stress or adaptation responses, or die (Fulda et al., 2010; Chovatiya and Medzhitov, 2014). One of the key regulators of cellular responses to endogenous and/or exogenous stress is the nuclear factor E2-related factor 2 (Nrf2) protein. Nrf2 is a redox and xenobiotics sensitive transcriptional factor, assuring the expression of proteins involved in cellular adaptation to oxidative stress, adjustment of metabolism and detoxification of drugs (Kensler et al., 2007). Under normal cellular conditions, Nrf2 functions as a tumor suppressor. However, it has been shown that Nrf2 might also act as an oncogene (Shelton and Jaiswal, 2013). Among gene targets regulated by Nrf2 are metallothioneins (MTs), which are small, cysteine rich and metal ion binding proteins. MTs play an important role in the protection of cells against metal toxicity, but are also involved in responses to oxidative stress, and exposure to glucocorticoids and cytokines (Miles et al., 2000).

The aim of this study was to investigate how the colorectal adenocarcinoma epithelial cell line (Caco-2), an in vitro model of the intestinal route of exposure to nanoparticles, responds to AuNPs treatments at RNA gene expression level. We selected undifferentiated cells mainly because in this way we looked at populations of heterogenic pool of Caco-2 cells prior to differentiation, therefore having wider plasticity in the cellular physiology, sensing and adaptation/response to stress, as compared to mature and polarized enterocytes (Tadiali et al., 2002). Keeping this in mind, when running both the cytotoxicity and RNA transcript profiling experiments, we explored Caco-2 cells (in undifferentiated stage) as potentially more suitable model for detecting

alterations in gene expression patterns upon exposure to NPs. For that purpose, we tested citrate-stabilized spherical AuNPs of two sizes (5 nm and 30 nm, synthesized and characterized in-house) for their cytotoxic potential, internalization and induction of changes in mRNA and long non-coding RNAs expression patterns using transcriptomics approach (Agilent microarrays platform). The microarray data were further validated with quantitative real-time reverse-transcriptase PCR (qPCR) for a set of mRNAs which were differentially expressed upon exposure of Caco-2 cells to AuNPs. Several biological pathways affected by treatment of Caco-2 cells with AuNPs (5 nm, 300 μM, 72 h) were identified in microarray datasets using bioinformatical tools. The novelty of this work is the integration of classical in vitro testing with the chemico-physical characterization of NPs, Omics and advanced analytical techniques to better understand the mechanisms of potential nanomaterials' toxicity. Their use has the potential to provide a description of the bio-responses and allows highlighting critical biochemical pathways affected by nanoparticle exposure. Huge progresses have been made in the genomic field and here we integrated this discipline to investigate in detail modifications caused by AuNPs exposure at gene level. The results of this work established a starting point in understanding and disseminating which cellular processes can be linked to the observed cytotoxic effect of 5 nm AuNPs on cancer Caco-2 cells.

2. Materials and methods

2.1. AuNPs synthesis and characterization

AuNPs of approximately 5 nm and 30 nm size in diameter were synthesized and concentrated as described in literature (Coradeghini et al., 2013; Turkevich et al., 1951). Detailed description of the chemicals used for AuNPs synthesis, description of the equipment used for particles size distribution and characterization, sample preparation, image acquisition and processing, can be found in Supplementary methods.

The stability of AuNPs dispersions was studied both using a centrifugal particle sedimentation (CPS) instrument and by zeta-potential measurements in representative media. Citrate-stabilized AuNPs (5 and 30 nm) were incubated at two different concentrations (100 and 300 μM) in three different media (milliQ-water, serum-free cell culture medium and complete cell culture medium). Measurements were made immediately after mixing AuNPs samples with the corresponding medium (time 0) and then again after 24 and 72 h incubation times at 37 °C.

AuNPs dispersions for cell exposure experiments were freshly prepared by diluting the AuNPs suspensions (after concentration step, as described in the Supplementary methods) in complete culture medium, and were added directly to Caco-2 cell cultures. The concentration step produced two solutions containing all the reagents used for the NPs synthesis and they were used as solvent controls for biological testing.

2.2. Cell culture

Human epithelial colorectal adenocarcinoma cells (Caco-2) are from the European collection of cell cultures (ECACC) and were purchased from Sigma (Catalogue number: 86010202; passage 45). Experimental cultures were prepared from deep-frozen stock vials and maintained in a sub-confluent state. They were grown in complete cell culture medium composed of high glucose (4.5 g/mL) Dulbecco's modified Eagle medium (DMEM), supplemented with 10% (v/v) fetal bovine serum (FBS), 4 mM L-glutamine and 1% (v/v) pen/strep (all from Invitrogen, Italy). Cultures were maintained in cell culture incubator (HERAEUS, Germany) under standard culture conditions (37 °C, 5% CO_2 and 95% humidity). Caco-2 cells used in

this work were screened for the presence of *Mycoplasma* with quantitative PCR (qPCR) using the Venor®GeM Prime kit and were *Mycoplasma* free.

2.3. Cytotoxicity assays

Cytotoxic effect of AuNPs in Caco-2 cells was studied by colony forming efficiency (CFE) and Trypan blue exclusion assays.

For the CFE, cells were seeded at the density of 200 cells per 60×15 mm dish (Corning, Italy) in 3 mL complete culture medium (three replicates) for each treatment. Twenty four hours after plating, the medium was changed and 3 mL of fresh medium containing the AuNPs was added to obtain the final AuNP concentrations of 10, 50, 100, 200 and 300 μM corresponding to 0.02, 9.85, 19.70, 39.40 and 59.10 μg/mL, respectively. After 24 and 72 h of exposure, the medium was replaced with fresh complete culture medium. On the 13th day from seeding, cells were fixed with 3.7% (v/v) formaldehyde solution (Sigma–Aldrich, Italy) in phosphate-buffered saline (PBS) without calcium, magnesium and sodium bicarbonate (Invitrogen, Italy) and stained with 10% (v/v) Giemsa GS-500 solution (Sigma–Aldrich) in ultra pure water. Solvent controls (cells exposed to two different solvents obtained after AuNPs of 5 nm and 30 nm filtration, as used for the highest concentration tested) and a positive control (1 mM) sodium meta chromate (Sigma–Aldrich) were included. Colonies were scored using a cell colony counter GelCount (Oxford Optronix Ltd., UK).

For Trypan blue exclusion assay, 2.5×10^5 and 0.9×10^5 cells were seeded for 24 h and 72 h exposures, respectively, in 6 well plates (Falcon, Italy) with 2 mL of complete cell culture medium. Twenty four hours after plating, cells were exposed to 50, 100 and 300 μM of 5 and 30 nm AuNPs, corresponding to 9.85, 19.70, and 59.10 μg/mL. At the end of the exposure time (24 or 72 h), cells were washed twice with PBS, detached with 0.5 mL of 0.05% trypsin sodium ethylene diamine tetraacetic acid (Trypsin-EDTA) from Invitrogen, and harvested with 1 mL of complete culture medium. Next, 30 μL of each sample was stained with 30 μL of Trypan Blue (Sigma–Aldrich) and cells were counted with the TC10 automated cell counter (Biorad, Italy) according to the supplier's protocol. Negative control, solvent control and positive control were also included in the test, as described for CFE assay.

In the CFE and Trypan blue assays, the results were normalized to the solvent control. For the CFE assay, they are expressed as CFE (%) ([average number of treatment colonies/average number of solvent control colonies] $\times$ 100). For the Trypan blue assay, they are expressed as viability (%) ([number of cells in treatment/number of cells in solvent control] $\times$ 100). One-way analysis of variance (ANOVA) with *post-hoc* test (Dunnett's multiple comparison test) for comparing groups of data against one control group was used. Data are reported as mean values $\pm$ SEM (standard error mean = standard deviation/$\sqrt{}$number of replicates). The data represents mean value of three independent biological replicas, where *p* values of less than 0.05 (*) and 0.001 (***) were considered statistically significant. Statistical calculations were carried out using GraphPad Prism Version 5.0 (GraphPad Software, USA).

2.4. Nanoparticle internalization

The uptake of AuNPs, their association with cellular membrane/matrix and internalization were quantified by Inductively Coupled Plasma Mass Spectrometry (ICP-MS). The uptake of AuNPs, association of AuNPs with cellular membrane/matrix and the internalization of AuNPs was quantified by ICP-MS. For the ICP-MS, 7×10^5 and 3×10^5 CaCo-2 cells were seeded in dishes from Corning (100 mm $\times$ 15 mm) for 24 and 72 h exposure time respectively, in 5 mL of complete culture medium. Twenty four hours after seeding, cells were treated for 24 and 72 h with 5 and 30 nm AuNPs

(100 and 300 μM). At the end of the exposure time, the medium was removed and collected for each sample, cells were washed twice with PBS and each wash collected in a separate tube. Cells were then detached with 1 mL of Trypsin-EDTA (Invitrogen, Italy) and harvested with 5 mL of complete culture medium. After this, cells suspension was centrifuged at $200 \times g$ for 5 min (4 °C), and the supernatant was transferred into a new tube. The cellular pellet was suspended in 1 mL of culture medium. An aliquot of each sample (20 μL) was taken for cell count with TC10 automated counter. The total content of Au in the cells (cellular pellet) as well as in all the fractions collected from each cell culture sample: (i) medium at the end of the treatment (24 and 72 h), (ii) supernatants from the two washes, (iii) cellular pellet, and (iv) the final supernatant (representing a third wash), were analyzed by ICP-MS after mineralization with Aqua Regia (HNO$_3$:HCl at 1:3 ratio) and microwave digestion (2 cycles at 950 W for 10 min) in a Discover-Explorer microwave instrument (CEM Corporation, USA). These extensive washing of cells and sample collection steps for Au content measurements were applied to remove weakly bound AuNPs and to assure that the total starting amount of Au given to the cells was recovered among different fractions (including both, strongly associated with and/or internalized by cells and not taken up by cells). Three independent experimental replicas were carried out and the results were expressed as pg Au/cell, % of the external exposure concentration and as a number of NPs/cell. Calculations were performed as described in Coradeghini et al. (2013).

2.5. Exposures to AuNPs and RNA extraction

For the gene expression experiments, 2.5×10^5 and 0.9×10^5 Caco-2 cells were seeded in 2 mL complete cell culture medium, in a 6 well/plate (Falcon, Italy), and incubated for 24 and 72 h with 5 nm or 30 nm AuNPs, at either 100 and 300 μM concentrations. At the end of the treatment, the exposure medium was removed and cells were washed twice with PBS, and harvested with 300 μL of RLT plus RNeasy lysis buffer (Qiagen, USA). Cell lysates were collected from wells and stored at -80 °C until the RNA extraction step was performed. The details of RNA isolation are available in Supplementary methods.

2.6. Microarray expression profiling

The microarray (Agilent Whole Human Genome Oligo Microarray: 4×44 k 60 mer slide format) experiments were designed to perform three biological replicates for each time point (24 and 72 h), AuNPs size (5 and 30 nm) and concentration (100 and 300 μM) with complete medium and solvent controls. All the cRNA synthesis/sample-labeling, hybridization, washing, and scanning steps were conducted following the manufacturer's specifications (Agilent Technologies Inc., USA). Procedures for microarrays based data generation are described in Supplementary methods.

2.7. Quantitative PCR validation of microarray data

A real-time quantitative PCR (qPCR) analysis has been done on the same RNA samples that were used for the microarray hybridization, with the aim to validate the microarray results. All reagents for the qPCR and equipment were from Applied Biosystems, USA. The details of qPCR validation process and data analysis using delta–delta Ct method (Livak and Schmittgen, 2001) are available in Supplementary methods.

2.8. Gene expression data analysis

Quality control and array normalization were performed in the *R* statistical environment using the Agi4x44PreProcess (v 1.18.0)

package, downloaded from the Bioconductor web site (Gentleman et al., 2004). The normalization and filtering steps were based on those described in the Agi4x44PreProcess reference manual. Briefly, Agi4x44PreProcess options were set to use the mean signal and the BG median signal as foreground and background signals, respectively. Data were normalized between arrays by the quantile method (Bolstad et al., 2003). In this approach, the distribution of intensities of different microarray chips are transformed to become equal so that intensities can be compared between each other. In order to detect expression changes among different treatment conditions, the moderated t test was applied. Moderated t statistics were generated by Limma Bioconductor package. Modulated genes were chosen as those with a fold change greater than 1.5 $\log_2$ fold change and a false discovery rate (Benjamini and Hochberg's method) corrected p-value smaller than 0.05 (Smyth, 2004). Microarray results have been submitted to NCBI's gene expression omnibus (GEO) repository and are available under accession number GSE55349.

2.9. Bioinformatics

Up regulated and down regulated genes were analyzed in the Kyoto Encyclopedia of Genes and Genomes (KEGG) database (http://www.genome.jp/kegg/) in order to identify genes with similar functions. Expression analysis systematic explorer (EASE) biological theme analysis was conducted online using DAVID bioinformatics resources server (http//david.abcc.ncifcrf.gov/). Phylogenetic tree creation (rVISTA), co-expression network visualization (FunCoup) and *in silico* miRNA binding sites prediction (DIANA-mirExTra) are described in Supplementary methods (Alexeyenko et al., 2011; Alexiou et al., 2010; Dubchak et al., 2013).
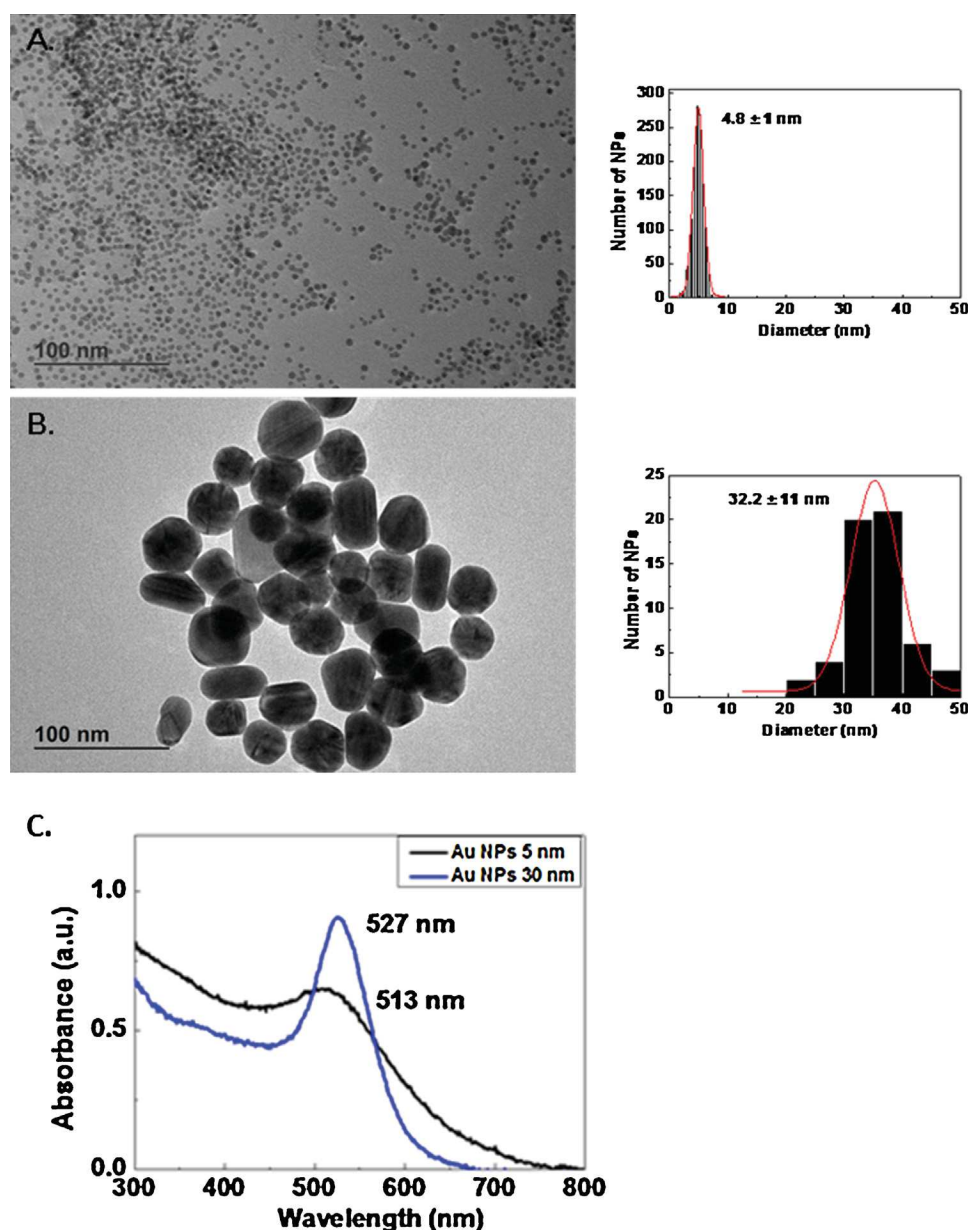
Fig. 1. Transmission electron microscopy (TEM) images and UV–vis absorption spectra of AuNPs. Morphology and size distributions of citrate-stabilized AuNPs of 5 nm (A) and 30 nm (B) in diameter. The histograms show size distributions of given AuNPs size, estimated with ImageJ software. UV–vis absorption spectra (C) of 5 nm AuNPs (black line) and 30 nm AuNPs (blue line). (For interpretation of the references to color in this figure legend, the reader is referred to the web version of this article.)

Table 1

Mean size distribution of AuNPs as measured by centrifugal sedimentation (CPS). Mean sizes of AuNPs samples (5 and 30 nm) incubated in water, Caco-2 cell culture medium without and with 10% (v/v) serum for 0, 24 and 72 h. Incubations took place in a cell culture incubator (in the dark). Abbreviations – HW: half width; PdI: polydispersity index; nd: not determined.

AuNPs	Au conc. (μM)	Mean size in water (nm) HW/PdI			Mean size in serum free cell medium (nm) HW/PdI			Mean size in cell medium with serum (nm) HW/PdI		
Sampling time		0 h	24 h	72 h	0 h	24 h	72 h	0 h	24 h	72 h
AuNPs 5 nm	100	3.9	4.1	4.5	41.0	52.2	47.3	5.5	4.5	4.4
		1.4/1.9	1.5/1.8	nd/1.8	21.5/1.2	26.0/1.2	23.7/1.2	nd/5.1	5.2/2.7	5.6/2.6
	300	3.9	4.0	4.5	51.1	53.8	50.5	4.9	5.5	5.5
		1.7/1.3	1.6/1.3	2.0/1.3	28.3/1.2	27.2/1.2	25.3/1.2	nd/2.6	5.2/1.6	4.9/1.9
AuNPs 30 nm	100	22.5	30.4	30.3	56.7	105.1	101.1	23.2	21.8	21.5
		6.4/1.3	6.7/1.1	6.4/1.1	26.2/1.3	64.4/1.4	57.8/7.0	6.6/1.4	6.4/1.3	6.3/1.3
	300	30.8	30.2	30.7	63.1	109.3	103.1	22.7	22.6	22.5
		6.0/1.1	6.3/1.1	5.9/1.1	41.6/1.4	73.7/1.5	81.4/1.6	7.0/1.3	5.9/1.2	5.8/1.4

3. Results

3.1. Characterization of AuNPs

Fig. 1A and B shows representative TEM images of the two nano gold samples used in this study. The morphologies observed were mainly spherical, although for 30 nm AuNPs it could also be observed a certain degree of faceting. Size distributions determined by TEM image analysis were narrow 4.8 ± 1.0 and 32.2 ± 11.0 nm, and the absorption band maximum measured by UV–vis spectrometry were in agreement with expected diameters of 5 nm and 30 nm AuNPs (Fig. 1C). It has been shown that the position of the surface plasmon resonance peak of Au NPs can be used to determine both size and concentration of gold nanoparticles (Haiss et al., 2007). Dynamic light scattering size measurements were also in agreement with the rest of characterization techniques (Suppl. Fig. 1) showing a mean size distribution, expressed as intensity (%), of 7.5 nm and 37.3 nm for 5 nm and 30 nm AuNPs, respectively.

Disc centrifuge sedimentation analysis using CPS technology was considered as an appropriate technique to monitor and measure the size distributions of AuNPs suspension samples in water, culture medium without serum and in complete cell culture medium, supplemented with 10% of serum (Table 1). The particles size distributions in water when measured by CPS are in agreement with those determined by TEM image analysis. As expected, in the absence of serum in cell medium, AuNPs aggregated, showing increase in AuNPs diameters. Aggregation was more noticeable at higher concentrations and for longer incubation times. However, in complete cell medium supplemented with serum proteins, no aggregation was observed and the NPs size was slightly larger to the one obtained in water due to the formation of a protein corona.

Zeta-potential measurements (Suppl. Fig. 2) were also performed in order to determine the evolution of the AuNP surface charge after incubation in cell culture media (with or without serum) and in water. Zeta-potential of AuNPs showed initial values between −30 and −40 mV in water. After incubation with cell culture medium in the presence of serum proteins, for both sizes (5 and 30 nm) and concentrations (100 and 300 μM) of AuNPs, a sudden change of the negative value of zeta-potential already occurring after mixing (time 0), is observed. At longer incubation times, zeta-potential values evolved toward the average charge of serum proteins (zeta-potential about −13.5 mV in our experimental system), which is indicative of the absorption of proteins at the surface of the NPs.

Finally, the concentration of ions released from the AuNPs suspensions, when measured by ICP-MS for up to 72 h in complete culture medium, was for both sizes of AuNPs below the detection limit of the technique (<1 ppb).

3.2. Cytotoxicity

Nano gold cytotoxicity in Caco-2 cells was evaluated using two methods: CFE assay and Trypan blue exclusion assay. The CFE is a standard test, already optimized for studying the toxicity of NPs (Ponti et al., 2010) and which is undergoing an inter-laboratory comparison of performance and reproducibility testing in the frame of the OECD working party of manufactured nanomaterials (work in progress). Cells were exposed to 5 and 30 nm AuNPs for 24 and 72 h, at concentrations ranging from 10 to 300 μM, as described in Supplementary methods.

Statistically significant cytotoxicity was observed only for 5 nm AuNPs when tested by CFE (Fig. 2A and B). Under the same exposure conditions, small decrease in cell viability at 100 and 300 μM was detected by Trypan blue assay. Although the observed drop in the membrane integrity was statistically not significant (Fig. 2C and D), its biological effects as a results of exposure of Caco-2 cells to 5 nm AuNPs, in particular to the highest concentration tested (300 μM), were evident when looking at detected changes in gene expression patterns. Interestingly, the cytotoxicity end-points based on changes in the membrane permeability detected by Trypan blue assay or efficiency in colony formation observed in CFE, were not statistically significant in Caco-2 cells exposed to 30 nm AuNPs, even for the highest concentration (300 μM) and at the longest (72 h) exposure time tested (Fig. 2). No significant difference in the number of colonies scored in the negative controls was observed in comparison to the solvent controls. As expected, for both *in vitro* cytotoxicity assays, treatment of Caco-2 cells with 1 mM sodium meta chromate (positive control) resulted in complete cell death (data not shown).

3.3. Nanoparticles internalization

The interaction of 5 and 30 nm AuNPs with Caco-2 cells was studied and quantified by ICP-MS after exposure to 100 and 300 μM nano gold suspensions (Fig. 3).

Internalization of gold in Caco-2 cells is expressed as pg/cell of Au, as % of Au *vs* total or number of NPs/cell. After 24 and 72 h of exposure at both 100 or 300 μM of Au 5 nm, cells incorporated approximately the same amount of Au; while we observed a dose-dependent increase of the Au 30 nm internalisation after both 24 and 72 h of exposure (Fig. 3A).

Interestingly, when the results are expressed as % of Au *vs* total exposure, for both AuNPs 5 and 30 nm a time-dependent increase in cell interaction and uptake was observed (Fig. 3B); and when expressing the data as a number of NPs in each cell the internalization of AuNPs 5 nm seems to be more efficient as compared to AuNPs 30 nm and no dose or time-dependent uptake manner was observed (Fig. 3C).
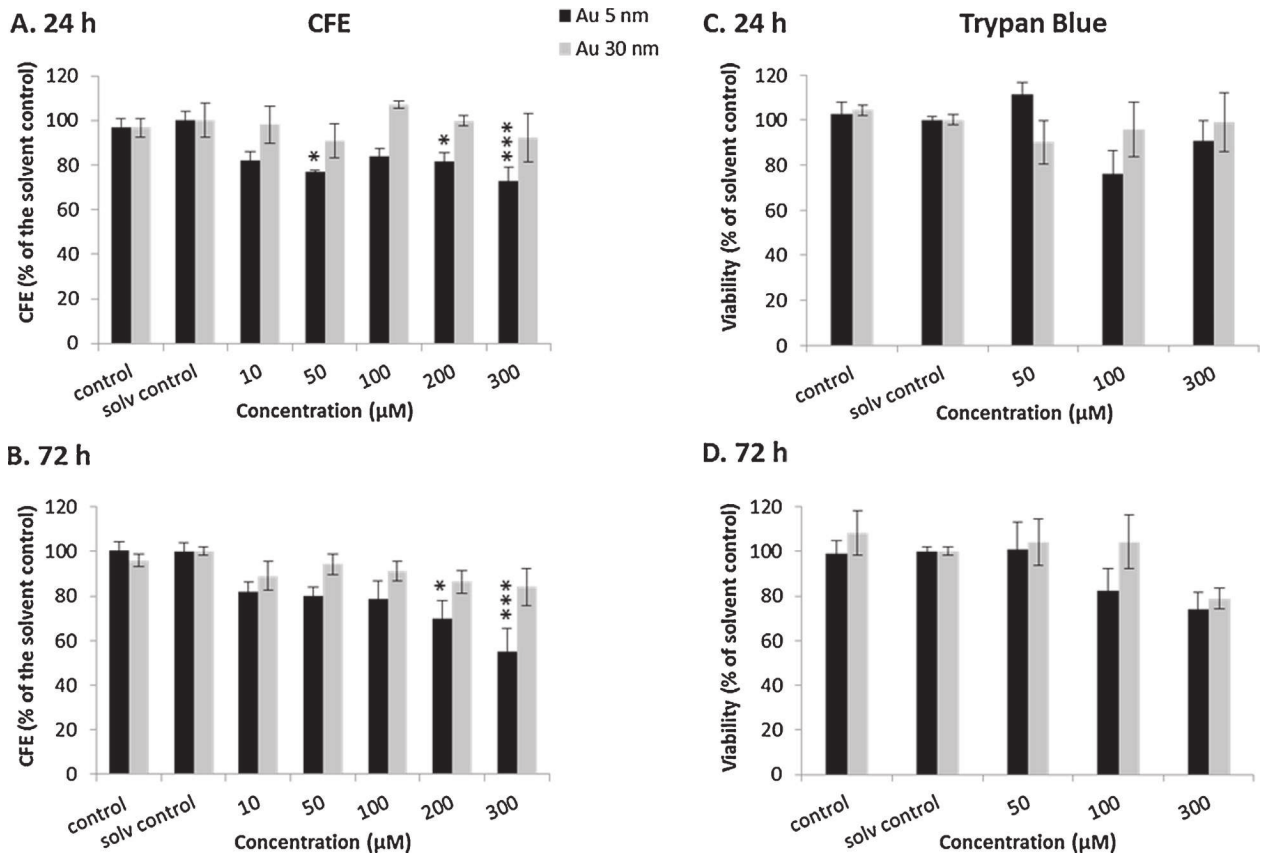
Fig. 2. Cytotoxic effects of 5 nm and 30 nm AuNPs on Caco-2 cells. The cytotoxicity of 5 nm AuNPs (black bars) and 30 nm AuNPs (gray bars) were estimated by colony forming efficiency (CFE) and Trypan blue exclusion assays. CFE assay: Caco-2 cells were exposed to increasing concentrations (10–300 μM) of AuNPs for 24 (A) and 72 h (B). In this range of concentrations and time points tested, no cytotoxicity was found in Caco-2 cells exposed to 30 nm AuNPs; while statistically significant cytotoxicity was observed for 5 nm AuNPs after 24 and 72 h of exposure to 200 μM ($*p < 0.05$) and 300 μM ($***p < 0.001$). Trypan blue exclusion assay: cell viability was tested on Caco-2 cells exposed for 24 (C) and 72 h (D) to increasing concentrations of 5 and 30 nm AuNPs (50–300 μM). Results of both assays represent a mean of three independent experiments (three replicates each) ± standard error of the mean (SEM) and are expressed in (A) and (B) as CFE (% of solvent control), while in (C) and (D) as viability (% of solvent control), respectively.

3.4. Gene expression profiling

As the major goal of our work was to get a better understanding of which molecular pathways might be affected by gold nanoparticles, we investigated the gene expression profiles of Caco-2 cells treated for 24 and 72 h with 5 and 30 nm nano gold, at two concentrations (100 and 300 μM), and compared them with the RNA transcripts levels of untreated cells (negative control).

First, a comparison of gene expression in cells treated with solvent (solvent control) vs the negative control was run and since almost no change was observed in the solvent control of

Caco-2 cells (data not shown), we used untreated cells as reference control for gene expression profiling experiments. Thereafter, an induction or repression greater than 1.5 $\log_2$ fold change (that corresponds to an increase/decrease of 50%) and with a false discovery rate (FDR) corrected p value smaller than 0.05, were used to compare control data sets vs different treatment conditions for AuNPs exposures.

At the lower concentration of AuNPs (100 μM), a minimal number of differentially expressed genes was found. There were no gene transcripts that were regulated by the 5 nm AuNPs neither at 24 nor at 72 h. However, there were four mRNAs induced in Caco-2
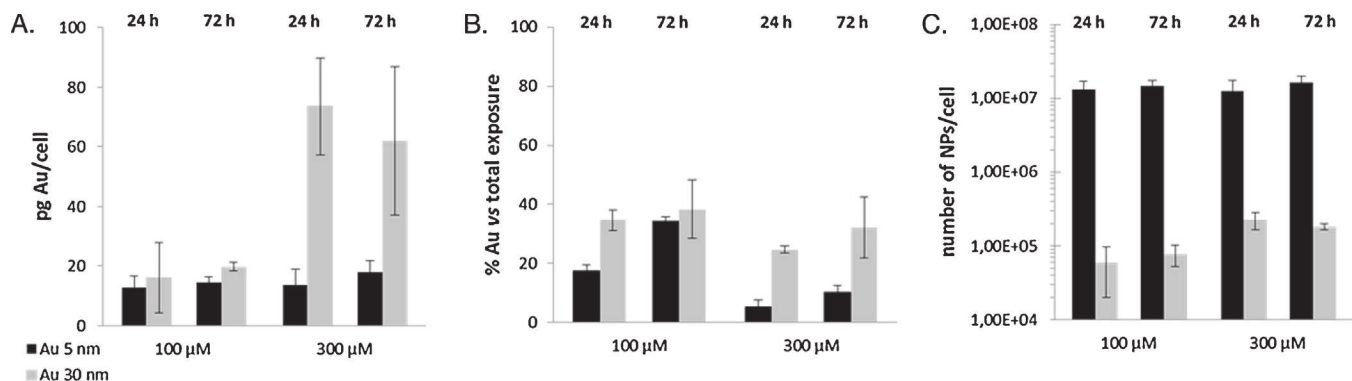
Fig. 3. Internalization of AuNPs by Caco-2 cells. The AuNPs cell interaction and uptake were measured by ICP-MS in Caco-2 cells incubated in the presence of 5 and 30 nm AuNPs (100 and 300 μM) for 24 and 72 h. Data are reported as pg Au/cell (A), % of Au in respect to the total Au exposure (B), and number of AuNPs/cell (C).

cells exposed to 30 nm nano gold (100 μM) after 24 h, and none of these genes was further affected after 72 h (Fig. 4A). Among these genes which mRNAs are increased, we find neurotensin receptor 2 (NTSR2) and two zinc finger containing transcriptional factors: human immunodeficiency virus type I enhancer binding protein 2 (HIVEP2) and zinc finger, DHHC-type containing 11 protein (ZDHHC11) involved in palmitoylation of proteins (Evers, 2006; Fukuda et al., 2002; Oku et al., 2013). Moreover, a gene locus LOC644662, which encodes yet uncharacterized novel long intergenic non-coding RNA (Zhang et al., 2011) was induced by 30 nm AuNPs (100 μM, 24 h).

At the highest AuNPs concentration tested (300 μM), a clear effect on gene expression can be observed, especially in 5 nm AuNPs treated Caco-2 cells. Here, at the earlier time point (24 h), we were able to detect 177 regulated genes (all down regulated). At the later time point (72 h) 811 transcripts were differentially expressed, with 103 up and 708 being down regulated. We observed a large fraction of genes which were down regulated already at 24 h (163), with their mRNAs levels being also decreased at 72 h (Fig. 4B).

Among the mRNAs highly up regulated upon exposure of Caco-2 cells to 5 nm AuNPs (300 μM, 72 h), were found the RNA transcripts of seven members of the methallothionein (MT) family genes, as well as genes of heme oxigenase (decycling) 1 (HMOX1), gastrointestinal glutathione peroxidase 2 (GPX2) and glucose-6-phosphate dehydrogenase (G6PD). Interestingly, already at 24 h time point of 5 nm AuNPs treatment (300 μM), the decrease of two selenoproteins' mRNAs (SELT and 15 kDa selenoprotein) was detected. A further decrease of SELT and 15 kDa selenoprotein expression levels, as well as mRNAs of two other selenoproteins (SELK and SEPP1) was observed at 72 h after exposure to 5 nm nano gold.

Under the same treatment conditions (300 μM) exposure of Caco-2 cells to larger AuNPs (30 nm) had no or very limited effects on gene expression patterns. For example, after 24 h we could not detect changes in RNA transcripts levels, and only four transcripts were detected as down regulated 72 h after treatment. The RNA transcripts of the following genes were altered in response to 30 nm AuNPs exposure: cadherin 16 (CDH16), carboxypeptidase A2 (CPA2), TSC22 domain family, member 3 protein (TSC22D3) and cysteine-rich PAK1 inhibitor (CRIPAK). The CDH16 gene product is a member of the cadherin family of cell adhesion, calcium dependent, membrane associated glycoproteins. Another mRNA induced by larger in size nano gold particle tested (30 nm), is a gene product of CPA2, which encodes a secreted protein involved in catabolic and digestion processes of other proteins (Vendrell et al., 2000). The third differentially expressed gene TSC22D3 encodes a leucine zipper transcription factor. Several studies showed that TSC22D3 gene, also known as GLIZ/DIP/TSC-22R, is induced by glucocorticoids (GCs), and plays a very important role as mediator in the anti-inflammatory and immunosuppressive action of GCs (Ayroldi and Riccardi, 2009). The fourth up regulated gene, CRIPAK is a novel endogenous inhibitor of p21-activated protein kinase 1 (Pak1). This kinase plays an important role in cytoskeleton organization, promotion of the cell survival responses and estrogen receptor (ER) mediated signaling (Talukder et al., 2006). Among these four genes, the mRNA of TSC22D gene was also down regulated in response to 5 nm AuNPs exposure (300 μM, 72 h). Thus, the other three genes (CDH16, CPA2, CIRPAK) showed decrease in their corresponding mRNAs levels only when the Caco-2 cells were treated with 30 nm nano gold particles.

3.5. Validation of microarray data with PCR

A subset of genes identified during microarray profiling was chosen for validation with real-time quantitative PCR (qPCR). The target selection of mRNAs (12 targets) for validation study was based on manual screening of differentially expressed genes, with
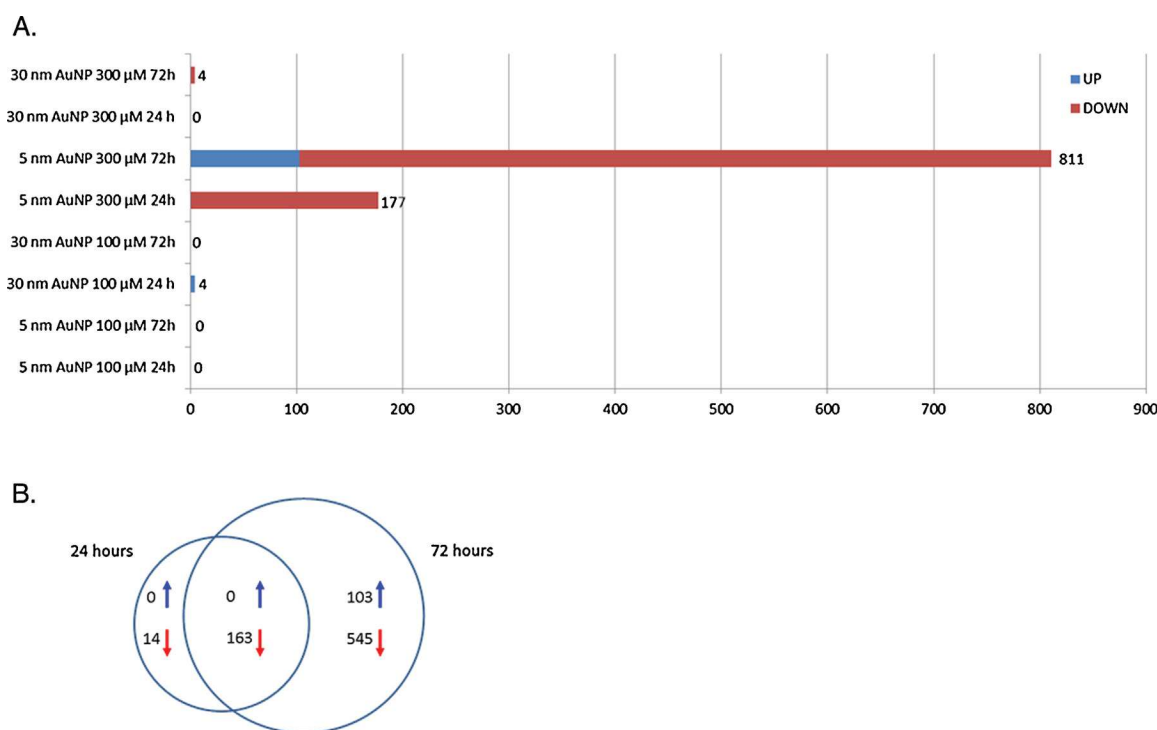
Fig. 4. Differentially expressed genes in Caco-2 cells exposed to 5 and 30 nm AuNPs. The bar graph (A) shows numbers of differentially expressed genes across RNA transcripts present on Agilent Whole Human Genome Oligo Microarray (4 × 44 k 60 mer slide format) and which were up and down regulated in Caco-2 cells as result of diverse exposure conditions to AuNPs. The Venn diagram (B) represents shared and time-specific numbers of genes regulated at 24 and 72 h after exposure to 5 nm AuNPs (300 μM).

Table 2

Validation of selected mRNAs with qPCR. Fold change expresses the difference of the mean log control and mean log stimulated data. Genes identified as regulated (log 2 fold greater than 1.5 and with false discovery rate (FDR) corrected p value smaller than 0.05) are coloured in red (down regulated) and blue (up regulated). The cells in the table are coloured in gray, when log 2 fold change is greater than 1.5 but the p value is not significant.

Gene symbol	QPCR				Microarray			
	5 nm AuNP 100 μM 24 h	5 nm AuNP 100 μM 72 h	5 nm AuNP 300 μM 24 h	5 nm AuNP 300 μM 72 h	5 nm AuNP 100 μM 24 h	5 nm AuNP 100 μM 72 h	5 nm AuNP 300 μM 24 h	5 nm AuNP 300 μM 72 h
ATF1	−0.21	−0.22	−0.86	−0.86	−0.28	−0.56	−0.87	−1.31
BIRC2	−0.54	−0.64	−1.06	−1.17	−0.32	−0.44	−0.98	−1.10
C1D	−0.43	−0.46	−1.09	−1.13	−0.46	−0.63	−0.95	−1.28
DNAJC21	−0.24	0.09	−0.43	−0.15	−0.18	−0.35	−0.22	−0.63
GPX2	−0.20	0.17	0.37	1.19	0.18	0.47	0.31	0.91
HAT1	−0.51	−0.64	−0.55	−0.55	−0.26	−0.49	−0.44	−0.76
HMOX1	0.00	0.36	0.36	1.82	0.16	0.39	0.29	1.42
MT2A	−1.32	0.30	0.48	3.95	0.15	1.94	0.30	3.55
OSGIN1	−0.07	−0.21	0.32	0.85	0.23	0.29	0.27	0.64
POLK	−0.17	−0.10	−0.82	−0.68	−0.48	−0.26	−0.67	−0.73
SRSF10	−0.17	−0.21	−0.66	−0.52	−0.26	−0.35	−0.61	−0.70
UBA2	−0.11	−0.02	−0.59	−0.40	−0.14	−0.18	−0.61	−0.52

an aim to select mRNAs covering diverse biological and biochemical functions which might be altered in Caco-2 cells when exposed to AuNPs.

Several members of genes involved in responses to oxidative stress, metal exposure and changes in cellular redox status were chosen for qPCR validation. To this group of validation targets belong mRNAs of the following genes: oxidative stress induced growth inhibitor 1 (OSGIN1), HMOX1, MT2A and GPX2 (Gozzelino et al., 2010; Li et al., 2006; Vašák and Meloni, 2011; Wingler et al., 1999). As the data from the CFE assay indicated cytotoxic effect of 5 nm AuNPs (300 μM, 72 h), we included for qPCR validation two genes encoding regulators of apoptosis: the inhibitor of apoptosis baculoviral IAP repeat containing 2 (BIRC2) and the apoptosis-inducing, DNA binding C1D protein (Dubrez-Daloz et al., 2008; Rothbarth et al., 1999).

We also included gene transcripts of activating transcription factor 1 (ATF1) and genes involved in post-translational protein modifications: histone acetyltransferase 1 (HAT1) and ubiquitin-like modifier SUMO-activating enzyme subunit 2 (UBA2) which is necessary for the sumoylation of proteins (Hay, 2005; Meyer and Habener, 1993; Parthun, 2007). Moreover, the set of mRNAs for validation contains genes encoding DnaJ (Hsp40) homolog, subfamily C, member 21 (DNAJC21), a chaperone which is important for protein translation, folding/unfolding, translocation, and degradation (Qiu et al., 2006); polymerase (DNA directed) kappa (POLK), with a unique DNA-damage bypass and fidelity characteristics (Zhang et al., 2000) and serine/arginine-rich splicing factor 10 (SRSF10) involved in regulation of constitutive and alternative splicing (Shin et al., 2005).

When selecting mRNAs for validation, we also took into consideration the trends in gene expression (up regulation and down regulation) observed in microarray assays, therefore genes

which were up (4) and down (8) regulated were included in the qPCR validation test (Table 2). As internal reference genes (RGs), the mRNA transcripts of the c-abl oncogene 1 (ABL1), a non-receptor tyrosine kinase and a mitochondrial ribosomal protein L19 (MRPL19) were used. Under given experimental conditions, these RGs showed to be not affected by exposures of Caco-2 cells to neither size/concentration/exposure time of studied AuNPs (data not shown).

Generally, as shown in Table 2, gene expression levels and trends of regulation (increase/decrease) detected with microarrays vs detection and quantification based on qPCR are in agreement with each other. However, expression levels of mRNAs of HAT1 and SRSF10 were lower when detecting them with qPCR, indicating that for these RNA transcripts, the microarray data (300 μM, 72 h) over estimated the levels of their down regulation. On the contrary, for gene BIRC2, HAT1 and MT2A, the qPCR was more sensitive in detecting the alterations of these particular mRNA expression levels (100 μM, 24 and 72 h), where microarrays data was not indicating their decreased RNA transcripts abundances (Table 2).

3.6. Bioinformatics

After validation of transcriptomics data with qPCR, we proceeded with a search for significantly enriched gene classes among differentially expressed genes, as defined by both gene ontology (GO) annotation and KEGG. This was applied to data sets obtained from microarray profiling experiments of Caco-2 cells treated with 5 nm AuNPs (300 μM) and harvested at 24 and 72 h after exposure.

The genes that were down regulated at 24 h time point, show an enrichment of categories related to transcription co-repressor/co-factors activities and transcription factor binding, binding of

Table 3

GO and KEGG enrichment of altered genes (down regulated) by 5 nm AuNPs treatment (300 mM, 24 h). The p value refers to how significant an association of a particular term has with the gene list. Where there are more than 10 genes regulated by AuNPs treatment, then only ten most regulated ones are displayed.

Term	Count	P value	Genes
GO:0003714 – transcription corepressor activity	6	0.0035	HSBP1, TBL1XR1, SP100, TAF9B, TFEC, C1D
GO:0008134 – transcription factor binding	10	0.0097	HSBP1, RAB18, TBL1XR1, NPM1, UBA2, SP100, TAF9B, TFEC, TADA1, C1D
GO:0003712 – transcription cofactor activity	8	0.0137	HSBP1, TBL1XR1, NPM1, SP100, TAF9B, TFEC, TADA1, C1D
GO:0000287 – magnesium ion binding	9	0.0139	IMPA1, SAR1B, RFK, POLK, HPRT1, MST4, MMGT1, ACVR1C, DUT
GO:0042802 – identical protein binding	11	0.0014	CLDN12 SP100, AK3, NPM1, ATL2, IMPA1, GCA, HPRT1, SNX6, MST4
GO:0032555 – purine ribonucleotide binding	21	0.0276	ATL2, UBE2W, HSPA13, RAB11A, ARL1, RAB18, ARL5B, RP2, MST4, RFK,
GO:0032553 – ribonucleotide binding	21	0.0276	ATL2, UBE2W, HSPA13, RAB11A, ARL1, RAB18, ARL5B, RP2, MST4, RFK,
GO:0017076 – purine nucleotide binding	21	0.0414	ATL2, UBE2W, HSPA13, RAB11A, ARL1, RAB18, ARL5B, RP2, MST4, RFK,
GO:0005525 – GTP binding	7	0.0464	SAR1B, RAB18, ARL5B, AK3, ARL1, ATL2, RAB11A
KEGG:hsa04120:ubiquitin mediated proteolysis	4	0.0537	UBE2N, BIRC2, UBA2, UBE2W

Table 4

GO and KEGG enrichment of altered genes (down regulated) by 5 nm AuNPs treatment (300 μM, 72 h). The p value refers to how significant an association of a particular term has with the gene list. Where there are more than 10 genes regulated by AuNPs treatment, then only ten most regulated ones are displayed.

Term	Count	P value	Genes
GO:0003723 – RNA binding	37	0.0002	ZCRB1, KIN, STAU2, SNRPB2, DCP2, SRSF3, TRUB1, C1D, EIF1AY, SRP9,
GO:0008270 – zinc ion binding	82	0.0048	RNF219, ZNF124, MOBKL3, PTS, ZFAND6, THAP1, BIRC2, RFK, ZFAND1, PLEKHF2,
GO:0046914 – transition metal ion binding	93	0.0133	RNF219, ZNF124, MOBKL3, PTS, ZFAND6, THAP1, BIRC2, RFK, ZFAND1, PLEKHF2
GO:0031072 – heat shock protein binding	7	0.0141	DNAJB9, DNAJC10, CDK1, DNAJB14, DNAJC19, GNG10, DNAJB6
GO:0004843 – ubiquitin-specific protease activity	4	0.0225	USP33, USP15, USP1, USP16
GO:0016565 – general transcriptional repressor activity	3	0.0224	SP100, HMGB2, CBX3
GO:0019783 – small conjugating protein-specific protease activity	4	0.0253	USP33, USP15, USP1, USP16
GO:0008353 – RNA polymerase II carboxy-terminal domain kinase activity	3	0.0394	MNAT1, CDK1, GTF2H2D
KEGG:hsa00563:glycosylphosphatidylinositol(GPI)-anchor biosynthesis	4	0.0189	PIGA, PIGF, PIGY, PIGK
KEGG:hsa03018:RNA degradation	5	0.0413	C1D, DCP2, CNOT7, LSM5, LSM6
KEGG: hsa00740:riboflavin metabolism	3	0.0510	MTMR6, ACP1, RFK

magnesium and purine (ribo) nucleotide, and ubiquitin mediated proteolysis (Table 3; Suppl. Table I). Examples of genes belonging to these categories include, e.g., HSB1, SP100, TAF9B, MMGT1, POLK, ATL2, RAB18, UBE2N and UBA2. In the group of genes down regulated 72 h after exposure to 5 nm AuNPs, enrichment in categories related to RNA and Zn ion/transition metal ion binding, heat shock protein binding, RNA degradation among others were found (Table 4; Suppl. Table II). These groups of GO/KEGG categories contain proteins encoded by, e.g., genes of STAU2, SRP9, RNF219, BIRC2, DNAJB9, DNAJC21, C1D, DCP2.

As shown in Table 5, the up regulated genes at 72 h after exposure of Caco-2 cells to 5 nm AuNPs (300 μM) turned out to be significantly enriched in GO biological process classes mainly related to ion (Cd and Cu) binding, amino acid/amine transmembrane transporter activity, peptide antigen binding (several MTs and SLC family members) and KEGG pathways, represented by GPX2 and G6PD, involved in the glutathione metabolism. The top highly induced transcripts with 3.55 log$_2$ fold change (increase in the mRNA levels of about 12 times) belong to genes encoding metallothioneins (MTs).

In humans, there are at least 18 genes encoding four distinct isoforms of MTs proteins: MT1, MT2, MT3 and MT4 (Laukens et al., 2009). The sequence homology grouping of MTs mRNAs is shown in Suppl. Fig. 3A. For the construction of phylogenetic trees, all members of the human MT gene family were plotted and analyzed against the mRNA of MT2A as a reference sequence. The MTs which mRNAs were induced in Caco-2 cells treated with 5 nm AuNPs (300 μM, 72 h) are in red, while the MTs which expression was not altered by exposure are in black. The exposure of Caco-2 cells to 5 nm AuNPs (300 μM, 72 h) resulted in up regulation of seven MTs mRNAs belonging to MT1 and MT2 groups only. Actually, there are 6 mRNAs of MTs (MT2A, MT1l, MT1E, MT1B, MT1X and MT1H) among 10 top up regulated genes (Suppl. Fig. 3B), with the most highly up regulated gene being the MT2A. Noteworthy, the increased mRNA level of MT2A gene detected in the microarray assay was confirmed with qPCR (Table 2).

When we analysed functions of genes which were among the highly down regulated (Suppl. Fig. 3C), the gene encoding selenoprotein T (SELT) was noticed once more. The SELT attracted our attention because another selenoprotein, namely GPX2 was highly up regulated (Tables 2 and 5) under the same exposure conditions (5 nm AuNP, 300 μM, 72 h).

The data analysis for information on mRNA co-expression and protein-protein interaction of highly up-regulated genes (MT2A, GPX2 and G6PD) and their connections with oxidative stress pathway [Hs_Oxidative_Stress_WP408_38774] revealed that MT2A is connected with 1 gene, while G6PD is connected with 5 genes belong to this biological network (Suppl. Fig. 4A). Notably, the MT1X gene, connected with MT2A, is also up regulated by 5 nm AuNPs (300 μM, 72 h). When looking at interactomes of most significantly up regulated and down regulated genes, the following was found: (i) in the set of genes which were up regulated, grouping of MTs genes with their mRNA and protein co-regulation was observed (Suppl. Fig. 4B); (ii) the density of mRNA/protein co-expression networks of up regulated genes was not as dense as for genes which were significantly down regulated (Suppl. Fig. 4C) and showed strong connections between each other.

The observation of a high number of down regulated RNA transcripts in Caco-2 cells exposed to 5 nm AuNPs, in particular at 72 h time point (300 μM), raised a question: at which level the repression of genes might have occurred? With the microarrays data in hand and with the freely available DIANA mirExTra tool for predicting potential microRNAs (miRNAs) binding targets sequences in differentially expressed mRNAs, we decided to run an in silico experiment. In this way, we were able to probe 25 most significantly down regulated genes, in parallel with 50 not affected by AuNPs (control genes), for analyzing ad hoc potential epigenetic regulators of gene expression, at miRNA-mRNA interface levels (Flynt and Lai, 2008). The results of the prediction test are presented in Suppl. Table III and in Fig. 5.

We found that, the following miRNAs: miR 340, miR 181a, miR 410 and miR 520 d 5p (Fig. 5A), are being frequently identified by

Table 5

The p value refers to how significant an association of a particular term has with the gene list.

Term	Count	P value	Genes
GO:0046870 – cadmium ion binding	4	0.0000026	MT1L, MT1A, MT1B, MT1F
GO:0005507 – copper ion binding	4	0.0009	MT1L, MT1A, MT1B, MT1F
GO:0015171 – amino acid transmembrane transporter activity	3	0.0117	SLC6A6, SLC7A5, SLC43A2
GO:0005275 – amine transmembrane transporter activity	3	0.0182	SLC6A6, SLC7A5, SLC43A2
GO:0042605 – peptide antigen binding	2	0.0341	SLC7A5, CLEC4M
KEGG:Hsa00480:glutathione metabolism	2	0.0999	GPX2, G6PD
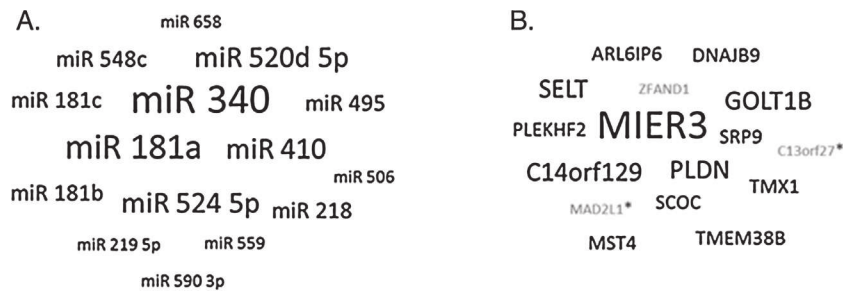
Fig. 5. Predicted miRs with the corresponding target genes that were decreased upon exposure of Caco-2 cells to 5 nm AuNPs (300 μM, 72 h). Group of miRs having 5–9 predicted target mRNAs (A). Set of genes with the highest number of predicted miRs binding sites in their mRNAs sequences (B). In gray are indicated mRNAs with no miRs binding site prediction. Asterics (*) denotes the most down regulated genes. Both word clouds were generated using the data presented in Suppl. Table 3.

the DIANA mirExTra algorithm and might represent potential mediators of down regulation of several mRNAs in the analyzed data set (Fig. 5B). Interestingly, the most down regulated genes (ZCCHC10, MAD2L1, C13orf27, CNPK, COMMD8) were not among the best targets for miRNAs mediated post-transcriptional gene regulation in the given experimental data set prediction context (Suppl. Table III, Fig. 5B). On the contrary, gene encoding selenoprotein SELT has 12 predicted binding sites for miRNAs, in the same number range for predicted miRNA binding sites (10–17), as the other down regulated genes have (PLDN, TMEM38B, ARL6IP6, C14orf129 and GOLT1B). The gene that has the highest number of predicted miRNAs binding sites (27), encodes mesoderm induction early response 1, family member 3 protein (MIER3).

4. Discussion

Several factors are involved in determining cytotoxicity of engineered nanomaterials (ENMs). Our work focused mainly on comparing cytotoxic potentials, in the context of inhibitory effect on colony forming efficiency (CFE) with changes in gene expression patterns (transcriptomics) induced in Caco-2 cells exposed to 5 nm and 30 nm citrate-stabilized AuNPs. Chemico-physical characterization tests of AuNPs used in this study confirmed that AuNPs were of expected size/shape and behaved in the experimental media as previously reported by Coradeghini et al. (2013).

In this work we selected undifferentiated Caco-2 cells an *in vitro* model of the intestinal route of exposure to nanoparticles. When Caco-2 cells are cultured over confluence for 21 days, these cells undergo spontaneous cell cycle arrest and differentiation. In his process, the enterocyte-like monolayer is formed serving as a model of the intestinal barrier (Sambuy et al., 2005; Natoli et al., 2012). Due to the intrinsic heterogeneity of the original parental cell line and culture-related conditions upon differentiation the expression of morphological and functional characteristics of mature enterocytes varies greatly between experiments and laboratories. Taking this into consideration, we have chosen to use in our work undifferentiated Caco-2 cultures to study their biological responses to AuNPs exposure. In this way we looked at populations of heterogenic pool of Caco-2 cells prior to differentiation, therefore having wider plasticity in the cellular physiology, sensing and adaptation/response to stress, as compared to mature and polarized enterocytes (Tadiali et al., 2002). Keeping this in mind, when running both the cytotoxicity and RNA transcript profiling experiments, we explored Caco-2 cells (in undifferentiated stage) as potentially more suitable model for detecting alterations in gene expression patterns upon exposure to NPs. We have to stress, that in that particular case, undifferentiated Caco-2 cells might have shown culture growth condition specific routes and efficiency in uptake of NPs. This in turn may contributed

in part to alternative cellular responses to stress and gene expression patterns, as compared with possibly different responses of classical model of mature enterocyte-like Caco-2 monolayer cells (Tremblay et al., 2006; Natoli et al., 2011).

When exposed to AuNPs, Caco-2 cells efficiently uptake AuNPs at both incubation times tested (24 and 72 h). However, we did not detect further increase in cellular uptake at later time point (72 h), maybe due to reaching of a steady-state of the uptake. These findings are in line with data reported earlier, supporting the notion that extending the incubation times above 24 h might not be useful for enhancing cellular uptake of nanoparticles, as observed in primary HUVECs, C17.2 neural progenitor cells and rat PC12 cells (Soenen et al., 2012), but in contrast with results obtained with mouse Balb/3T3 cells (Coradeghini et al., 2013). In the later case, time dependent increase in uptake of AuNPs, even after 24 h exposure time, was observed. We have also observed that if we express the uptake in number of NPs/cell or % of AuNPs versus total exposure, at the same external dose of exposure, the 5 nm AuNPs cell internalisation is higher than 30 nm AuNPs. This result is probably due to the fact that cells are exposed to a number of small NPs that is approximately 100 times higher than bigger NPs. In addition, as previously observed for Balb/3T3 cells (Coradeghini et al., 2013) by TEM analysis, both 5 and 30 nm NPs are internalised by endocytic patway.

When testing cytotoxic effects of AuNPs at the cellular level, we observed inhibition of Caco-2 cell growth and decrease in colony forming efficiency, induced by smaller AuNPs (5 nm). We must admit that this cytotoxic effect was observed only at relatively high levels of exposure (200 μM and 300 μM), with the most evident inhibitory effect detected at concentration 300 μM at 72 h. At the molecular level, when measuring biomarkers related to AuNPs exposures by changes in RNA expression levels, broad range of responses which potentially mediate inhibition of cellular growth and other functions of Caco-2 cells in response to nano gold, were identified. These cellular processes affected by exposure to 5 nm AuNPs include, for the early time point examined (24 h), down regulation of genes involved in regulation of transcription (transcriptional factors), biogenesis of RNA and GTP binding among others. At the later time point studied (72 h), more dramatic changes in differentially expressed gene expression patterns evoked by 5 nm AuNPs were detected. Beside 708 down regulated genes, an increase in abundance of 103 RNA transcripts was also observed. Thus, our gene expression profiling experiments demonstrated that RNA/zinc ion/transition metal ion binding, heat shock protein binding, RNA degradation and splicing (decreased); cadmium/copper ion binding, amino acid/amine transmembrane transporter activity and glutathione metabolism (increased), were among the cellular response processes correlated with exposure of Caco-2 cells and were associated with cytotoxicity induced by smaller AuNPs (5 nm, 300 μM).

Interestingly, although the larger (30 nm) AuNPs had rather limited effect on Caco-2 cell mRNAs expression, these AuNPs were still able to induce expression of couple of genes already at 100 μM exposure level at 24 h time point (CDH16, CPA2, TSC22D3 and CRIPAK). Noteworthy, the CDH16 protein was shown to be exclusively expressed in the kidney (Thomson et al., 1995); however its mRNA transcript induction was evident when the Caco-2 cells, originating from the colon, were exposed to 30 nm AuNPs.

As mentioned earlier, treatment of cells with 5 nm AuNPs had very pronounced effect on increase in mRNAs levels of metallothioneins (MTs) genes belonging to the MT1 and MT2 isoforms only. Exposure to nano gold had no effect on the MT3 or MT4 mRNAs expression in Caco-2 cells (gastrointestinal origin) due to the fact that MT3 is usually expressed in neurons (Masters et al., 1994), while MT4 is exclusively found in stratified squamous epithelium (Quaife et al., 1994).

Differential expression of selenoproteins (GPX2↑ while SELT, SEPP1, SELK and 15 kDa selenoprotein↓), might be related to changes in levels of selenium. Selenoproteins belong to a group of proteins which play important role in, e.g., oxidative stress signaling and protection, redox homeostasis, thyroid hormone metabolism, protection of some forms of cancer among others (Papp et al., 2010). It has been shown that the mRNA stability of selenoproteins differs depending on the availability of selenium within the cell (Schomburg and Schweizer, 2009). Therefore, we have hypothesized that Caco-2 cells might have responded to high concentration of AuNPs as if they have faced selenium "deficiency". It is also possible that high concentration of gold within the cell or/and extra cellular milieu had an effect on selenium homeostasis or/and its availability for uptake by Caco-2 cells.

Lowered cellular selenium content can evoke Nrf2 and Wnt stress response signaling via disturbed redox state as demonstrated by Brigelius-Flohé and Kipp (2013). The changes we found in expression of genes belonging to Nrf2 mediated signaling cascades (metallothioneins, HMOX, OSGIN1, G6PD, GPX2 and other selenoproteins) are indeed well described targets of regulation by transcriptional factor Nrf2 (Kensler et al., 2007; Miles et al., 2000). Therefore, changes in expression of genes being under Nrf2 control and induced by small AuNPs (5 nm) might be the result of different triggers: metal exposure, oxidative stress, disturbed redox and selenium status, and/or combination of them. Noteworthy, it was recently observed that Nrf2 is activated in Caco-2 cells upon exposure to high concentrations of silver NPs (Aueviriyavit et al., 2014) supporting our reasoning that induction of mRNA levels of the genes mentioned above, involves Nrf2 mediated signaling events, at least to some extent.

The results presented here clearly indicate that the cancer cells used in this study were able to recognize the AuNPs not only as metal entities but also as potential "danger" signals and stress inducers. Although Caco-2 cells showed the capacity to activate Nrf2-mediated defense networks (Kensler et al., 2007), these responses were not sufficient in preventing toxic effect of 5 nm AuNPs that were observed in CFE assay. Consequently, stress resulting from cytotoxic level of smaller AuNPs had an effect on down regulation of genes important for RNA biogenesis (transcription, splicing) and post-translational modifications (ubiquitination, sumoylation) of proteins that are vital for protein stability, activity and turn-over (proteolysis), especially when the misfolding of proteins occurs, for example during oxidative stress. Therefore, Caco-2 cells exhibited slower growth and lower efficiency in forming colonies.

It is well known that gene expression can be regulated at chromatin level (histone code) and RNA level (transcription, splicing, post-transcriptional RNA modifications, RNA stability/turn over of RNA transcripts, cellular localization of RNA molecules,

their translation etc.). These processes quite often involve and are regulated by non-coding RNAs (ncRNAs), including small (20–22 nt long) non-coding microRNAs (Venkatesh et al., 2013; Ullah et al., 2014). For that reason, we tested in silico the microarrays expression data for the presence of miRNAs binding sites across highly down regulated mRNAs (300 μM, 72 h, 5 nm AuNP). Indeed, prediction analysis pointed out that some miRNAs (miR 340, miR 181a, miR 410, miR 520 d5p) could play to some extend a role in down regulating many of tested mRNA targets.

The explanation of the very weak response of Caco-2 cells at transcriptome level, upon exposure to larger AuNPs (30 nm), remains still unclear. When interpreting our results the following explanation(s) can be suggested. As already reported in literature, the cellular uptake of engineered nanoparticles depends on the size of nanoparticles (Wang et al., 2010; Labens et al., 2013; Li and Schneider, 2014). In our experimental settings, the number of AuNPs taken up by the cells is much higher in the case of smaller NPs (5 nm), and this by itself might represent more biologically significant "stimulus". Thereafter, combination of the frequency of cellular membrane association/engulfment, uptake and exocytosis of 5 nm AuNPs, may trigger much stronger effect on signaling events, as compared to 30 nm AuNPs that are present in lower number but at the same molar Au concentration (Bahrami et al., 2014; Oh and Park, 2014). Moreover, it is also possible that smaller AuNPs (5 nm), with higher surface area to volume ratio, resulting in higher reactivity toward biological molecules (Nel et al., 2009), are more "disruptive" to the homeostasis of exposed cells as compared to larger AuNPs (30 nm). The different expression profiles observed in Caco-2 cells exposed to the two different sizes of nano gold particles, gave an additional support to previously published findings demonstrating that isotropic AuNPs larger than 5 nm seem to be biologically inert (Li et al., 2014).

We must stress however, that although the larger AuNPs showed very limited activity at transcriptional level, the picture of cellular responses might be different when looking at different exposure time (e.g., earlier sampling time), end-points/markers (protein expression, post-translational modifications, cellular metabolism, intracellular trafficking/secretion of bio-molecules, etc.). Also, the fact that Caco-2 cells were exposed to much higher number of small AuNPs as compared to larger AuNPs, points out that some cytotoxic effects might be observed even for 30 nm AuNPs, if given to cells in adequately higher numbers.

Interestingly, Caco-2 cells actually responded to 30 nm AuNPs already at 24 h by up regulating four gene transcripts after being exposed to this AuNPs (100 μM). Notably, under the same exposure conditions, presence of 5 nm AuNPs in the cell culture medium and/or as adsorbed/internalized AuNPs by cells, did not affect gene expression patterns in Caco-2 cells. One possible explanation is that the mass transfer of larger AuNPs (30 nm) to the cellular surface and interaction with cellular membrane, as a result of more rapid gravitational settling/sedimentation (Wittmaack, 2011; Li and Schneider, 2014) which is higher as compared to smaller AuNPs, triggering diverse signaling events, at different time points and with possible different effects on gene expression as compared to these evoked by exposure to 5 nm AuNPs.

The observed cytotoxic properties of smaller AuNPs might be of practical use for enhancement of already existing AuNPs based thermal therapies, as well as in other cancer treatment regimes (Schütz et al., 2013). Nevertheless, we should not ignore the fact that changes in gene expression induced by 5 nm AuNPs exposure might lead to potentially hazardous effect for healthy cells and/or tissues that still need to be estimated and characterized despite the absence of acute toxicity effects. This is of great concern, especially for individuals who are undergoing long-term AuNPs-based treatment.

5. Conclusions

A combination of standard cytotoxicity methods, such as CFE and Trypan blue exclusion assays, with gene expression profiling (transcriptomics) allowed us to identify cellular signaling and stress response pathways that might be associated with the cytotoxicity observed upon exposure of Caco-2 cells to citrate-stabilized AuNPs (5 nm). However, it is critical to point out that changes in gene expression at mRNA level do not necessarily correlate with observed trends (up/down regulation) in the amount of corresponding protein (Walker and Hughes, 2008). Therefore, validation(s) of alterations in mRNA expression, observed in Caco-2 cells as response to AuNPs exposures, requires further work to estimate the changes in the corresponding expression of encoded protein(s), their activity, proper localization and/or secretion. The very same approach also applies for testing whatever the predicted involvement of miRNAs and/or other ncRNAs takes place and might contribute to cellular responses evoked by treatment of Caco-2 cells with AuNPs.

Nevertheless, data presented here provide a starting point in exploration of possible mechanisms related to cytotoxicity observed in cells exposed to AuNPs and can be applied for designing more efficient and safe nano gold nanomedicines.

Funding

Transparency document

The Transparency document associated with this article can be found in the online version.

Conflict of interest

The authors declare that there are no conflicts of interest.

Acknowledgements

Appendix A. Supplementary data

Supplementary data associated with this article can be found, in the online version, at http://dx.doi.org/10.1016/j.toxlet.2014.12.008.

References

Alexeyenko, A., Schmitt, T., Tjärnberg, A., Guala, D., Frings, O., Sonnhammer, E.L., 2011. Comparative interactomics with Funcoup 2.0. Nucleic Acids Res. 40, D821–D828. doi:http://dx.doi.org/10.1093/nar/gkr1062.

Alexiou, P., Maragkakis, M., Papadopoulos, G.L., Simmosis, V.A., Zhang, L., Hatzigeorgiou, A.G., 2010. The DIANA-mirExTra web server: from gene expression data to microRNA function. PLoS One 5, e9171. doi:http://dx.doi.org/10.1371/journal.pone.0009171.

Aueviriyavit, S., Phummiratch, D., Maniratanachote, R., 2014. Mechanistic study on the biological effects of silver and gold nanoparticles in Caco-2 cells induction of the Nrf2/HO-1 pathway by high concentrations of silver nanoparticles. Toxicol. Lett. 224, 73–83. doi:http://dx.doi.org/10.1016/j.toxlet.2013.09.020.

Ayroldi, E., Riccardi, C., 2009. Glucocorticoid-induced leucine zipper (GILZ): a new important mediator of glucocorticoid action. FASEB J. 23, 3649–3658. doi:http://dx.doi.org/10.1096/fj.09-134684.

Bahrami, A.H., Raatz, M., Agudo-Canalejo, J., Michel, R., Curtis, E.M., Hall, C.K., Gradzielski, M., Lipowsky, R., Weikl, T.R., 2014. Wrapping of nanoparticles by membranes. Adv. Colloid. Interface Sci. 208, 214–224. doi:http://dx.doi.org/10.1016/j.cis.2014.02.012.

Bhattacharya, R., Mukherjee, P., 2008. Biological properties of naked metal nanoparticles. Adv. Drug Deliv. Rev. 60, 1289–1306. doi:http://dx.doi.org/10.1016/j.addr.2008.03.013.

Bolstad, B.M., Irizarry, R.A., Astrand, M., Speed, T.P., 2003. A comparison of normalization methods for high density oligonucleotide array data based on variance and bias. Bioinformatics 19, 185–193. doi:http://dx.doi.org/10.1093/bioinformatics/19.2.185.

Brigelius-Flohé, R., Kipp, A.P., 2013. Selenium in the redox regulation of the Nrf2 and the Wnt pathway. Methods Enzymol. 527, 65–86. doi:http://dx.doi.org/10.1016/B978-0-12-405882-8.00004-0.

Chovatiya, R., Medzhitov, R., 2014. Stress, inflammation, and defense of homeostasis. Mol. Cell. 54, 281–288. doi:http://dx.doi.org/10.1016/j.molcel.2014.03.030.

Chuang, S.M., Lee, Y.H., Liang, R.Y., Roam, G.D., Zeng, Z.M., Tu, H.F., Wang, S.K., Chueh, P.J., 2013. Extensive evaluations of the cytotoxic effects of gold nanoparticles. Biochim. Biophys. Acta 496, 4960–4973. doi:http://dx.doi.org/10.1016/j.bbagen.2013.06.025.

Connor, E.E., Mwamuka, J., Gole, A., Murphy, C.J., Wyatt, M.D., 2005. Gold nanoparticles are taken up by human cells but do not cause acute cytotoxicity. Small 1, 325–327. doi:http://dx.doi.org/10.1002/smll.200400093.

Coradeghini, R., Gioria, S., García, C.P., Nativo, P., Franchini, F., Gilliland, D., Ponti, J., Rossi, F., 2013. Size-dependent toxicity and cell interaction mechanisms of gold nanoparticles on mouse fibroblasts. Toxicol. Lett. 217, 205–216. doi:http://dx.doi.org/10.1016/j.toxlet.2012.11.022.

Dubchak, I., Munoz, M., Poliakov, A., Salomonis, N., Minovitsky, S., Bodmer, R., Zambon, A.C., 2013. Whole-Genome rVISTA: a tool to determine enrichment of transcription factor binding sites in gene promoters from transcriptomic data. Bioinformatics 129, 2059–2061. doi:http://dx.doi.org/10.1093/bioinformatics/btt318.

Dubrez-Daloz, L., Dupoux, A., Cartier, J., 2008. IAPs: more than just inhibitors of apoptosis proteins. Cell Cycle 7, 1036–1046. doi:http://dx.doi.org/10.4161/cc.7.8.5783.

Dykman, L., Khlebtsov, N., 2012. Gold nanoparticles in biomedical applications: recent advances and perspectives. Chem. Soc. Rev. 41, 2256–2282. doi:http://dx.doi.org/10.1039/c1cs15166e.

Esther, R.J., Bhattacharya, R., Ruan, M., Bolander, M.E., Mukhopadhyay, M.E., Sarkar, D., Mukherjee, G., 2005. Gold nanoparticles do not affect the global transcriptional program of human umbilical vein endothelial cells: a DNA microarray analysis. J. Biomed. Nanotechnol. 3, 328–335.

Evers, B.M., 2006. Neurotensin and growth of normal and neoplastic tissues. Peptides 27, 2424–2433. doi:http://dx.doi.org/10.1016/j.peptides.2006.01.028.

Flynt, A.S., Lai, E.C., 2008. Biological principles of microRNA-mediated regulation: shared themes amid diversity. Nat. Rev. Genet. 9, 831–842. doi:http://dx.doi.org/10.1038/nrg2455.

Fukuda, S., Yamasaki, Y., Iwaki, T., Kawasaki, H., Akieda, S., Fukuchi, N., Tahira, T., Hayashi, K., 2002. Characterization of the biological functions of a transcription factor, c-myc intron binding protein 1 (MIBP1). J. Biochem. 131, 349–357.

Fulda, S., Gorman, A.M., Hori, O., Samali, A., 2010. Cellular stress responses: cell survival and cell death. Int. J. Cell. Biol. 2010, 214074. doi:http://dx.doi.org/10.1155/2010/214074.

Gentleman, R.C., Carey, V.J., Bates, D.M., Bolstad, B., Dettling, M., Dudoit, S., Ellis, B., Gautier, L., Ge, Y., Gentry, J., et al., 2004. Bioconductor: open software development for computational biology and bioinformatics. Genome Biol. 5, R80. doi:http://dx.doi.org/10.1186/gb-2004-5-10r80.

Gioria, S., Chassaigne, H., Carpi, D., Parracino, A., Meschini, S., Barboro, P., Rossi, F., 2014. A proteomic approach to investigate AuNPs effects in Balb/3T3 cells. Toxicol. Lett. 228, 111–126. doi:http://dx.doi.org/10.1016/j.toxlet.2014.04.016.

Gozzelino, R., Jeney, V., Soares, M.P., 2010. Mechanisms of cell protection by heme oxygenase-1. Annu. Rev. Pharmacol. Toxicol. 50, 323–354. doi:http://dx.doi.org/10.1146/annurev.pharmtox.010909.105600.

Hainfeld, J.F., Slatkin, D.N., Focella, T.M., Smilowitz, H.M., 2006. Gold nanoparticles: a new X-ray contrast agent. Br. J. Radiol. 79, 248–253. doi:http://dx.doi.org/10.1259/bjr/13169882.

Haiss, W., Thanh, N.T.K., Aveyard, J., Fernig, D.G., 2007. Determination of size and concentration of gold nanoparticles from UV–vis spectra. Anal. Chem. 79, 4215–4221. doi:http://dx.doi.org/10.1021/ac0702084.

Hamadeh, H.K., Amin, R.P., Paules, R.S., Afshari, C.A., 2002. An overview of toxicogenomics. Curr. Issues Mol. Biol. 4, 45–56.

Hay, R.T., 2005. SUMO: a history of modification. Mol. Cell. 18, 1–12. doi:http://dx.doi.org/10.1016/j.molcel.2005.03.012.

Kensler, T.W., Wakabayashi, N., Biswal, S., 2007. Cell survival responses to environmental stresses via the Keap1-Nrf2-ARE pathway. Annu. Rev. Pharmacol. Toxicol. 47, 89–116. doi:http://dx.doi.org/10.1146/annurev.pharmtox.46.120604.141046.

Kunzmann, A., Andersson, B., Thurnherr, T., Krug, H., Scheynius, A., Fadeel, B., 2011. Toxicology of engineered nanomaterials: focus on biocompatibility,

biodistribution and biodegradation. Biochim. Biophys. Acta 1810, 361–373. doi: http://dx.doi.org/10.1016/j.bbagen.2010.04.007.

Labens, R., Lascelles, B.D., Charlton, A.N., Ferrero, N.R., Van Wettere, A.J., Xia, X.R., Blikslager, A.T., 2013. Ex vivo effect of gold nanoparticles on porcine synovial membrane. Tissue Barriers 1, e24314. doi:http://dx.doi.org/10.4161/tisb.24314.

Laukens, D., Waeytens, A., De Bleser, P., Cuvelier, C., De Vos, M., 2009. Human metallothionein expression under normal and pathological conditions: mechanisms of gene regulation based on in silico promoter analysis. Crit. Rev. Eukaryot. Gene Expression 19, 301–317. doi:http://dx.doi.org/10.1615/CritRevEukarGeneExpr.v19. i4.40.

Li, K., Schneider, M., 2014. Quantitative evaluation and visualization of size effect on cellular uptake of gold nanoparticles by multiphoton imaging-UV/vis spectroscopic analysis. J. Biomed. Opt. 19, 101505. doi:http://dx.doi.org/10.1117/1. JBO.19.10.101505.

Li, R., Chen, W., Yanes, R., Lee, S., Berliner, J.A., 2006. OKL38 is an oxidative stress response gene stimulated by oxidized phospholipids. J. Lipid Res. 48, 709–715. doi:http://dx.doi.org/10.1194/jlr.M600501-JLR200.

Li, J.J., Lo, S.L., Ng, C.T., Gurung, R.L., Hartono, D., Hande, M.P., Ong, C.N., Bay, B.H., Yung, L.Y., 2011. Genomic instability of gold nanoparticle treated human lung fibroblast cells. Biomaterials 32, 5515–5523. doi:http://dx.doi.org/10.1016/j. biomaterials.2011.04.023.

Li, N., Zhao, P., Astruc, D., 2014. Anisotropic gold nanoparticles: synthesis, properties, applications, and toxicity. Angew. Chem. Int. Ed. Engl. 53, 1756–1789. doi:http://dx.doi.org/10.1002/anie.201300441.

Livak, K.J., Schmittgen, T.D., 2001. Analysis of relative gene expression data using real-time quantitative PCR and the 2(-Delta Delta C(T)) method. Methods 25, 402–408. doi:http://dx.doi.org/10.1006/meth.2001.1262.

Masters, B.A., Quaife, C.J., Erickson, J.C., Kelly, E.J., Froelick, G.J., Zambrowicz, B.P., Brinster, R.L., Palmiter, R.D., 1994. Metallothionein III is expressed in neurons that sequester zinc in synaptic vesicles. J. Neurosci. 14, 5844–5857.

Maynard, R.L., 2012. Nano-technology and nano-toxicology. Emerg. Health Threats J. 5, 17508. doi:http://dx.doi.org/10.3402/ehtj.v5i0.17508.

Meyer, T.E., Habener, J.F., 1993. Cyclic adenosine 3′,5′-monophosphate response element binding protein (CREB) and related transcription-activating deoxyribonucleic acid-binding proteins. Endocr. Rev. 14, 269–290. doi:http://dx.doi.org/10.1210/edrv-14-3-269.

Miles, A.T., Hawksworth, G.M., Beattie, J.H., Rodilla, V., 2000. Induction regulation, degradation, and biological significance of mammalian metallothioneins. Crit. Rev. Biochem. Mol. Biol. 35, 35–70.

Mironava, T., Hadjiargyrou, M., Simon, M., Rafailovich, M.H., 2014. Gold nanoparticles cellular toxicity and recovery: adipose derived stromal cells. Nanotoxicology 8, 189–201. doi:http://dx.doi.org/10.3109/17435390.2013.769128.

Natoli, M., Leoni, B.D., D'Agnano, I., D'Onofrio, M., Brandi, R., Arisi, I., Zucco, F., Felsani, A., 2011. Cell growing density affects the structural and functional properties of Caco-2 differentiated monolayer. J. Cell Physiol. 226 (6), 1531–1543. doi:http://dx.doi.org/10.1002/jcp.22487.

Natoli, M., Leoni, B.D., D'Agnano, I., Zucco, F., Felsani, A., 2012. Good Caco-2 cell culture practices. Toxicol. In Vitro 26 (8), 1243–1246. doi:http://dx.doi.org/10.1016/j.tiv.2012.03.009.

Nel, A.E., Mädler, L., Velegol, D., Xia, T., Hoek, E.M., Somasundaran, P., Klaessig, F., Castranova, V., Thompson, M., 2009. Understanding biophysicochemical interactions at the nano-bio interface. Nat. Mater. 8, 543–557. doi:http://dx.doi.org/10.1038/nmat2442.

Oh, N., Park, J.-H., 2014. Endocytosis and exocytosis of nanoparticles in mammalian cells. Int. J. Nanomed. 9 (Suppl. 1), 51–63. doi:http://dx.doi.org/10.2147/IJN.S26592.

Oku, S., Takahashi, N., Fukata, Y., Fukata, M., 2013. In silico screening for palmitoyl substrates reveals a role for DHHC1/3/10 (zDHHC1/3/11)-mediated neurochondrin palmitoylation in its targeting to Rab5-positive endosomes. J. Biol. Chem. 288, 19816–19829. doi:http://dx.doi.org/10.1074/jbc.M112.431676.

Papp, L.V., Holmgren, A., Khanna, K.K., 2010. Selenium and selenoproteins in health and disease. Antioxid. Redox Signal. 12, 793–795. doi:http://dx.doi.org/10.1089/ars.2009.2973.

Parthun, M.R., 2007. Hat1: the emerging cellular roles of a type B histone acetyltransferase. Oncogene 26, 5319–5328. doi:http://dx.doi.org/10.1038/sj.onc.1210602.

Pernodet, N., Fang, X., Sun, Y., Bakhtina, A., Ramakrishnan, A., Sokolov, J., Ulman, A., Rafailovich, M., 2006. Adverse effects of citrate/gold nanoparticles on human dermal fibroblasts. Small 2, 766–773. doi:http://dx.doi.org/10.1002/smll.200500492.

Ponti, J., Colognato, R., Rauscher, H., Gioria, S., Broggi, F., Franchini, F., Pascual, C., Giudetti, G., Rossi, F., 2010. Colony forming efficiency and microscopy analysis of multi-wall carbon nanotubes cell interaction. Toxicol. Lett. 197, 29–37. doi:http://dx.doi.org/10.1016/j.toxlet.2010.04.018.

Qiu, X.B., Shao, Y.M., Miao, S., Wang, L., 2006. The diversity of the DnaJ/Hsp40 family, the crucial partners for Hsp70 chaperones. Cell. Mol. Life Sci. 63, 2560–2570. doi:http://dx.doi.org/10.1007/s00018-006-6192-6.

Qu, Y., Huang, Y., Lü, X., 2013. Proteomic analysis of molecular biocompatibility of gold nanoparticles to human dermal fibroblasts-fetal. J. Biomed. Nanotechnol. 9, 40–52. doi:http://dx.doi.org/10.1166/jbn.2013.1428.

Quaife, C.J., Findley, S.D., Erickson, J.C., Froelick, G.J., Kelly, E.J., Zambrowicz, B.P., Palmiter, R.D., 1994. Induction of a new metallothionein isoform (MT-IV) occurs during differentiation of stratified squamous epithelia. Biochemistry 33, 7250–7259. doi:http://dx.doi.org/10.1021/bi00189a029.

Rothbarth, K., Spiess, E., Juodka, B., Yavuzer, U., Nehls, P., Stammer, H., Werner, D., 1999. Induction of apoptosis by overexpression of the DNA-binding and DNA-PK-activating protein C1D. J. Cell Sci. 112, 2223–2232.

Sambuy, Y., De Angelis, I., Ranaldi, G., Scarino, M.L., Stammati, A., Zucco, F., 2005. The Caco-2 cell line as a model of the intestinal barrier: influence of cell and culture-related factors on Caco-2 cell functional characteristics? Altern. Lab. Anim. 33 (6), 603–618.

Schütz, C.A., Juillerat-Jeanneret, L., Mueller, H., Lynch, I., Riediker, M., 2013. Therapeutic nanoparticles in clinics and under clinical evaluation. Nanomedicine 8, 449–467. doi:http://dx.doi.org/10.2217/nnm.13.8.

Schomburg, L., Schweizer, U., 2009. Hierarchical regulation of selenoprotein expression and sex-specific effects of selenium. Biochim. Biophys. Acta 1790, 1453–1462. doi:http://dx.doi.org/10.1016/j.bbagen.2009.03.015.

Shelton, P., Jaiswal, A.K., 2013. The transcription factor NF-E2-related factor 2 (Nrf2): a protooncogene? FASEB J. 27, 414–423. doi:http://dx.doi.org/10.1096/fj.12-217257.

Shin, C., Kleiman, F.E., Manley, J.L., 2005. Multiple properties of the splicing repressor SRp38 distinguish it from typical SR proteins. Mol. Cell. Biol. 25, 8334–8343. doi:http://dx.doi.org/10.1128/MCB.25.18.8334-8343.2005.

Smyth, G.K., 2004. Linear models and empirical bayes methods for assessing differential expression in microarray experiments. Stat. Appl. Genet. Mol. Biol. 3, 1–25. doi:http://dx.doi.org/10.2202/1544-6115.1027 (Article 3).

Soenen, S.J., Manshian, B., Montenegro, J.M., Amin, F., Meermann, B., Thiron, T., Cornelissen, M., Vanhaecke, F., Doak, S., Parak, W.J., et al., 2012. Cytotoxic effects of gold nanoparticles: a multiparametric study. ACS Nano 6, 5767–5783. doi:http://dx.doi.org/10.1021/nn301714n.

Staggers, N., McCasky, T., Brazelton, N., Kennedy, R., 2008. Nanotechnology: the coming revolution and its implications for consumers, clinicians, and informatics. Nurs. Outlook 56, 268–274. doi:http://dx.doi.org/10.1016/j.outlook.2008.06.004.

Tadiali, M., Seidelin, J.B., Olsen, J., Troelsen, J.T., 2002. Transcriptome changes during intestinal cell differentiation. Biochim. Biophys. Acta 1589 (2), 160–167.

Talukder, A.H., Meng, Q., Kumar, R., 2006. CRIPak a novel endogenous Pak1 inhibitor. Oncogene 25, 1311–1319. doi:http://dx.doi.org/10.1038/sj.onc.1209172.

Thomson, R.B., Igarashi, P., Biemesderfer, D., Kim, R., Abu-Alfa, A., Soleimani, M., Aronson, P.S., 1995. Isolation and cDNA cloning of Ksp-cadherin, a novel kidney-specific member of the cadherin multigene family. J. Biol. Chem. 270, 17594–17601. doi:http://dx.doi.org/10.1074/jbc.270.29.17594.

Tremblay, E., Auclair, J., Delvin, E., Levy, E., Ménard, D., Pshezhetsky, A.V., Rivard, N., Seidman, E.G., Sinnett, D., Vachon, P.H., Beaulieu, J.F., 2006. Gene expression profiles of normal proliferating and differentiating human intestinal epithelial cells: a comparison with the Caco-2 cell model? J. Cell Biochem. 99 (4), 1175–1186.

Turkevich, J., Stevenson, P.C., Hillier, J., 1951. A study of nucleation and growth process in the synthesis of colloidal gold. Discuss. Faraday Soc. 11, 55–75.

Ullah, S., John, P., Bhatti, A., 2014. MicroRNAs with a role in gene regulation and in human diseases. Mol. Biol. Rep. 41, 225–232. doi:http://dx.doi.org/10.1007/s11033-013-2855-1.

Vašák, M., Meloni, G., 2011. Chemistry and biology of mammalian metallothioneins. J. Biol. Inorg. Chem. 16, 1067–1078. doi:http://dx.doi.org/10.1007/s00775-011-0799-2.

Vendrell, J., Querol, E., Avilés, F.X., 2000. Metallocarboxypeptidases and their protein inhibitors. Structure, function and biomedical properties. Biochim. Biophys. Acta 28, 4–298. doi:http://dx.doi.org/10.1016/S0167-4838(99)00280-0.

Venkatesh, S., Workman, J.L., Smolle, M., 2013. UpSETing chromatin during non-coding RNA production. Epigenetics Chromatin 6, 16. doi:http://dx.doi.org/10.1186/1756-8935-6-16.

Walker, M.S., Hughes, T.A., 2008. Messenger RNA expression profiling using DNA microarray technology: diagnostic tool, scientific analysis or un-interpretable data? Int. J. Mol. Med. 21, 13–17. doi:http://dx.doi.org/10.3892/ijmm.21.1.13.

Wang, S.H., Lee, C.W., Chiou, A., Wei, P.K., 2010. Size-dependent endocytosis of gold nanoparticles studied by three-dimensional mapping of plasmonic scattering images. J. Nanobiotechnol. 8, 33. doi:http://dx.doi.org/10.1186/1477-3155-8-33.

Wingler, K., Böcher, M., Flohé, L., Kollmus, H., Brigelius-Flohé, R., 1999. mRNA stability and selenocysteine insertion sequence efficiency rank gastrointestinal glutathione peroxidase high in the hierarchy of selenoproteins. Eur. J. Biochem. 259, 149–157. doi:http://dx.doi.org/10.1046/j.1432-1327.19999.00012.x.

Wittmaack, K., 2011. Excessive delivery of nanostructured matter to submersed cells caused by rapid gravitational settling. ACS Nano 5, 3766–3778. doi:http://dx.doi.org/10.1021/nn200112u.

Yang, Y., Qu, Y., Lü, X., 2010. Global gene expression analysis of the effects of gold nanoparticles on human dermal fibroblasts. J. Biomed. Nanotechnol. 6, 234–246. doi:http://dx.doi.org/10.1166/jbn.2010.1128.

Zhang, Y., Yuan, F., Wu, X., Wang, M., Rechkoblit, O., Taylor, J.S., Geacintov, N.E., Wang, Z., 2000. Error-free and error-prone lesion bypass by human DNA polymerase kappa in vitro. Nucleic Acids Res. 28, 4138–4146.

Zhang, S.L., Tang, Y.P., Wang, T., Yang, J., Rao, K., Zhao, L.Y., Zhu, W.Z., Meng, X.H., Wang, S.G., Liu, J.H., et al., 2011. Clinical assessment and genomic landscape of a consanguineous family with three Kallmann syndrome descendants. Asian J. Androl. 13, 166–171. doi:http://dx.doi.org/10.1038/aja.2010.83.

SCIENTIFIC REP⚙RTS

High variability of genomic instability and gene expression profiling in different HeLa clones

Annalisa Frattini[1,2], Marco Fabbri[2], Roberto Valli[2], Elena De Paoli[2], Giuseppe Montalbano[2], Laura Gribaldo[3], Francesco Pasquali[2] & Emanuela Maserati[2]

The HeLa cell line is one of the most popular cell lines in biomedical research, despite its well-known chromosomal instability. We compared the genomic and transcriptomic profiles of 4 different HeLa batches and showed that the gain and loss of genomic material varies widely between batches, drastically affecting basal gene expression. Moreover, different pathways were activated in response to a hypoxic stimulus. Our study emphasizes the large genomic and transcriptomic variability among different batches, to the point that the same experiment performed with different batches can lead to distinct conclusions and irreproducible results. The HeLa cell line is thought to be a unique cell line but it is clear that substantial differences between the primary tumour and the human genome exist and that an indeterminate number of HeLa cell lines may exist, each with a unique genomic profile.

Since HeLa was first established as a human cancer cell line in 1952[1], it has become probably the most-used human cell line in biological research. The cell line was established from the invasive cervical adenocarcinoma of a young patient, Henrietta Lacks, who eventually died in 1951, and it was the first successful attempt to establish a culture of immortalized human cells. Starting with the pioneering research of Jonas Salk, who developed the first polio vaccine[2], the use of HeLa cells has contributed to many fundamental scientific breakthroughs.

HeLa cells have been employed to investigate cancer, AIDS mechanisms[3], and the effects of drugs[4], toxins[5] and radiation[6]. These cells have also been used in the Nobel-winning experiments that led to the discovery of telomeric activity[7,8].

Furthermore, to verify the gene-editing effects involved in specific cellular processes, gene expression profiles and proteome analyses have been applied to HeLa cells[9–11]. The widespread use of this cell line is mainly due to the ease with which they can be handled and manipulated in different conditions.

Starting from the 1950 s, approximately 80,000 studies have reported results obtained using the HeLa cell line as a physiological model. In the majority of these studies, the source of the HeLa cell line is not specified, implying a lab-to-lab origin (Supplementary Table S1).

Several published studies reported that HeLa cells are characterized by extensive chromosome instability (CIN)[12–19] (Supplementary Table S1), although one study concluded that they are stable and able to maintain a constant number of chromosomes mitosis after mitosis[20].

A few years after the establishment of the line, one of the first studies on the metaphase spreads of clonal cell strains of HeLa was published in 1958[21], showed a relatively narrow chromosome number distribution between 75 and 82. The large number of duplications and deletions compared with the normal human genome has already been extensively described[19] (Supplementary Table S1), and as chromosomes provide genome identity, it might even be argued that the HeLa genome is no longer a human one[22]. In 1991, it was even proposed that the HeLa cell could be considered a new species (*Helacyton gartleri*)[23].

[1]Institute of Genetic and Biomedical Research (IRGB), National Research Council (CNR), via Fantoli 15/16, 20090 Milan, Italy. [2]Department of Clinical and Experimental Medicine (DMCS), University of Insubria, via J.H. Dunant 5, 21100 Varese, Italy. [3]Institute for Health and Consumer Protection, European Commission, I Via Enrico Fermi 2749, 21027 Ispra (VA), Italy. Correspondence and requests for materials should be addressed to A.F. (email: annalisa. frattini@irgb.cnr.it)

To our knowledge, all of the reports regarding HeLa CIN have been conducted on a single cell clone or on sub-clones[20,24]. Recently, the HeLa genome and transcriptome was exhaustively characterized by deep RNA and DNA sequencing performed on a single clone from CLS Cell Lines Service GmbH (the HeLa Kyoto cell line)[25]. To investigate the reported instability of the HeLa cell lines and to verify the possibility that erroneous conclusions could be generated by the use of HeLa cells obtained from different laboratories, we compared different "batches" obtained from four Italian laboratories (HeLaSR, HeLaV, HeLaP, and HeLaH). HeLaP and HeLaH were derived from the same batch but had been cultured in two different laboratories for approximately 8 years; similarly, HeLaV was derived from the same batch as HeLaSR but had been cultured in two different laboratories for approximately 12 years.

Results

HeLa karyotyping and a-CGH show genomic instability.
We evaluated the genomic stability of these "batches" by karyotyping, array-comparative genomic hybridization (a-CGH) and fluorescent *in situ* hybridization (FISH described in the next section).

Cytogenetic analysis was performed on 20 metaphase spreads stained using the quinacrine-based Q-banding technique (QFQ). The HeLa cells were near-triploid, containing a range of 60–66 chromosomes in HeLaSR, 56–79 in HeLaV, 71–79 in HeLaP, and 63–79 in HeLaH. In addition, approximately 10% of the metaphase spreads of clone HeLaSR exhibited chromosome numbers ranging from 101 to 148, whereas HeLaV (derived from the HeLaSR batch) exhibited a range of 124–198 chromosomes in approximately 30% of its metaphase spreads. We excluded the coexistence of two different sub-clones by monoclonal sub-culturing.

Ten HeLaV clones, derived from a monoclonal sub-culture, showed the presence of both metaphase populations (with a range of 49–81 and a range of 92–240 chromosomes), suggesting that a single cell could carry the inherent defect, possibly generated by new mutation events. For our FISH and transcriptomic analysis, we used the batch HeLaSR because it showed fewer mitoses with double the modal chromosome number compared to HeLaV.

To characterize all of the genomic imbalances of the four "batches", we performed a-CGH. As showed in the Circos plot[26] (Fig. 1A), a comparison between the HeLa DNA content and the diploid human genome evinced a substantial difference among the four lines analysed. The comparison of the 4 HeLa clones underscored that although the amount of gain and loss of genomic material compared to the human diploid genome is highly variant among the 4 clones, there is similarity within the pairs with a common origin, i.e., HeLaH/HeLaP vs HeLaSR/HeLaV (Fig. 1B).

To express the similarities among the HeLa clones, we calculated the percentage of the genomes with the same annotation (diploid, deleted or amplified). The results, depicted in Fig. 1C, show high similarity within the two pairs HeLaSR/HeLaV and HeLaH/HeLaP. We emphasize that even recently split-out batches (HeLaSR vs HeLaV and HeLaH vs HeLaP) present specific gains or losses and that these new events are acquired and stably maintained. A possible hypothesis to explain the different chromosome imbalances between the two pairs could be ancestral mutational events that conferred an evolutionary advantage in DNA losses or gains.

FISH analysis highlights new specific markers.
To identify chromosomal rearrangements and to verify the presence of HeLa-specific markers observed by karyotyping[17,20], we performed a FISH analysis to paint chromosomes 1, 3, 5, 9, 13 and 19 in HeLaSR and HeLaP because they appeared to be the two most different clones by a-CGH. As shown in Table 1, HeLaP displays almost all of the HeLa-specific markers previously identified[12,20,25], whereas HeLaSR has lost most of them. In addition, we found in each clone the presence of new specific markers (Supplementary Fig. S1), confirming an independent evolution of each batches.

Transcriptomic analysis reveals that different batches exposed to hypoxic stimulus display differences in gene expression.
Our genomic analysis uncovered deep variability between the batches, and because genomic gains or losses or whole-chromosome aneuploidy can have drastic consequences on gene expression[27], we performed a whole-transcriptome analysis to verify the transcriptional effects of this differential chromosome instability. The microarray expression analysis was performed on HeLaSR and HeLaP, the batches most different in terms of genomic content. These cell lines were exposed to hypoxic conditions, chosen because the induced hypoxic pathway is well characterized[28,29].

A principal-component analysis (PCA) was performed to determine the expression trends within the dataset. PCA is a useful technique to reduce the dimensionality of large data sets and to visually assess similarities and differences between samples[30]. PCA was used to identify trends in the regulation of genes induced by hypoxic exposure and to map the entire dataset on a two-axis graph (principal components, PC1 and PC2) where the distances account for similarity (Fig. 2A); the closer the distance between samples, the more they are similar. The main divergence was due to two different clones, HeLaSR vs HeLaP (triangles and circles, respectively), as demonstrated by the first principal component (PC1). The second component (PC2), summarizing the effects of hypoxia, highlighted strong changes in HeLaSR and mild changes in HeLaP. Indeed, untreated HeLaP and HeLaP after hypoxia are closer to each other than untreated HeLaSR is to HeLaSR after hypoxia, meaning that hypoxia has a stronger effect in HeLaSR than in HeLaP (Fig. 2A). Furthermore, we identified the genes regulated by hypoxic treatment in these
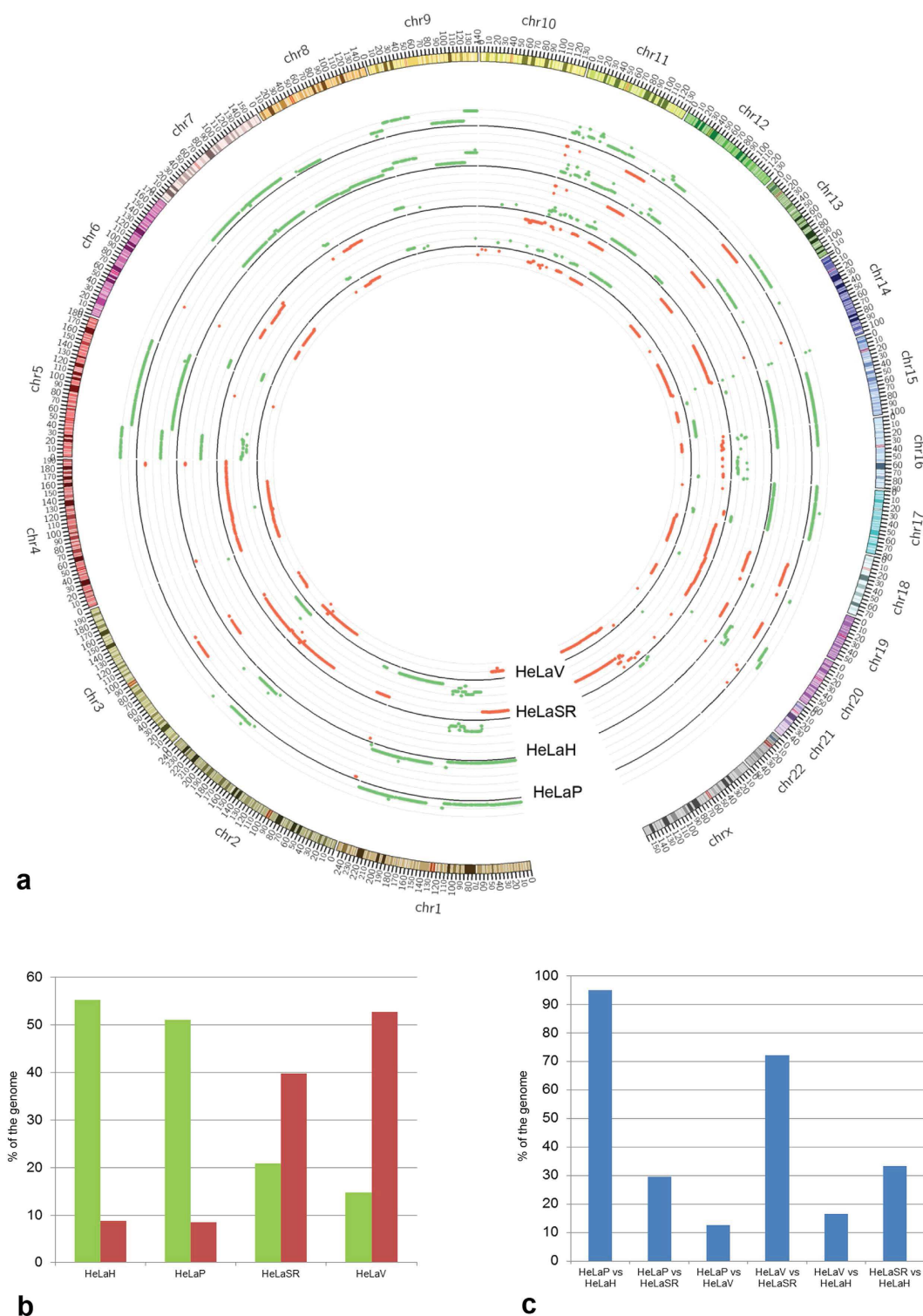
Figure 1. The genomic landscape of the 4 HeLa cell lines. (**a**) Circos plot of the four HeLa genomes compared with the diploid human genome, with tracks representing the gain (green) and loss (red) of genomic material. (**b**) The histogram summarizes the percentage of the gain (green) and loss (red) of genomic material in the 4 cell lines compared to the diploid human genome, highlighting the separate evolution of the two pairs of HeLa clones (HeLaH and HeLP vs HeLaSR and HeLaV). (**c**) The histogram shows the percentage of similarity in genomic content in each HeLa clone compared with the other lines and emphasizes that the two more similar lines, based on their common origin (HeLaH and HeLaP; HeLaSR and HeLaV), bear differences in their genomic content.

Chromosome markers previously reported[17–20]	HeLaSR	HeLaP
M1 der(1)t(1;3)(q11;q11)	10/10	9/10
M2 der(1;9)(p11;q11)	0/10	4/10
M4 der(3;5)(p11;q11)	10/10	0/10
M5 der(3;20)(q10;q?10)	8/10	8/10
M7 i(5)(p10)	10/10	10/10
M8 der(7)t(7;19)(q35;?)	0/10	9/10
M10 der(9)t(3;9)(p21;p11)	0/10	8/10
M11 der(11)t(9;11;9) (?;p14?q33?;?dup(11)(p?)dup(11)(q?)	0/10	10/10
M14 der(19)t(13;19)(q21;p13)	10/10	10/10
M22 der (5;9)(p10;p10)	0/10	10/10
Loss or acquired chromosomes		
+chr.1	9/10	5/10
− chr. 3	10/10	10/10
− 2 chrs. 5	0/10	10/10
+chr.9	2/10	1/10
− chr. 9	0/10	3/10
− chr. 13	10/10	1/10
− chr. 19	2/10	10/10
Specific new markers		
i(1p)	1/10	0/10
i(5q)	0/10	10/10
t(3p;13q)	10/10	1/10
t(6;19)	10/10	1/10

Table 1. HeLa cell line's specific markers of HeLaSR and HeLaP lines. Marker identification by FISH using WCP (Whole Chromosome Painting) for chr.1 vs chr. 3; chr. 5 vs chr. 9; chr.13 vs chr.19 (see Supplementary Fig. S1). Ten metaphases for each HeLa clone were analysed.

two clones: 2,900 (1,666 genes upregulated and 1,234 downregulated) genes were mis-regulated only in HeLaSR, whereas 145 genes were mis-regulated only in HeLaP (104 up and 41 down). A total of 89 genes (88 up and 1 down) were mis-regulated in both cell lines (Fig. 2B).

These three gene lists were analysed for gene ontology (GO) enrichment (Fig. 2C). The more significant GO classes those that are differentially expressed between HeLaSR and HeLaP, demonstrating the large differences in the expression profiles of the two cell lines in response to hypoxia.

The classes related to hypoxia were present in both, but they were not the most significant (Fig. 2C). On the contrary, when we analysed the 89 mis-regulated genes common to both cell lines, the most enriched classes are related to hypoxia (Fig. 2B,C). These results suggest that the different genomic contents of the two clones have a remarkable influence on basal gene expression and, consequently, on the response to a hypoxic stimulus. The cells activate different pathways, but interestingly, the regulation of hypoxia-related genes is preserved.

Real-time RT-PCR confirmed the microarray data. A subset of regulated genes identified for their relevance in the hypoxic response were validated by real-time RT-PCR (qPCR) (Supplementary Table S2). The trend of the array data was confirmed by qRT-PCR (Supplementary Table S3).

Copy number variation influences gene expression. Because significant chromosome copy number alterations are frequently associated with gene expression changes in the affected regions[31], we evaluated the possible effects of copy number variation on gene expression[32] in our samples. Based on the data obtained with a-CGH and the expression array performed on HeLaP and HeLaSR samples as previously described, a general lack of dosage compensation was observed in HeLaP (Fig. 3A) and in HeLaSR (Fig. 3B), meaning that gene dosage is correlated to gene expression.

Discussion

Genetic aberrations, such as gene amplification, deletions, and loss of heterozygosity, are hallmarks of cancer and are major contributors to the neoplastic process through the accumulation of mutations in
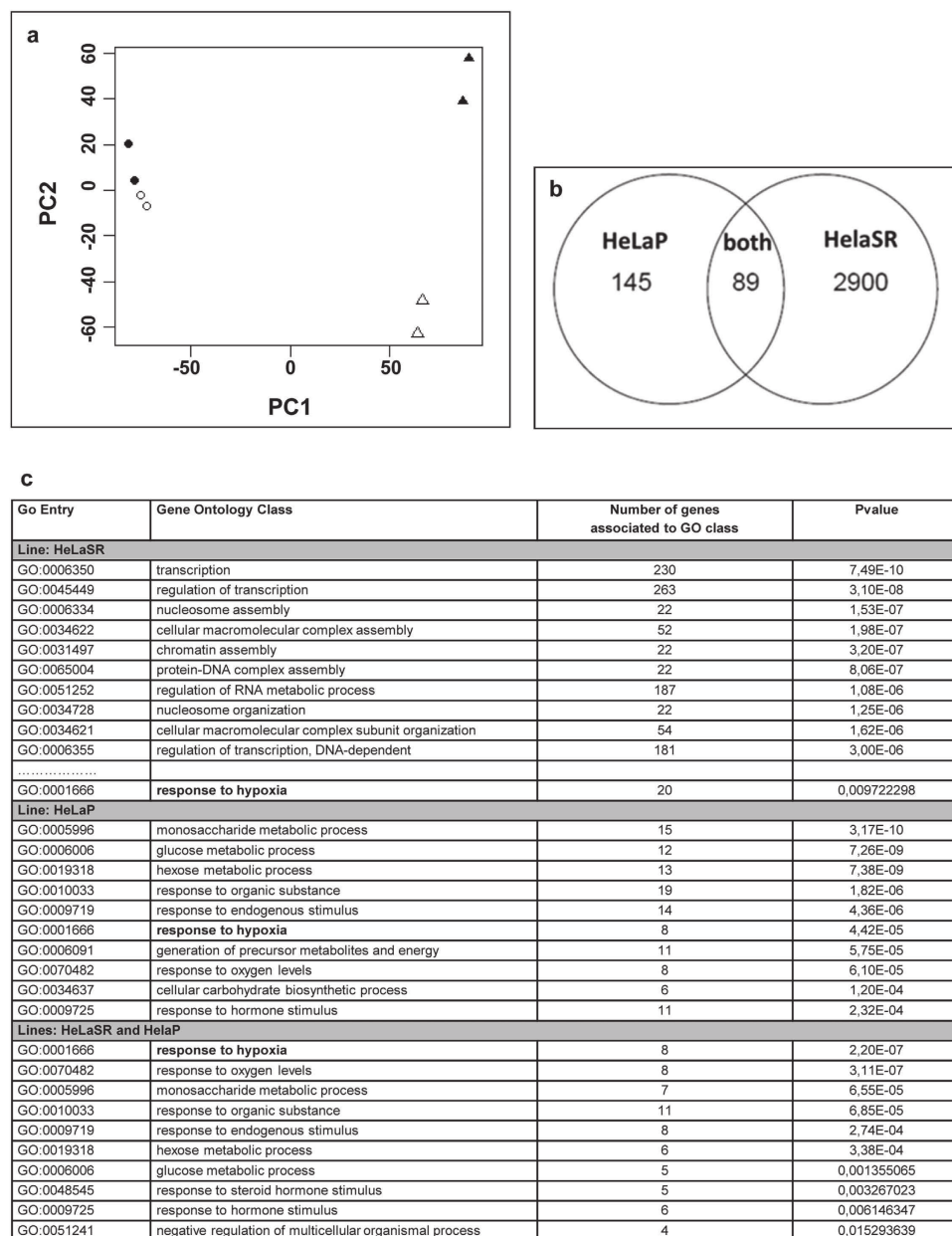
a

b

HeLaP	both	HelaSR
145	89	2900

c

Go Entry	Gene Ontology Class	Number of genes associated to GO class	Pvalue
Line: HeLaSR			
GO:0006350	transcription	230	7,49E-10
GO:0045449	regulation of transcription	263	3,10E-08
GO:0006334	nucleosome assembly	22	1,53E-07
GO:0034622	cellular macromolecular complex assembly	52	1,98E-07
GO:0031497	chromatin assembly	22	3,20E-07
GO:0065004	protein-DNA complex assembly	22	8,06E-07
GO:0051252	regulation of RNA metabolic process	187	1,08E-06
GO:0034728	nucleosome organization	22	1,25E-06
GO:0034621	cellular macromolecular complex subunit organization	54	1,62E-06
GO:0006355	regulation of transcription, DNA-dependent	181	3,00E-06
....			
GO:0001666	**response to hypoxia**	20	0,009722298
Line: HeLaP			
GO:0005996	monosaccharide metabolic process	15	3,17E-10
GO:0006006	glucose metabolic process	12	7,26E-09
GO:0019318	hexose metabolic process	13	7,38E-09
GO:0010033	response to organic substance	19	1,82E-06
GO:0009719	response to endogenous stimulus	14	4,36E-06
GO:0001666	**response to hypoxia**	8	4,42E-05
GO:0006091	generation of precursor metabolites and energy	11	5,75E-05
GO:0070482	response to oxygen levels	8	6,10E-05
GO:0034637	cellular carbohydrate biosynthetic process	6	1,20E-04
GO:0009725	response to hormone stimulus	11	2,32E-04
Lines: HeLaSR and HelaP			
GO:0001666	**response to hypoxia**	8	2,20E-07
GO:0070482	response to oxygen levels	8	3,11E-07
GO:0005996	monosaccharide metabolic process	7	6,55E-05
GO:0010033	response to organic substance	11	6,85E-05
GO:0009719	response to endogenous stimulus	8	2,74E-04
GO:0019318	hexose metabolic process	6	3,38E-04
GO:0006006	glucose metabolic process	5	0,001355065
GO:0048545	response to steroid hormone stimulus	5	0,003267023
GO:0009725	response to hormone stimulus	6	0,006146347
GO:0051241	negative regulation of multicellular organismal process	4	0,015293639

Figure 2. Transcriptional landscape. (a) Principal component analysis (PCA) of the transcriptome. The PCA maps the entire dataset on a two-axis graph (principal components, PC1 and PC2), where the distances account for similarity. Untreated HeLaP cells (white circles) and HeLaP cells after hypoxia (black circles) are closer to each other than untreated HeLaSR cells (white triangles) are to hypoxic HeLaSR cells (black triangles), suggesting that hypoxia exerts a stronger effect on HeLaSR cells than on HeLaP cells. **(b)** Venn diagram showing the number of genes either upregulated or downregulated due to hypoxia in the HeLaP and HeLaSR clones compared to their respective controls. **(c)** Gene ontology of genes either upregulated or downregulated by hypoxia in HeLaSR and HeLaP cells.

specific genes. The mechanisms through which these mutations are generated are the subject of continued debate[33–37], and several cancer-predisposing mutations affect genes that are responsible for maintaining the integrity and number of chromosomes during cell division.

The main factors that control chromosome stability are telomere maintenance, cell division mechanisms, and the mitotic checkpoint that ensures correct chromosome segregation[38–40].

Consequently, the archetypical transformation of tumour cells results in CIN[41,42]. Established cell lines have been traditionally used to characterize the biological significance of specific genomic aberrations identified in primary tumours[43] and to test the therapeutic efficacy of anticancer agents[44].

HeLa was the first cultured cancer line[45]. Although its CIN has already been extensively investigated[19] (see Supplementary Table S1), demonstrating the low degree of similarity with the initial tumour and
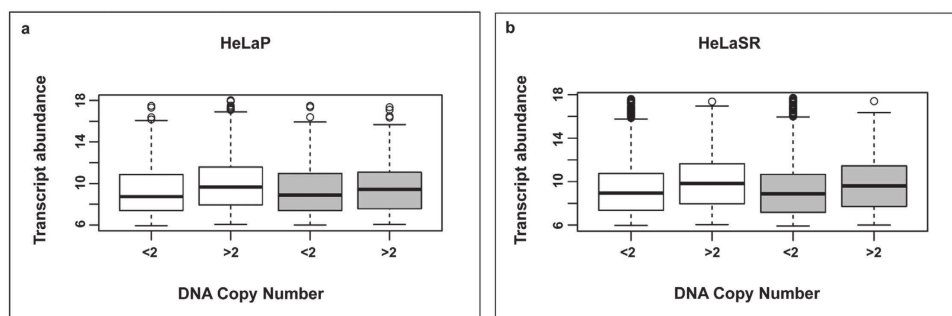
Figure 3. Gene expression by copy number in HeLaP and HeLaSR cells. Transcript abundance (arbitrary unit) is positively correlated with gene copy number. (**a**) HeLaP gene expression in untreated (white) and hypoxic (grey) cells. (**b**) HeLaSR gene expression in untreated (white) and hypoxic (grey) cells. A general lack of dosage compensation was observed in both cell lines.

with the human diploid genome, this cell line is largely used in biomedical research. The HeLa cell line is among the most frequently utilized models in research to validate drugs for cancer therapy[46] and for genetic/epigenetic manipulation using demethylation agents[47], siRNA and expression vectors to study gene function[48–50].

Here, we report the high level of CIN in HeLa clones obtained from different laboratories. We demonstrated that each clone accumulates genomic variability in a time-dependent manner. We speculate that some chromosomal rearrangements or point mutations that randomly arose in each clone increased survival, leading to a kind of "genetic drift" in clonal variants.

This conclusion is evident in the differing DNA content of the clones HeLaSR and HeLaV, which showed a loss of genomic DNA, whereas HeLaH and HeLaP exhibited a gain of genomic DNA in comparison with the diploid human genome. We speculate that even slightly different culture conditions may produce this divergence. The number of passages that a cell line undergoes can certainly lead to extensive modifications in growth rate, morphology, aneuploidy, chromosome alterations, gene expression and drug sensitivity, depending on the culture environment[51–55]. In addition, we demonstrated that the genomic gains or losses or whole-chromosome aneuploidy is specific to each analysed clone (Fig. 1A) and that these differences in genomic content have a remarkable influence on basal gene expression (Fig. 2A). We showed that in response to a hypoxic stimulus, each cell line activates different pathways, although the regulation of genes related to hypoxia is conserved (Fig. 2A,C).

These results suggest that different HeLa batches used for the same experiment may yield different results. The large differences in the basal gene expression profiles suggest that the use of uncharacterized clones may lead to faulty conclusions and to irreproducible results in studies of gene function and pathway analysis. With respect to genomic content, the use of uncharacterized batches of HeLa cells[56] may result in different behaviours between clones in response to specific stimuli, such as cancer drugs, used in biomedical research.

Our results suggest that not a single HeLa cell line, or even a set of similar HeLa cell lines, exists. Rather, an indeterminate number of clones exist, each carrying large genomic differences that lead to different expression profiles. The HeLa cell recalls the main character of the novel by Pirandello (the Italian poet awarded the 1934 Nobel Prize in Literature): "One, no one, one hundred thousand"[57]: the HeLa cell line is thought to be a unique cell line ("one"), but it is clear that large differences exist between the tumour from which it was derived and the human genome ("no one") and that an indeterminate number of HeLa cell lines are scattered in laboratories worldwide ("one hundred thousand" or more), each with a unique genomic profile.

Methods

Cell lines.
The cell lines HeLaP, HeLaH, HeLaSR and HeLaV were obtained from four Italian laboratories. HeLaP and HeLaH were derived from the same cell-line batch but were cultured in two different laboratories for approximately 8 years. Similarly, HeLaSR and HeLaV were derived from the same cell-line batch but were cultured in two different laboratories for approximately 12 years. In our lab, the mycoplasma-free cell lines were cultured in DMEM-F12 (Euroclone SpA, Milan, Italy) with 10% heat-inactivated foetal bovine serum (Euroclone), 1 mM glutamine, 100 U/ml penicillin and 100 μg/ml streptomycin and were incubated at 37 °C and 5% CO_2. The cells were cultured to reach a confluence of 80–90%.

Cytogenetic analysis.
Metaphase spreads were obtained from the four cell lines. After culturing, the cells were treated with 0.04 μg/ml colcemid for 2 hours. The cells were harvested by treatment with a 1× trypsin/EDTA solution for approximately 5 min. A hypotonic treatment was performed with 0.96% Na citrate for 15 min at 37 °C, and the cells were subsequently fixed in a fresh methanol/acetic acid

(3/1, v/v) solution. Metaphase spreads were stained overnight with 0.005% quinacrine mustard solution in McIlvaine buffer (QFQ-banding), and standard cytogenetic analyses were performed with a Leica D5000B fluorescent microscope.

Monoclonal subculturing by limiting dilution.   To exclude the possibility that the HeLaV and HeLaSR cell lines arose from 2 different HeLa subclones, we obtained a cell culture derived from a single cell by limiting-dilution culture. We prepared serial dilutions to obtain a suspension containing 1 cell/µl. A single µl of the final cell suspension was seeded into each well of a 96-well plate containing growth medium. The presence of a single cell was evaluated by microscopy, and the cells were incubated at 37 °C and 5% CO_2 overnight. After one day, we used microscopy to confirm the presence of a single cluster of cells (2 or more) per well, implying a single-cell origin, and we excluded any wells with double or multiple clusters of cells. The monoclonal cell lines were trypsinised and seeded in T25 flasks to obtain sufficient cells for the metaphase spread analysis.

Fluorescence *in situ* hybridization experiments.   Metaphase spreads were hybridized with Cytocell Aquarius Whole Chromosome Painting probes (WCP Probes) using the codenaturation protocol. Briefly, 20 µl of ready-to-use probes were deposited on the slide and sealed with a coverslip using rubber cement. Codenaturation was performed on a HyChrome hybridization machine at 75 °C for 2 min, and hybridization was conducted overnight. The slides were then washed for 2 min in 0.4× SSC buffer at 72 °C and for 30 min in 2× SSC/0.05% Tween 20 at room temperature. Metaphases spreads were then counterstained in 2× SSC buffer with 200 ng/ml of 4,6-diamidino-2-phenylindole (DAPI) and then mounted with an anti-fade solution (Vector Laboratories INC., Burlingame, CA, USA). The samples were analysed with a Leica DM5000B fluorescence microscope, and images were captured with the Leica QFISH software system.

DNA extraction.   DNA was extracted from approximately 10×10^7 cells using the DNeasy Blood and Tissue kit (Qiagen S.r.l. Milan, Italy) according to the manufacturer's protocol. Genomic DNA was quantified using an ND-1000 UV-Vis spectrophotometer (Thermo Scientific, Wilmington, DE, USA).

a-CGH analysis.   a-CGH was performed on an Agilent microarray platform (Agilent Technologies Inc., Santa Clara, CA USA) with an Agilent's human 4×180K CGH slide. Sample preparation, labelling, and microarray hybridization were performed according to the Agilent CGH Enzymatic Protocol version 7.3. Slides were scanned using the Agilent G2565CA scanner and analysed using the Agilent Feature Extraction 10.7.3.1 software. The a-CGH profile was extrapolated using the Agilent Genomic Workbench 6.5.0.18 software with the following parameters: ADM-2 threshold 6, Fuzzy Zero ON, and Centralization OFF. Coverage plots were generated using the Circos visualization tool compared with the 2.2×10^9 genome covered by the Agilent probes.

Hypoxic treatment.   Before administering the hypoxia treatment, the HeLaP and HeLaSR cells were maintained at 70–80% confluence. The medium was refreshed before the hypoxia treatment. Cells (two flasks per cell line) were maintained under hypoxic (1% O_2, 5% CO_2, 94% N_2) conditions or normoxic (95% air and 5% CO_2) conditions for 24 h.

RNA extraction.   Total RNA was purified from the HeLa cells using the RNeasy Plus kit (Qiagen). RNA was quantified using an ND-1000 UV-Vis spectrophotometer (Thermo Scientific, Wilmington, DE, USA), and the integrity of the RNA was assessed with the Agilent 2100 Bioanalyzer (Agilent Technologies Inc.) according to the manufacturer's instructions. All of the RNA samples used in this study exhibited a 260/280 ratio above 1.9 and an RNA Integrity Number (RIN) above 9.0.

Microarray expression profiling.   The microarray experiment included two biological replicates per treatment. All sample-labelling, hybridization, washing, and scanning steps were conducted according to the manufacturer's specifications. Briefly, Cy3-labelled cRNA was generated from 50 ng input total RNA using the One Color Quick Amp Labelling Kit (Agilent Technologies Inc.). For every sample, 600 ng cRNA from each labelling reaction (with a specific activity above 9.0) was hybridized using the Gene Expression Hybridization Kit (Agilent Technologies Inc.) to the Agilent Whole Human Genome Oligo Microarray (Agilent Technologies Inc.), which is in a 4×44k 60-mer slide format, where each of the 4 arrays represents approximately 41,000 unique genes and transcripts. After hybridization, the slides were washed and then scanned with the Agilent G2565BA Microarray Scanner (Agilent Technologies Inc.). The fluorescence intensities of the scanned images were extracted and pre-processed using the Agilent Feature Extraction Software (10.7.3.1).

Gene expression data analysis.   Quality control and array normalization were performed in the R statistical environment using the Agi4 × 44PreProcess (v 1.18.0) package, which was downloaded from the Bioconductor web site. The normalization and filtering steps were based on those described in the Agi4 × 44PreProcess reference manual. Briefly, the Agi4 × 44PreProcess options were set to use the Mean Signal and the BG Median Signal as foreground and background signals, respectively. The data were normalized between arrays using the quantile method. Genes with a fold change greater than 1 $\log_2$ were

designated as modulated. All of the above computations were conducted using the R statistical programming environment. Principal-component analysis (PCA) was performed on all genes under investigation to determine their expression trends within the dataset. PCA is a useful technique to reduce the dimensionality of large data sets. The expression analysis systematic explorer (EASE) biological theme analysis of the regulated genes was conducted online using DAVID.

Quantitative real-time PCR validation of microarray data. A real-time quantitative PCR (qRT-PCR) analysis was performed, in triplicate, on the same RNA samples that were used for the microarray hybridization to validate the microarray results. One μg of total RNA was retro-transcribed using SuperScript II (Life Technologies, Carlsbad, CA, USA). qRT-PCR was performed using the iQ SYBR® Green supermix (Bio-Rad, Hercules, CA, USA,) on the ABI Prism 7000 platform (Applied Biosystems) with the following thermal cycling protocol: denaturation for 1 min at 95 °C followed by 40 cycles of 15 sec at 95 °C and 1 min at 60 °C. The primers are listed in Supplementary Table S3. A relative quantitative analysis was performed using the $2^{-\Delta\Delta}$Ct method.

References

1. Gey, G. O., Coffman, W. D. & Kubicek, M. T. Tissue culture studies of the proliferative capacity of cervical carcinoma and normal epithelium. Scientific Proceedings American Association for Cancer Research. *Cancer Res.* **12,** 264–265 (1952).
2. Salk, J. E. Considerations in the preparation and use of poliomyelitis virus vaccine. *J Am Med Assoc.* **158,** 1239–1248 (1955).
3. Berg, J., Doe, B., Steimer, K. S. & Wabl, M. HeLa-LAV, an epithelial cell line stably infected with HIV-1. *J Virol Methods.* **34,** 173–180 (1991).
4. al-Allaf, T. A. & Rashan, L. J. Cis- and trans-platinum and palladium complexes: a comparative study review as antitumour agents. *Boll Chim Farm.* **140,** 205–210 (2001).
5. Khan, A. A. *et al.* Biophysical interactions of novel oleic acid conjugate and its anticamcer potential in HeLa cells. *J Fluoresc.* **25,** 519–525 (2015).
6. Murray, J. I. *et al.* Diverse and specific gene expression responses to stresses in cultured human cells. *Mol. Biol. Cell* **15,** 2361–2374 (2004).
7. Greider, C. W. & Blackburn, E. H. Identification of a specific telomere terminal transferase activity in Tetrahymena extracts. *Cell.* **43,** 405–413 (1985).
8. Morin, G. B. The human telomere terminal transferase enzyme is a ribonucleoprotein that synthesizes TTAGGG repeats. *Cell.* **59,** 521–529 (1989).
9. Chaudhry, M. A., Chodosh, L. A., McKenna, W. G. & Muschel, R. J. Gene expression profiling of HeLa cells in G1 or G2 phases. *Oncogene.* **21,** 1934–1942 (2002).
10. Whitfield, M. *et al.* Identification of genes periodically expressed in the human cell cycle and their expression in tumors. *Mol. Biol. Cell.* **13,** 1977–2000 (2002).
11. Hnilicová, J. *et al.* Histone deacetylase activity modulates alternative splicing. *PLoS ONE.* **6,** e16727 (2011).
12. Chen, T. R., Re-evaluation of HeLa, HeLa S3, and HEp-2 karyotypes *Cytogenet. Cell Genet.* **48,** 19–24 (1988).
13. Francke, U., Hammond, D. S. &. Schneider, J. A. The band patterns of twelve D 98-AH-2 marker chromosomes and their use for identification of intraspecific cell hybrids. *Chromosoma* **41,** 111–121 (1973).
14. Kraemer, P. M., Deaven, L. L., Crissman, H. A., Steinkamp, J. A. & Petersen D. F. On the nature of heteroploidy. Cold Spring Harb. Symp. *Quant. Biol.* **38,** 133–144 (1974).
15. Heneen, W. K. HeLa cells and their possible contamination of other cell lines: karyotype studies. *Hereditas* **82,** 217–248 (1976).
16. Nelson-Rees, W. A., Hunter, L., Darlington, G. J. & O'Brien, S. J. Characteristics of HeLa strains: permanent vs. variable features. *Cytogenet. Cell Genet.* **27,** 216–231 (1980).
17. Stanbridge, E. J., Flandermeyer, R. R., Daniels, D. W. & Nelson- Rees, W. A. Specific chromosome loss associated with the expression of tumorigenicity in human cell hybrids. *Somatic Cell Genet.* **7,** 699–712 (1981).
18. Ruess, D., Ye, L. Z. & Grond-Ginsbach, C. HeLa D98/aH-2 studied by chromosome painting and conventional cytogenetical techniques. *Chromosoma.* **102,** 473–477 (1993).
19. Rutledge, S. What HeLa Cells Are You Using? *The Winnower.* (2014). Website Available at: https://thewinnower.com/papers/what-hela-cells-are-you-using (Accessed: 19th May 2015).
20. Macville, M. *et al.* Comprehensive and definitive molecular cytogenetic characterization of HeLa cells by spectral karyotyping. *Cancer Res.* **59,** 141–150 (1999).
21. Tjio, J. H. & Puck T. T. Genetics of somatic mammalian cells. II. Chromosomal constitution of cells in tissue culture. *J Exp Med.* **108,** 259–268 (1958).
22. Callaway E. Most popular human cell in science gets sequenced. *Nature News Mar.* **15,** doi: 10.1038/nature.2013.12609 (2013).
23. Val Valen, L. M. & Maiorana, V. C. HeLa, a new microbial species. *Evolutionary Theory.* **10,** 71–74 (1991).
24. Adey, A. *et al.* The haplotype-resolved genome and epigenome of the aneuploid HeLa cancer cell line. *Nature.* **500,** 207–211 (2013).
25. Landry, J. J. *et al.* The genomic and transcriptomic landscape of a HeLa cell line. *G3 (Bethesda).* **3,** 1213–1224 (2013).
26. Krzywinski, M. *et al.* Circos: an Information aesthetic for comparative genomics. *Genome Res.* **19,** 1639–1645 (2009).
27. Pavelka, N., Rancati, G. & Li, R. Dr Jekyll and Mr Hyde: role of aneuploidy in cellular adaptation and cancer. *Curr Opin Cell Biol.* **22,** 809–815 (2010).
28. Masson, N. & Ratcliffe, P. J. Hypoxia signalling pathways in cancer metabolism: the importance of co-selecting interconnected physiological pathways *Cancer Metab.* **2,** 1–17 (2014).
29. Tian, X. *et al.* Hypoxia-inducible factor-1α enhances the malignant phenotype of multicellular spheroid HeLa cells *in vitro*. *Oncol Lett.* **1,** 893–897 (2010).
30. Pearson, K. On lines and planes of closest fit to systems of points in space (PDF). *Philosophical Magazine.* **2,** 559–572 (1991).
31. Lynch, M. Gene duplication and evolution. *Science.* **297,** 945–947 (2002).
32. Henrichsen, C. N., Chaignat, E. & Reymond A. Copy number variants, diseases and gene expression. *Hum Mol Genet.* **18,** R1–R8 (2009).
33. Lengauer, C. Aneuploidy and genetic instability in cancer. *Semin Cancer Biol.* **15,** 1 (2005).
34. Loeb, L. A. Mutator phenotype may be required for multistage carcinogenesis. *Cancer Res.* **51,** 3075–3079 (1991).
35. Hartwell, L. Defects in a cell cycle checkpoint may be responsible for the genomic instability of cancer cells. *Cell* **71,** 543–546 (1992).
36. Mitelman, F. Recurrent chromosome aberrations in cancer. *Mutat Res.* **462,** 247–253 (2000).

37. Sandberg, A. A. & Meloni-Ehrig A. M. Cytogenetics and genetics of human cancer: methods and accomplishments *Cancer Genetics and Cytogenetics*. **203,** 102–126 (2010).
38. Jefford, C. E. & Irminger-Finger, I. Mechanisms of chromosome instability in cancers. *Crit Rev Oncol Hematol.* **59,** 1–14 (2006).
39. Bakhoum, S. F. & Swanton, C. Chromosomal instability, aneuploidy, and cancer. *Front Oncol.* **4,** 161 (2014).
40. Mitelman, F., Johansson, B. & Mertens, F. The impact of translocations and gene fusions on cancer causation. *Nat Rev Cancer.* **7,** 233–45 (2007).
41. Bakhoum, S. F. & Compton D. A. Chromosomal instability and cancer: a complex relationship with therapeutic potential *J Clin Invest.* **122,** 1138–1143 (2012).
42. Lengauer, C., Kinzler, K. W. & Vogelstein, B. Genetic instabilities in human cancers. *Nature.* **396,** 643–649 (1998).
43. Ferreira, D., Adega, F. & Chaves, R. *Novel Approaches in Biomarkers Discovery and Therapeutic Targets in Cancer* (ed. López-Camarillo, C. & Aréchaga-Ocampo, E.) 139–166 (InTech, 2013).
44. Sharma, S. V., Haber, D. A. & Settleman, J. Cell line-based platforms to evaluate the therapeutic efficacy of candidate anticancer agents. *Nat Rev Cancer.* **10,** 241–253 (2010).
45. Scherer, W. F., Syverton, J. T. & Gey, G. O. Studies on the propagation *in vitro* of poliomyelitis viruses. IV. Viral multiplication in a stable strain of human malignant epithelial cells (strain HeLa) derived from an epidermoid carcinoma of the cervix. *J Exp Med.* **97,** 695–710 (1953).
46. Guan, Y. Q. *et al.* Pathway of programmed cell death in HeLa cells induced by polymeric anti-cancer drugs. *Biomaterials.* **32,** 3637–3646 (2011).
47. Sood, S. & Srinivasan, R. Alterations in gene promoter methylation and transcript expression induced by cisplatin in comparison to 5-Azacytidine in HeLa and SiHa cervical cancer cell lines. *Mol Cell Biochem.* **404,** 181–191 (2015).
48. Tsai, K. W., Kao, H. W., Chen, H. C., Chen, S. J. & Lin, W. C. Epigenetic control of the expression of a primate-specific microRNA cluster in human cancer cells. *Epigenetics.* **4,** 587–592 (2009).
49. Rassmann, A. *et al.* Identification of gene expression profiles in HeLa cells and HepG2 cells infected with Coxsackievirus B3. *Journal of Virological Methods.* **187,** 190–194 (2013).
50. Chaudhry, M. A., Chodosh, L. A., McKenna, W. G. & Muschel, R. J. Gene expression profiling of HeLa cells in G1 or G2 phases. *Oncogene* **21,** 1934–1942 (2002).
51. Nelson-Rees, W. A., Owens, R. B., Arnstein, P. & Kniazeff, A. J. Source, alterations, characteristics and use of a new dog cell line (Cf2Th). *In Vitro.* **12,** 665–669 (1976).
52. Sakamoto, J. *et al.* Alteration of phenotype, morphology and drug sensitivity in colon cancer cell lines under various culture conditions. *Gan To Kagaku Ryoho.* **4,** 1864–1873 (1989).
53. Burdall, S. E., Hanby, A. M., Lansdown, M. R. J. & Speirs V. Breast cancer cell lines: friend or foe? *Breast Cancer Res.* **5,** 89–95 (2003).
54. van Staveren, W. C. *et al.* Human cancer cell lines: experimental models for cancer cells *in situ*?For cancer stem cells? *Biochim Biophys Acta.* **1795,** 92–103 (2009).
55. Borrell, B. How accurate are cancer cell lines? *Nature.* **463,** 858 (2010).
56. Domcke, S., Sinha, R., Levine, D. A., Sander, C. & Schultz, N. Evaluating cell lines as tumour models by comparison of genomic profiles. *Nat Commun.* **4,** 2126 (2013).
57. Pirandello, L. *One, No One, and One Hundred Thousand.* Vol. 18 (ed. Marsilio, Pub) (1990).

Author Contributions

A.F. conceived the project, designed the experiments, performed cell culture, hypoxia test and the microarray and qRT-PCR experiments; M.F. analysed the microarray and qRT-PCR data; R.V. performed the FISH and a-CGC experiment and analysed the data; G.M. and E.D.P. performed cell culture and metaphases preparation; E.M. analysed karyotypes and FISH and contributed to experimental design; L.G. contributed to study design; F.P. supervised the experimental design. M.F. and A.F. wrote the manuscript with input from all the authors. All the authors have read and approved the final manuscript.

Additional Information

Supplementary information accompanies this paper at http://www.nature.com/srep

Competing financial interests: The authors declare no competing financial interests.

How to cite this article: Frattini, A. *et al.* High variability of genomic instability and gene expression profiling in different HeLa clones. *Sci. Rep.* **5,** 15377; doi: 10.1038/srep15377 (2015).

Conclusion

The three papers presented in this thesis show that application of both gene expression analysis and cell lines to modern toxicology may bear several advantages but also some drawbacks.

The first paper shows the potential of gene expression to explain the toxic mechanism of cadmium cancerogenity using HepG2 cell line. The second paper utilizes Caco-2 cells to show that gene expression can be applied also to study toxic effects of a particular material, as nanoparticles. The third paper is a critical evaluation of cell lines reproducibility, as this study shows that batches of HeLa treated by hypoxia have some differences in the gene profile and the genetic analysis shows the presence of high genomic instability.

The first publication focuses on cadmium and cancer. A suggested mechanism of cadmium-induced carcinogenicity involves defects in the response DNA damage and the resistance to apoptosis: following this idea I focused on the tumour suppressor protein P53 since its inactivation is a common feature found in human cancers and it is a crucial component of the cellular response to DNA damage. P53 is primarily involved in defence mechanisms by transcriptional activation of genes responsible of growth arrest and apoptosis for the elimination of heavily damaged cells.

The results presented in this thesis demonstrated that in HepG2 cells exposed to cadmium the P53 was correctly moved and accumulated into the nucleus to accomplish its function of transcription factor. However, in spite of this correct nuclear localization, the signals for the cell cycle arrest were not activated.

In this context, P21, a P53 downstream protein, which is an important mediator of cell cycle arrest, was upregulated at gene level but not at protein level. These results could be explained by a post-transcriptional activity by the miRNA, as demonstrated by the upregulation of mir-372 in cadmium-treated HepG2 cells, able to affect p21 expression and to promote cell proliferation.

The second study focused on the toxic effect of nanoparticles. In this study, gene expression was applied to get insights in the mechanism of the cytotoxic effect of gold nanoparticle (AuNP) of two different sizes, 5 and 30 nm. The main focus was to compare the effect of the two sizes using Caco-2 cells as *in vitro* model of the intestine.

The smaller AuNPs (5 nm) inhibit Caco-2 cell growth, the gene expression analysis showed a broad range of responses induced by small size AuNPs which therefore mediate inhibition of Caco-2 cells growth.

The results presented indicate that the Caco-2 cells were able to recognize 5 nm AuNPs not only as metal but also as potential danger signals and stress inducers. This is shown by the bioinformatics reconstruction of regulated pathways that indicates that Caco-2 cells activate defence responses, even if it was not enough to prevent the observed toxic effect.

The stress resulting from cytotoxic level of smaller AuNPs induced down regulation of many genes. The observation of a high number of down regulated RNA transcripts in Caco-2 cells exposed to 5 nm AuNPs, suggested a possible involvement of miRNA. A

bioinformatics approach was applied to predict potential miRNA target sequences in mRNAs and a possible involvement of miRNAs in this process is suggested.

The response at the transcriptome level upon exposure to larger AuNPs (30nm) level is very weak. This effect can be due to the fact that, as already reported in literature, the cellular uptake is higher for smaller nanoparticles. In our study we observed the same phenomenon, and the higher uptake of smaller AuNPs (5 nm) might represent a stronger biologically stimulus. Moreover, it is also possible that smaller AuNPs (5nm), with higher surface area to volume ratio, have a higher reactivity toward biological molecules and are more "disruptive" to the homeostasis of exposed cells as compared to larger AuNPs (30 nm).

The different expression profiles observed in Caco-2 cells exposed to the two different sizes of nano-gold particles, gave an additional support to previously published findings demonstrating that isotropic AuNPs larger than 5 nm seem to be biologically inert [82].

The third paper focused on the issue about cell line variability using different batches of HeLa cells, collected from different laboratories. The microarray expression analysis was performed on these batches of HeLa cells exposed to hypoxic conditions, chosen because the induced hypoxic pathway is well characterized. In response to a hypoxic stimulus, each cell line batch activates different pathways, although the regulation of genes related to hypoxia is conserved. These outcomes strongly suggest that

different HeLa batches can give different results in gene expression.

A genetic analysis showed the high level of extensive chromosome instability in the HeLa clones obtained from different laboratories. Each clone accumulates genomic variability in a time-dependent manner, so it possible to speculate that some chromosomal rearrangements or point mutations that randomly arose in each clone increased survival, leading to a kind of "genetic drift" in clonal variants.

The large differences in gene expression profiles suggest that the use of uncharacterized clones may lead to faulty conclusions and to irreproducible results in studies of gene function and pathway analysis. With respect to genomic content, the use of uncharacterized batches of HeLa cells may result in different behaviours between clones in response to specific stimuli, such as cancer drugs, used in biomedical research.

In the three papers presented in this thesis I have not only shown the reproducibility of microarray by comparison to real time PCR, the gold standard for mRNA quantification, but also the capability to create possible model for the mechanistic effects on biological pathways. Furthermore microRNAs have been integrated in the modelling of mechanisms and should be considered important potential biomarkers.

In my thesis I have used different cell lines as *in vitro* models. They have shown that they have many advantages and that can give strong support for modern toxicology and can be used to study

biological mechanism, although the last publication shows some limits, due to the high variability in cell line batches, that have to be taken into account.

I can conclude that microarray and cell lines are powerful tools for modern toxicology to study mechanism of toxic compounds. Microarray is a mature and solid technology, whereas cell lines have been shown to be nice models but have to be used with attention.

Personal papers with results included in this thesis

- Urani, C., Melchioretto, P., Fabbri, M., Bowe, G., Maserati, E., and Gribaldo, L. (2014). Cadmium Impairs p53 Activity in HepG2 Cells. ISRN Toxicol. 2014, 976428.
- Bajak, E., Fabbri, M., Ponti, J., Gioria, S., Ojea-Jiménez, I., Collotta, A., Mariani, V., Gilliland, D., Rossi, F., and Gribaldo, L. (2015). Changes in Caco-2 cells transcriptome profiles upon exposure to gold nanoparticles. Toxicol. Lett. 233, 187–199.
- Frattini, A., Fabbri, M., Valli, R., De Paoli, E., Montalbano, G., Gribaldo, L., Pasquali, F., and Maserati, E. (2015). High variability of genomic instability and gene expression profiling in different HeLa clones. Sci. Rep. 5, 15377.

Personal papers not included in this thesis

- Martinez, F.O., Helming, L., Milde, R., Varin, A., Melgert, B.N., Draijer, C., Thomas, B., Fabbri, M., Crawshaw, A., Ho, L.P., et al. (2013). Genetic programs expressed in resting and IL-4 alternatively activated mouse and human macrophages: similarities and differences. Blood 121, e57–e69.
- Pallocca, G., Fabbri, M., Sacco, M.G., Gribaldo, L., Pamies, D., Laurenza, I., and Bal-Price, A. (2013). miRNA expression profiling in a human stem cell-based model as a tool for developmental neurotoxicity testing. Cell Biol. Toxicol. 29, 239–257.
- Pallocca, G., Fabbri, M., Nerini-Molteni, S., Pistollato, F., Zagoura, D., Sacco, M.G., Gribaldo, L., Bremer-Hoffmann, S., and Bal-Price, A. (2014). Changes in miRNA Expression Profiling during Neuronal Differentiation and Methyl Mercury-Induced Toxicity in Human in Vitro Models. Toxics 2, 443–463.
- Pamies, D., Sogorb, M.A., Fabbri, M., Gribaldo, L., Collotta, A., Scelfo, B., Vilanova, E., Harris, G., and Bal-Price, A. (2014). Genomic and phenotypic alterations of the neuronal-like cells derived from human embryonal carcinoma stem cells (NT2) caused by exposure to organophosphorus compounds paraoxon and mipafox. Int. J. Mol. Sci. 15, 905–926.

- Pamies, D., Bal-Price, A., Fabbri, M., Gribaldo, L., Scelfo, B., Harris, G., Collotta, A., Vilanova, E., and Sogorb, M.A. (2014). Silencing of PNPLA6, the neuropathy target esterase (NTE) codifying gene, alters neurodifferentiation of human embryonal carcinoma stem cells (NT2). Neuroscience 281C, 54–67.
- Urani, C., Melchioretto, P., Bruschi, M., Fabbri, M., Sacco, M.G., and Gribaldo, L. (2015). Impact of Cadmium on Intracellular Zinc Levels in HepG2 Cells: Quantitative Evaluations and Molecular Effects. BioMed Res. Int. 2015.

References

[1] G. T. Ankley, R. S. Bennett, R. J. Erickson, D. J. Hoff, M. W. Hornung, R. D. Johnson, D. R. Mount, J. W. Nichols, C. L. Russom, P. K. Schmieder, J. A. Serrrano, J. E. Tietge, and D. L. Villeneuve, "Adverse outcome pathways: A conceptual framework to support ecotoxicology research and risk assessment," *Environ. Toxicol. Chem.*, vol. 29, no. 3, pp. 730–741, Mar. 2010.

[2] J. Warringer, M. Hult, S. Regot, F. Posas, and P. Sunnerhagen, "The HOG Pathway Dictates the Short-Term Translational Response after Hyperosmotic Shock," *Mol. Biol. Cell*, vol. 21, no. 17, pp. 3080–3092, Sep. 2010.

[3] M. Chee, R. Yang, E. Hubbell, A. Berno, X. C. Huang, D. Stern, J. Winkler, D. J. Lockhart, M. S. Morris, and S. P. Fodor, "Accessing genetic information with high-density DNA arrays," *Science*, vol. 274, no. 5287, pp. 610–614, Oct. 1996.

[4] A. I. Su, M. P. Cooke, K. A. Ching, Y. Hakak, J. R. Walker, T. Wiltshire, A. P. Orth, R. G. Vega, L. M. Sapinoso, A. Moqrich, A. Patapoutian, G. M. Hampton, P. G. Schultz, and J. B. Hogenesch, "Large-scale analysis of the human and mouse transcriptomes," *Proc. Natl. Acad. Sci. U. S. A.*, vol. 99, no. 7, pp. 4465–4470, Apr. 2002.

[5] M. Chekulaeva and W. Filipowicz, "Mechanisms of miRNA-mediated post-transcriptional regulation in animal cells," *Curr. Opin. Cell Biol.*, vol. 21, no. 3, pp. 452–460, Jun. 2009.

[6] S. Choudhuri, "Small noncoding RNAs: biogenesis, function, and emerging significance in toxicology," *J. Biochem. Mol. Toxicol.*, vol. 24, no. 3, pp. 195–216, Jun. 2010.

[7] M. R. Fabian, N. Sonenberg, and W. Filipowicz, "Regulation of mRNA translation and stability by microRNAs," *Annu. Rev. Biochem.*, vol. 79, pp. 351–379, 2010.

[8] R. C. Friedman, K. K.-H. Farh, C. B. Burge, and D. P. Bartel, "Most mammalian mRNAs are conserved targets of microRNAs," *Genome Res.*, vol. 19, no. 1, pp. 92–105, Jan. 2009.

[9] W. P. Kloosterman and R. H. A. Plasterk, "The diverse functions of microRNAs in animal development and disease," *Dev. Cell*, vol. 11, no. 4, pp. 441–450, Oct. 2006.

[10] C. M. McHale, L. Zhang, A. E. Hubbard, and M. T. Smith, "Toxicogenomic profiling of chemically exposed humans in risk assessment," *Mutat. Res.*, vol. 705, no. 3, pp. 172–183, Dec. 2010.

[11] A. A. Gheyas and D. W. Burt, "Microarray resources for genetic and genomic studies in chicken: A review," *Genesis*, vol. 51, no. 5, pp. 337–356, 2013.

[12] T. D. Williams, K. Gensberg, S. D. Minchin, and J. K. Chipman, "A DNA expression array to detect toxic stress response in European flounder (Platichthys flesus)," *Aquat. Toxicol.*, vol. 65, no. 2, pp. 141–157, 2003.

[13] D. N. Keys, J. K. Au-Young, and R. A. Fekete, "TaqMan Array Cards in pharmaceutical research," *Methods Mol. Biol. Clifton NJ*, vol. 632, pp. 87–97, 2010.

[14] E. F. Nuwaysir, M. Bittner, J. Trent, J. C. Barrett, and C. A. Afshari, "Microarrays and toxicology: the advent of toxicogenomics," *Mol. Carcinog.*, vol. 24, no. 3, pp. 153–159, Mar. 1999.

[15] H. Zhu, J. Zhang, M. T. Kim, A. Boison, A. Sedykh, and K. Moran, "Big data in chemical toxicity research: the use of high-throughput screening assays to identify potential toxicants," *Chem. Res. Toxicol.*, vol. 27, no. 10, pp. 1643–1651, Oct. 2014.

[16] M. B. Eisen, P. T. Spellman, P. O. Brown, and D. Botstein, "Cluster analysis and display of genome-wide expression patterns," *Proc. Natl. Acad. Sci. U. S. A.*, vol. 95, no. 25, pp. 14863–14868, Dec. 1998.

[17] P. T. Spellman, G. Sherlock, M. Q. Zhang, V. R. Iyer, K. Anders, M. B. Eisen, P. O. Brown, D. Botstein, and B. Futcher, "Comprehensive identification of cell cycle-regulated genes of the yeast Saccharomyces cerevisiae by microarray hybridization," *Mol. Biol. Cell*, vol. 9, no. 12, pp. 3273–3297, Dec. 1998.

[18] J. F. Waring, R. Ciurlionis, R. A. Jolly, M. Heindel, and R. G. Ulrich, "Microarray analysis of hepatotoxins in vitro reveals a correlation between gene expression profiles and mechanisms of toxicity," *Toxicol. Lett.*, vol. 120, no. 1–3, pp. 359–368, Mar. 2001.

[19] S. Goto, H. Bono, H. Ogata, W. Fujibuchi, T. Nishioka, K. Sato, and M. Kanehisa, "Organizing and computing metabolic pathway data in terms of binary relations," *Pac. Symp. Biocomput. Pac. Symp. Biocomput.*, pp. 175–186, 1997.

[20] D. Croft, A. F. Mundo, R. Haw, M. Milacic, J. Weiser, G. Wu, M. Caudy, P. Garapati, M. Gillespie, M. R. Kamdar, B. Jassal, S. Jupe, L. Matthews, B. May, S. Palatnik, K. Rothfels, V. Shamovsky, H. Song, M. Williams, E. Birney, H. Hermjakob, L. Stein, and P. D'Eustachio, "The Reactome pathway knowledgebase," *Nucleic Acids Res.*, vol. 42, no. Database issue, pp. D472–477, Jan. 2014.

[21] R. Caspi, T. Altman, R. Billington, K. Dreher, H. Foerster, C. A. Fulcher, T. A. Holland, I. M. Keseler, A. Kothari, A. Kubo, M. Krummenacker, M. Latendresse, L. A. Mueller, Q. Ong, S. Paley, P. Subhraveti, D. S. Weaver, D. Weerasinghe, P. Zhang, and P. D. Karp, "The MetaCyc database of metabolic pathways and enzymes and the BioCyc collection of Pathway/Genome Databases," *Nucleic Acids Res.*, vol. 42, no. Database issue, pp. D459–471, Jan. 2014.

[22] A. R. Pico, T. Kelder, M. P. van Iersel, K. Hanspers, B. R. Conklin, and C. Evelo, "WikiPathways: pathway editing for the people," *PLoS Biol.*, vol. 6, no. 7, p. e184, Jul. 2008.

[23] J. Krol, I. Loedige, and W. Filipowicz, "The widespread regulation of microRNA biogenesis, function and decay," *Nat. Rev. Genet.*, vol. 11, no. 9, pp. 597–610, Sep. 2010.

[24] H. Guo, N. T. Ingolia, J. S. Weissman, and D. P. Bartel, "Mammalian microRNAs predominantly act to decrease target mRNA levels," *Nature*, vol. 466, no. 7308, pp. 835–840, Aug. 2010.

[25] Q. Jiang, Y. Wang, Y. Hao, L. Juan, M. Teng, X. Zhang, M. Li, G. Wang, and Y. Liu, "miR2Disease: a manually curated database for microRNA deregulation in human disease," *Nucleic Acids Res.*, vol. 37, no. Database issue, pp. D98–104, Jan. 2009.

[26] M. Ferracin, A. Veronese, and M. Negrini, "Micromarkers: miRNAs in cancer diagnosis and prognosis," *Expert Rev. Mol. Diagn.*, vol. 10, no. 3, pp. 297–308, Apr. 2010.

[27] Y. Yang, S. J. Abel, R. Ciurlionis, and J. F. Waring, "Development of a toxicogenomics in vitro assay for the efficient characterization of compounds," *Pharmacogenomics*, vol. 7, no. 2, pp. 177–186, Mar. 2006.

[28] F. Boess, M. Kamber, S. Romer, R. Gasser, D. Muller, S. Albertini, and L. Suter, "Gene Expression in Two Hepatic Cell Lines, Cultured Primary Hepatocytes, and Liver Slices Compared to the in Vivo Liver Gene Expression in Rats: Possible Implications for Toxicogenomics Use of in Vitro Systems," *Toxicol. Sci.*, vol. 73, no. 2, pp. 386–402, Jun. 2003.

[29] H. Jaeschke, "Are cultured liver cells the right tool to investigate mechanisms of liver disease or hepatotoxicity?," *Hepatol. Baltim. Md*, vol. 38, no. 4, pp. 1053–1055, Oct. 2003.

[30] T. Hartung, "Food for thought... on cell culture," *ALTEX*, vol. 24, no. 3, pp. 143–152, 2007.

[31] J. H. Chiu, C. P. Hu, W. Y. Lui, S. C. Lo, and C. M. Chang, "The formation of bile canaliculi in human hepatoma cell lines," *Hepatol. Baltim. Md*, vol. 11, no. 5, pp. 834–842, May 1990.

[32] W. G. E. J. Schoonen, J. A. D. M. de Roos, W. M. A. Westerink, and E. Débiton, "Cytotoxic effects of 110 reference compounds on HepG2 cells and for 60 compounds on HeLa, ECC-1 and CHO cells. II mechanistic assays on NAD(P)H, ATP and DNA contents," *Toxicol. Vitro Int. J. Publ. Assoc. BIBRA*, vol. 19, no. 4, pp. 491–503, Jun. 2005.

[33] J. V. Castell, R. Jover, C. P. Martínez-Jiménez, and M. J. Gómez-Lechón, "Hepatocyte cell lines: their use, scope and limitations in drug metabolism studies," *Expert Opin. Drug Metab. Toxicol.*, vol. 2, no. 2, pp. 183–212, Apr. 2006.

[34] S. Knasmüller, W. Parzefall, R. Sanyal, S. Ecker, C. Schwab, M. Uhl, V. Mersch-Sundermann, G. Williamson, G. Hietsch, T. Langer, F. Darroudi, and A. T. Natarajan, "Use of metabolically competent human hepatoma cells for the detection of mutagens and antimutagens," *Mutat. Res.*, vol. 402, no. 1–2, pp. 185–202, Jun. 1998.

[35] M. Zegers and D. HOEKSTRA, "Mechanisms and functional features of polarized membrane traffic in epithelial and hepatic cells," *Biochem J*, vol. 336, pp. 257–269, 1998.

[36] C. Urani, P. Melchioretto, C. Canevali, and G. F. Crosta, "Cytotoxicity and induction of protective mechanisms in HepG2 cells exposed to cadmium.," *Toxicol. Vitro Int. J. Publ. Assoc. BIBRA*, vol. 19, no. 7, pp. 887–92, 2005.

[37] I. J. Hidalgo, T. J. Raub, and R. T. Borchardt, "Characterization of the human colon carcinoma cell line (Caco-2) as a model system for intestinal epithelial permeability," *Gastroenterology*, vol. 96, no. 3, pp. 736–749, Mar. 1989.

[38] P. Artursson and J. Karlsson, "Correlation between oral drug absorption in humans and apparent drug permeability coefficients in human intestinal epithelial (Caco-2) cells," *Biochem. Biophys. Res. Commun.*, vol. 175, no. 3, pp. 880–885, Mar. 1991.

[39] P. Artursson, K. Palm, and K. Luthman, "Caco-2 monolayers in experimental and theoretical predictions of drug transport," *Adv. Drug Deliv. Rev.*, vol. 46, no. 1–3, pp. 27–43, Mar. 2001.

[40] S. Yee, "In vitro permeability across Caco-2 cells (colonic) can predict in vivo (small intestinal) absorption in man--fact or myth," *Pharm. Res.*, vol. 14, no. 6, pp. 763–766, Jun. 1997.

[41] L. Z. Benet and C. A. Larregieu, "The FDA should eliminate the ambiguities in the current BCS biowaiver guidance and make public the drugs for which BCS biowaivers have been granted," *Clin. Pharmacol. Ther.*, vol. 88, no. 3, pp. 405–407, Sep. 2010.

[42] Y. Yang, P. J. Faustino, D. A. Volpe, C. D. Ellison, R. C. Lyon, and L. X. Yu, "Biopharmaceutics classification of selected beta-blockers: solubility and permeability class membership," *Mol. Pharm.*, vol. 4, no. 4, pp. 608–614, Aug. 2007.

[43] Go. Gey, W. D. Coffman, and M. T. Kubicek, "Tissue culture studies of the proliferative capacity of cervical carcinoma and normal epithelium," in *Cancer research*, 1952, vol. 12, pp. 264–265.

[44] Lasso RA, "THe immortal life of henrietta lacks," *JAMA*, vol. 305, no. 11, pp. 1143–1144, Mar. 2011.

[45] W. F. Scherer, "STUDIES ON THE PROPAGATION IN VITRO OF POLIOMYELITIS VIRUSES: IV. VIRAL MULTIPLICATION IN A STABLE STRAIN OF HUMAN MALIGNANT EPITHELIAL CELLS (STRAIN HELA) DERIVED FROM AN EPIDERMOID CARCINOMA OF THE CERVIX," *J. Exp. Med.*, vol. 97, no. 5, pp. 695–710, May 1953.

[46] J. Berg, B. Doe, K. S. Steimer, and M. Wabl, "HeLa-LAV, an epithelial cell line stably infected with HIV-1," *J. Virol. Methods*, vol. 34, no. 2, pp. 173–180, Oct. 1991.

[47] J. I. Murray, M. L. Whitfield, N. D. Trinklein, R. M. Myers, P. O. Brown, and D. Botstein, "Diverse and specific gene expression responses to stresses in cultured human cells," *Mol. Biol. Cell*, vol. 15, no. 5, pp. 2361–2374, May 2004.

[48] C. W. Greider and E. H. Blackburn, "Identification of a specific telomere terminal transferase activity in Tetrahymena extracts," *Cell*, vol. 43, no. 2 Pt 1, pp. 405–413, Dec. 1985.

[49] M. L. Whitfield, G. Sherlock, A. J. Saldanha, J. I. Murray, C. A. Ball, K. E. Alexander, J. C. Matese, C. M. Perou, M. M. Hurt, P. O. Brown, and D. Botstein, "Identification of genes periodically expressed in the human cell cycle and their expression in tumors," *Mol. Biol. Cell*, vol. 13, no. 6, pp. 1977–2000, Jun. 2002.

[50] I. Ghosh and S. Ghosh, "Karyological studies on two HeLa lines," *Z. Für Krebsforsch.*, vol. 74, no. 1, pp. 103–109, 1970.

[51] V. Leone, T. C. Hsu, and C. M. Pomerat, "Cytological studies on HeLa, a strain of human cervical carcinoma. II. On rotatory movements of the nuclei," *Z. Für Zellforsch. Mikrosk. Anat. Vienna Austria 1948*, vol. 41, no. 5, pp. 481–492, 1955.

[52] "A Proposed Standard System on Nomenclature of Human Mitotic Chromosomes," *Am. J. Hum. Genet.*, vol. 12, no. 3, pp. 384–388, Sep. 1960.

[53] E. H. Chu and N. G. Giles, "Comparative chromosomal studies on mammalian cells in culture. I. The HeLa strain and its mutant clonal derivatives," *J. Natl. Cancer Inst.*, vol. 20, no. 2, pp. 383–401, Feb. 1958.

[54] S. Ghosh and I. Ghosh, "Variation of stemline karyotype in a HeLa cell line," *Z. Für Krebsforsch. Klin. Onkol. Cancer Res. Clin. Oncol.*, vol. 84, no. 2, pp. 129–133, Oct. 1975.

[55] M. Macville, E. Schröck, H. Padilla-Nash, C. Keck, B. M. Ghadimi, D. Zimonjic, N. Popescu, and T. Ried, "Comprehensive and definitive molecular cytogenetic characterization of HeLa cells by spectral karyotyping," *Cancer Res.*, vol. 59, no. 1, pp. 141–150, Jan. 1999.

[56] J. H. Tjio and T. T. Puck, "Genetics of somatic mammalian cells. II. Chromosomal constitution of cells in tissue culture," *J. Exp. Med.*, vol. 108, no. 2, pp. 259–268, Aug. 1958.

[57] P. B. Tchounwou, C. G. Yedjou, A. K. Patlolla, and D. J. Sutton, "Heavy Metal Toxicity and the Environment," in *Molecular, Clinical and Environmental Toxicology*, vol. 101, A. Luch, Ed. Basel: Springer Basel, 2012, pp. 133–164.

[58] S. Satarug and M. R. Moore, "Adverse health effects of chronic exposure to low-level cadmium in foodstuffs and cigarette smoke.," *Environ. Health Perspect.*, vol. 112, no. 10, pp. 1099–103, Jul. 2004.

[59] M. P. Waalkes, "Cadmium carcinogenesis in review," *J. Inorg. Biochem.*, vol. 79, no. 1–4, pp. 241–244, Apr. 2000.

[60] C. D. Klaassen, J. Liu, and S. Choudhuri, "Metallothionein: an intracellular protein to protect against cadmium toxicity," *Annu. Rev. Pharmacol. Toxicol.*, vol. 39, pp. 267–294, 1999.

[61] A. Hartwig, "Cadmium and cancer," *Met. Ions Life Sci.*, vol. 11, pp. 491–507, 2013.

[62] P. Joseph, "Mechanisms of cadmium carcinogenesis," *Toxicol. Appl. Pharmacol.*, vol. 238, no. 3, pp. 272–279, Aug. 2009.

[63] M. R. Cheung, J. Kang, D. Ouyang, and V. Yeung, "Association between urinary cadmium and all cause, all cancer and prostate cancer specific mortalities for men: an analysis of national health and nutrition examination survey (NHANES III) data," *Asian Pac. J. Cancer Prev. APJCP*, vol. 15, no. 1, pp. 483–488, 2014.

[64] A. Hartwig, "Carcinogenicity of metal compounds: possible role of DNA repair inhibition," *Toxicol. Lett.*, vol. 102–103, pp. 235–239, Dicembre 1998.

[65] D. Beyersmann and S. Hechtenberg, "Cadmium, Gene Regulation, and Cellular Signalling in Mammalian Cells," *Toxicol. Appl. Pharmacol.*, vol. 144, no. 2, pp. 247–261, Giugno 1997.

[66] S. Guo and E. Wang, "Noble metal nanomaterials: Controllable synthesis and application in fuel cells and analytical sensors," *Nano Today*, vol. 6, no. 3, pp. 240–264, Giugno 2011.

[67] G. Oberdörster, A. Maynard, K. Donaldson, V. Castranova, J. Fitzpatrick, K. Ausman, J. Carter, B. Karn, W. Kreyling, D. Lai, S. Olin, N. Monteiro-Riviere, D. Warheit, H. Yang, and ILSI Research Foundation/Risk Science Institute Nanomaterial Toxicity Screening Working Group, "Principles for characterizing the potential human health effects from exposure to nanomaterials: elements of a screening strategy," *Part. Fibre Toxicol.*, vol. 2, p. 8, Oct. 2005.

[68] R. Podila and J. M. Brown, "Toxicity of engineered nanomaterials: a physicochemical perspective," *J. Biochem. Mol. Toxicol.*, vol. 27, no. 1, pp. 50–55, Jan. 2013.

[69] S. Sharifi, S. Behzadi, S. Laurent, M. L. Forrest, P. Stroeve, and M. Mahmoudi, "Toxicity of nanomaterials," *Chem. Soc. Rev.*, vol. 41, no. 6, pp. 2323–2343, Mar. 2012.

[70] A. Nel, "Toxic Potential of Materials at the Nanolevel," *Science*, vol. 311, no. 5761, pp. 622–627, Feb. 2006.

[71] C. Carlson, S. M. Hussain, A. M. Schrand, L. K. Braydich-Stolle, K. L. Hess, R. L. Jones, and J. J. Schlager, "Unique cellular interaction of silver nanoparticles: size-dependent generation of reactive oxygen species," *J. Phys. Chem. B*, vol. 112, no. 43, pp. 13608–13619, Oct. 2008.

[72] E. E. Connor, J. Mwamuka, A. Gole, C. J. Murphy, and M. D. Wyatt, "Gold nanoparticles are taken up by human cells but do not cause acute cytotoxicity," *Small Weinh. Bergstr. Ger.*, vol. 1, no. 3, pp. 325–327, Mar. 2005.

[73] L. Dykman and N. Khlebtsov, "Gold nanoparticles in biomedical applications: recent advances and perspectives," *Chem. Soc. Rev.*, vol. 41, no. 6, pp. 2256–2282, Mar. 2012.

[74] J. F. Hainfeld, D. N. Slatkin, T. M. Focella, and H. M. Smilowitz, "Gold nanoparticles: a new X-ray contrast agent," *Br. J. Radiol.*, vol. 79, no. 939, pp. 248–253, Mar. 2006.

[75] R. Coradeghini, S. Gioria, C. P. García, P. Nativo, F. Franchini, D. Gilliland, J. Ponti, and F. Rossi, "Size-dependent toxicity and cell interaction mechanisms of gold nanoparticles on mouse fibroblasts," *Toxicol. Lett.*, vol. 217, no. 3, pp. 205–216, Mar. 2013.

[76] T. Mironava, M. Hadjiargyrou, M. Simon, and M. H. Rafailovich, "Gold nanoparticles cellular toxicity and recovery: adipose Derived Stromal cells," *Nanotoxicology*, vol. 8, no. 2, pp. 189–201, Mar. 2014.

[77] G. L. Semenza and G. L. Wang, "A nuclear factor induced by hypoxia via de novo protein synthesis binds to the human erythropoietin gene enhancer at a site required for transcriptional activation," *Mol. Cell. Biol.*, vol. 12, no. 12, pp. 5447–5454, Dec. 1992.

[78] P. H. Maxwell, C. W. Pugh, and P. J. Ratcliffe, "Inducible operation of the erythropoietin 3' enhancer in multiple cell lines: evidence for a widespread oxygen-sensing mechanism.," *Proc. Natl. Acad. Sci. U. S. A.*, vol. 90, no. 6, pp. 2423–2427, Mar. 1993.

[79] J. D. Firth, B. L. Ebert, C. W. Pugh, and P. J. Ratcliffe, "Oxygen-regulated control elements in the phosphoglycerate kinase 1 and lactate dehydrogenase A genes: similarities with the erythropoietin 3' enhancer," *Proc. Natl. Acad. Sci. U. S. A.*, vol. 91, no. 14, pp. 6496–6500, Jul. 1994.

[80] Y. Z. Gu, S. M. Moran, J. B. Hogenesch, L. Wartman, and C. A. Bradfield, "Molecular characterization and chromosomal localization of a third alpha-class hypoxia inducible factor subunit, HIF3alpha," *Gene Expr.*, vol. 7, no. 3, pp. 205–213, 1998.

[81] G. L. Semenza, "Regulation of mammalian O2 homeostasis by hypoxia-inducible factor 1," *Annu. Rev. Cell Dev. Biol.*, vol. 15, pp. 551–578, 1999.

[82] N. Li, P. Zhao, and D. Astruc, "Anisotropic gold nanoparticles: synthesis, properties, applications, and toxicity," *Angew. Chem. Int. Ed Engl.*, vol. 53, no. 7, pp. 1756–1789, Feb. 2014.